

Probing collision dynamics of atoms, ions and molecules via electron impact ionization

Ghanshyam Purohit

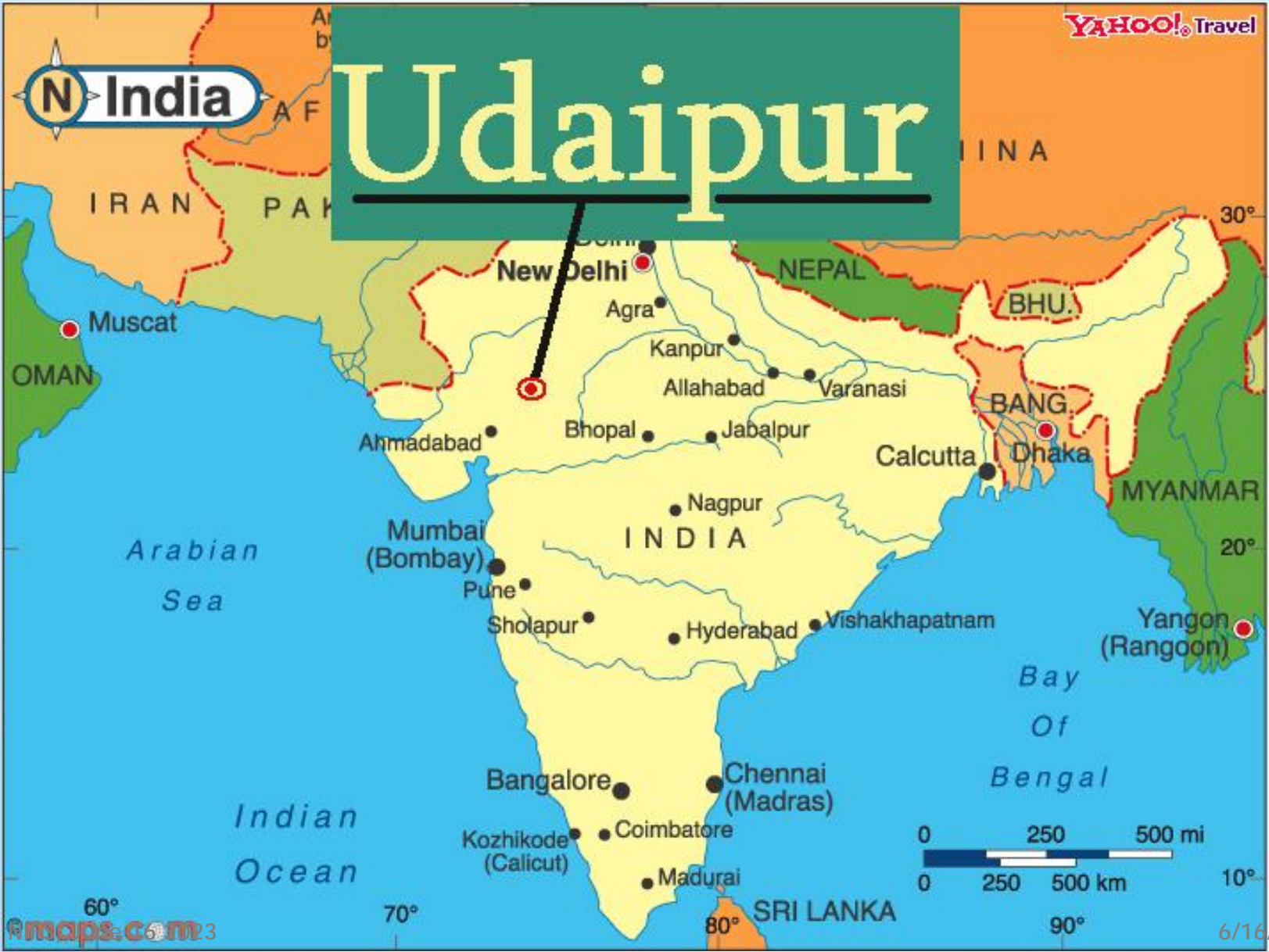
プロヒット ガンシャム

*Department of Physics, University College of Science,
Mohanlal Sukhadia Univesrity, Udaipur-313001, India (インド)*



N India

Udaipur



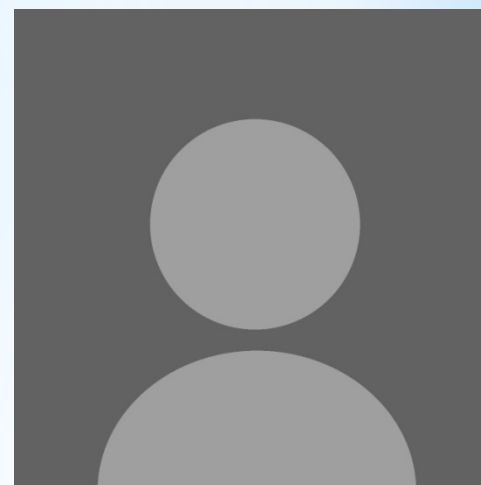
Research Group



Kailash Chandra Dhakar
Ph. D Student



Alpana Pandey
SERB JRF, Ph. D student



Suneel Kumar
Meena, Ph. D
Student

Email: ghanshyam.purohit@mlsu.ac.in
gvpurohit1974@gmail.com

* Researchers of the field

Experiments

Andrew Murray, Manchester University, UK

Alexander Dorn, Max Planck Institute for Nuclear Physics,
Heidelberg, Germany

A. Lehman Bennani, University Paris, Orsay, France

Robert DuBois, Missouri University of Science and Technology,
USA

Masahiko Takahashi, Tohoku University, Sendai, Japan

Jiro Itatani, ISSP, University of Tokyo, Japan

* Researchers of the field

Theory

Klaus Bartschat, Drake University, Des Moines, USA

Igor Bray, Curtin University, Perth, Australia

Claude Dal Cappello, University of Metz, France

Ugo Ancarani, University of Metz, France

Fumihiko Koike, Sophia University, Japan

Anatoli Kheifets, ANU, Canberra, Australia

* Researchers of the field

India

Lokesh Tribedi, TIFR, Mumbai

Sajid Rangwala, RRI, Bengaluru

C. P. Safyan, IUAC, Delhi

Bhas Bapat, IISER, Pune

Umesh Kadhane, IIST, Thriuvananthapuram

Rajesh Srivastava, IIT Roorkee

Minaxi Vinodkumar, Vallabh Vidyanagar

Bobby Antony, IIT-ISM Dhanbad

Chetan Limbachiya, M S University, Vadodra

Bijaya Sahoo, PRL, Ahemdabad

D.K. Mani, IIT Delhi

- INTRODUCTION
- KINEMATICS and GEOMETRY - ionization process
- THEORY
- RESULTS
 - TDCS for Ar, Xe, W, W⁺
 - TICS for W, W⁺ and Be
 - TDCS for N₂, H₂O and CO₂
- Conclusions
- Outlook

Introduction

Scattering – Important tool to know the structure of targets (Rutherford et al. (1909)).

Electron impact ionization – Important in many physical processes (The first theoretical paper on electron impact ionization of atoms - by Sir J. J. Thompson “**Ionization by moving electrified particles**”.)

- everyday processes both natural and man made are driven by collision between charged particle and atoms /or molecules
- Atomic and subatomic micro world information
- Interaction of complex target with charged projectile
- Development of Quantum Mechanics
- Recent advancement in experimental technique.

Applications

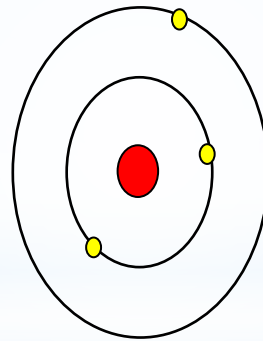
Few applications of a fundamental collision process;

- * plasma physics - Fusion Plasma, Industrial Plasmas
- * astrophysics
- * atmospheric modeling - Stellar and Planetary Atmospheres
- * discharge physics and radiobiology.

However, there are many more

What happens when target (atom, ion or molecule) is hit by a projectile?

Projectile ●



Scattering processes

There are basically following electron-atom

scattering processes:

Elastic scattering : $A+B \rightarrow A+B$

Inelastic scattering : $A+B \rightarrow A^{\#}+B$

Excitation processes : $A+B \rightarrow A^*+B$

Ionization processes : $A+B \rightarrow A+B^+$

Electron-Electron exchange:

$A^++B \rightarrow A+B^+$

Scattering cross sections

The collision which take place betw projectile and a target is conveniently described in terms of a cross section.

singly differential cross section (SDCS)

$$\sigma = \int \frac{d\sigma}{d\Omega} d\Omega$$

double differential cross section (DDCS)

$$\sigma = \int \frac{d^2\sigma(\theta)}{d\Omega dE} dE d\Omega$$

triple differential cross section (TDCS)

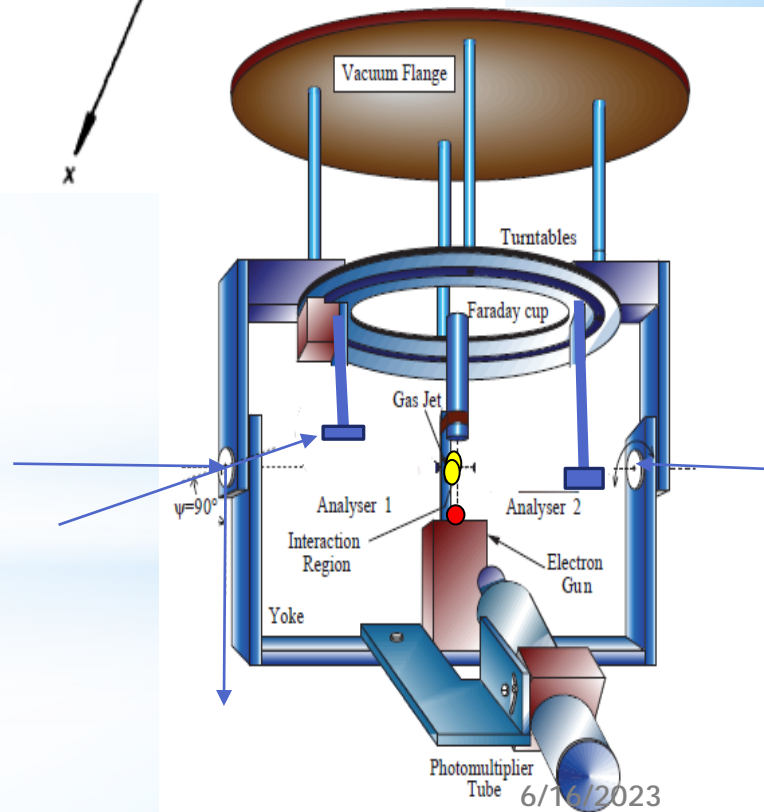
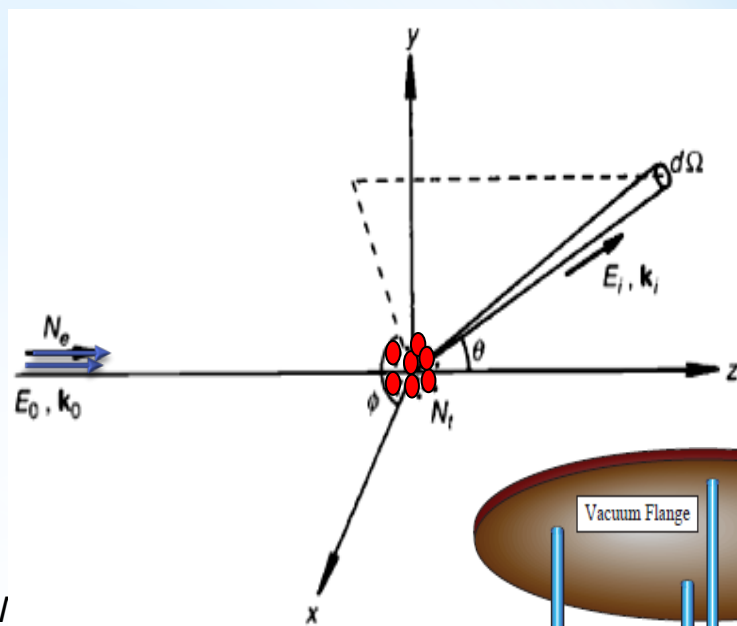
$$\frac{d^3\sigma}{d\Omega_1 d\Omega_2 dE_1}$$

NIFS, June 16 2023

five- fold differential cross section

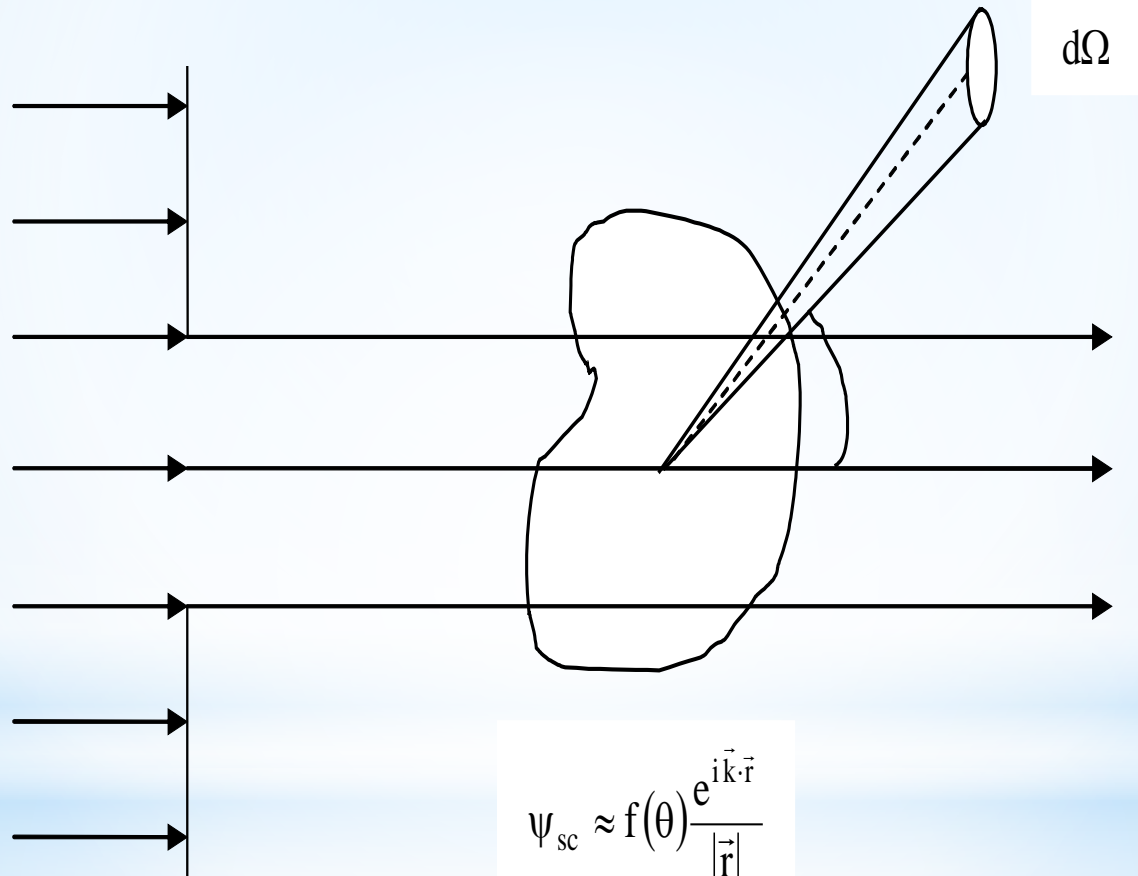
$$\frac{d^5\sigma}{d\Omega_1 d\Omega_2 d\Omega_s dE_1 dE_2}$$

11



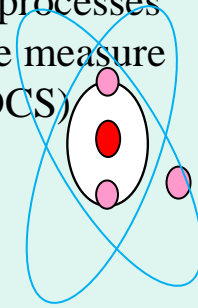
6/16/2023

Incident Beam



(e, 2e) Processes

Definition :- An electron impact single ionization, which is referred to as (e, 2e) processes. In order to gain information about the (e, 2e) ionization process, we measure the triple differential (TDCS) or fully differential cross section (FDCS).



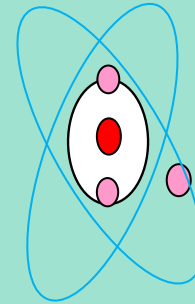
Scattered e_a

Ejected e_b



(e, 3e) Processes

Definition :- An electron impact double ionization, which is referred to as (e, 3e) processes. In order to gain information about the (e, 3e) ionization process, we measure the Five-fold differential cross section (FDCS).



scattered e_a

ejected e_b

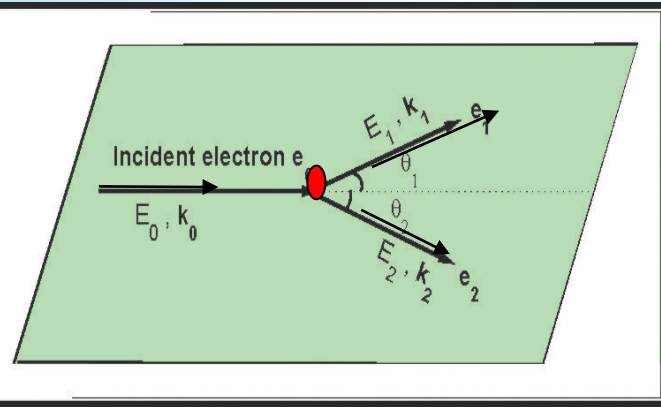
ejected e_b



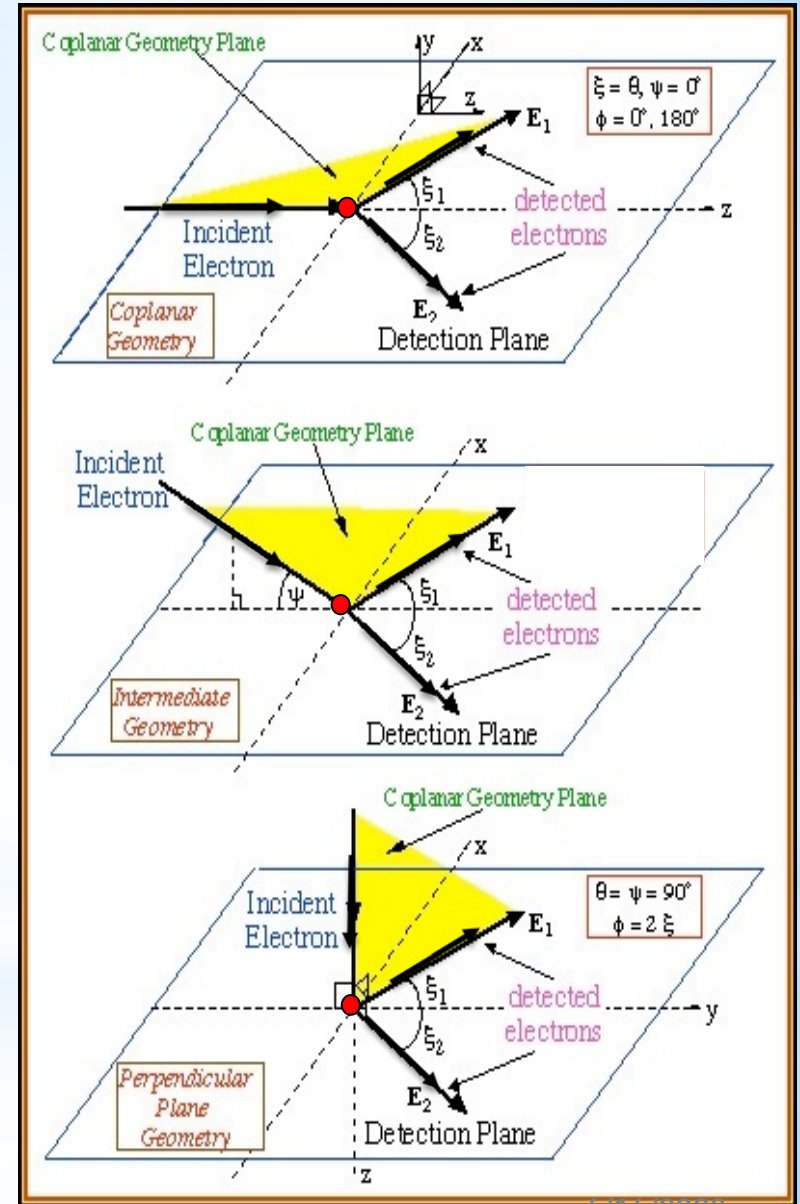
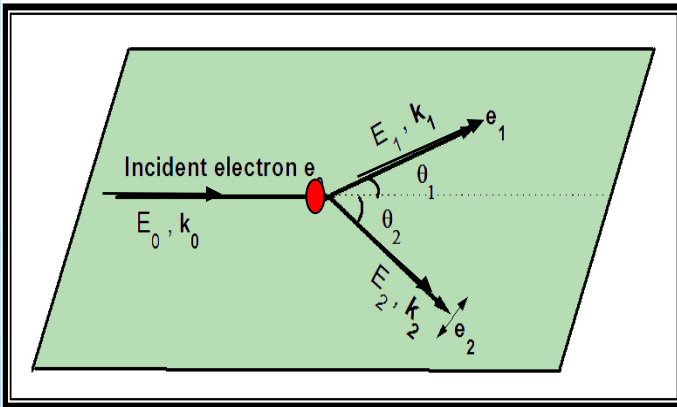
Motivation:- Theoretical modeling of few-body dynamics such as electron impact ionization is very challenging since the few-body problem is one of the most fundamental unsolved problems in physics.

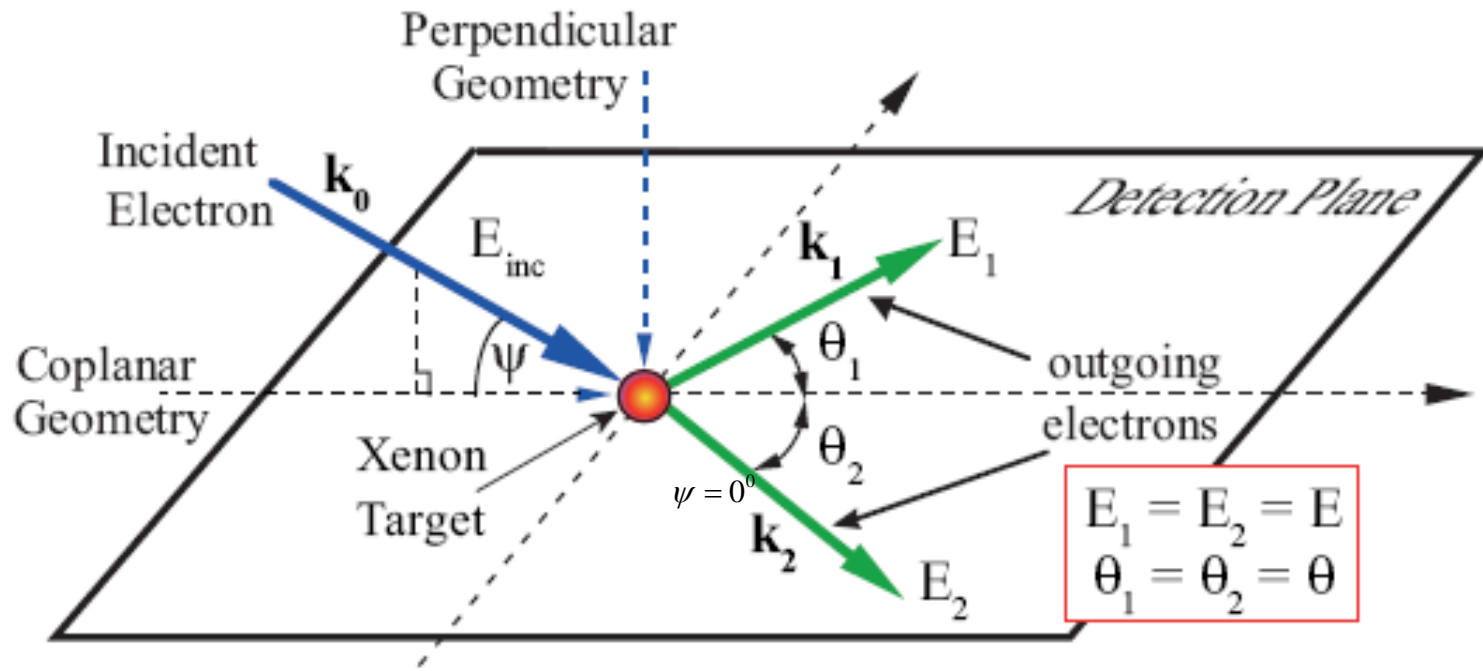
Kinematics

Coplanar symmetric kinematics :-



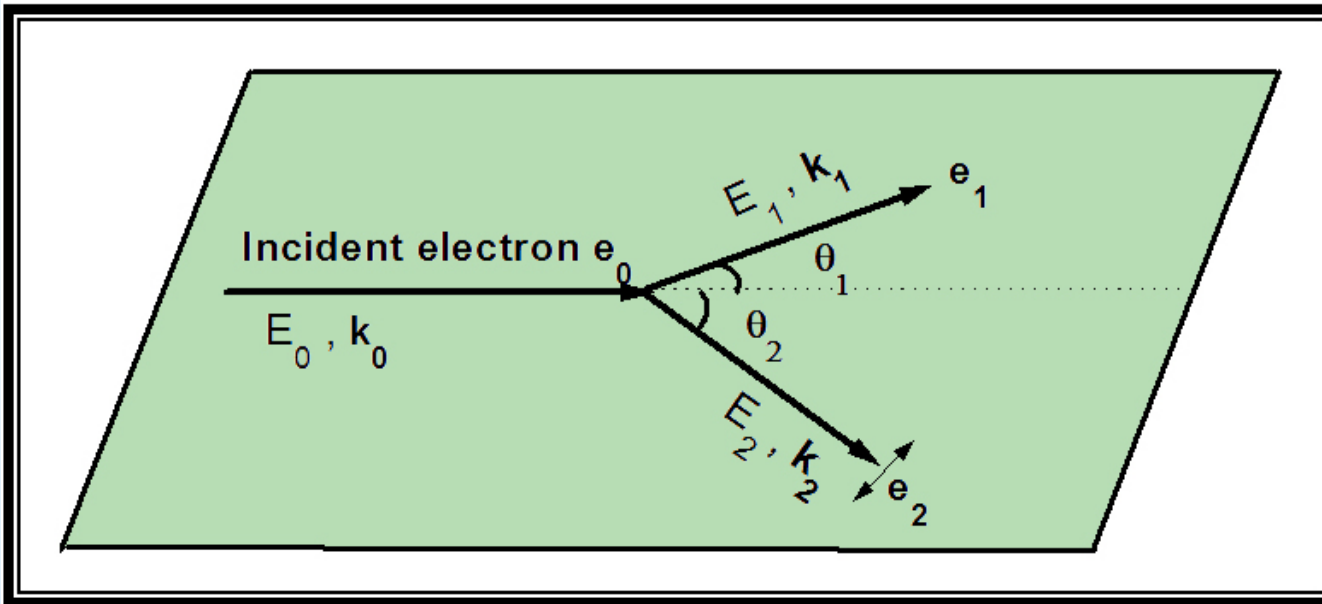
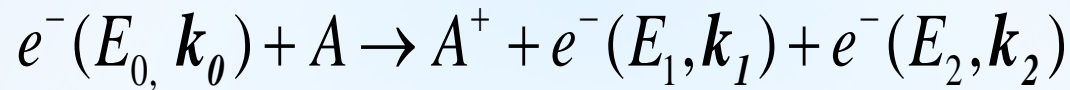
Coplanar asymmetric kinematics:-





The incident electron momentum can be moved from being in the detection plane to being perpendicular to this plane

THEORETICAL FORMALISM OF CHARGED PARTICLE IMPACT IONIZATION OF ATOMS, IONS AND MOLECULES



(e, 2e) - Coincidence technique

Delivers most precise data for the study of ionization by electron impact

(e, 2e) measurements - Differential cross sections (DCS) which depends on all three momenta

In the electron impact single ionization process, an incident electron of linear momentum k_i and energy E_i ionizes the target (atom / ion) and the two emerging electrons are described by the linear momentum and energy (k_f, E_f) and (k_e, E_e) , where the scattered (primary) electron is specified by subscript 'f' and the ejected (secondary) electron is specified by subscript 'e'.

The energy conservation principle states;

$$E_i = E_f + E_e + E_b \quad (1)$$

where E_b is the energy of the bound electron.

The momentum conservation equation is

$$\mathbf{k}_i = \mathbf{k}_e + \mathbf{k}_f + \mathbf{k}_r$$

Momentum transfer from incident electron to target is given by

$$\mathbf{K} = \left| \mathbf{k}_i - \mathbf{k}_f \right|$$

The triple differential cross section (TDCS) for the electron impact single ionization, which is the probability of single ionization, is expressed in atomic units as

$$\frac{d^3\sigma}{d\Omega_f d\Omega_e dE_f} = (2\pi)^4 \frac{k_f k_e}{k_i} \sum_{av} |T(k_f, k_e, k_i)|^2 \quad (2)$$

The expression in Eq. (2) includes a sum over final and average over initial magnetic and spin state degeneracy. The T matrix in Eq.(2), which is the subject of approximation, includes interaction between the incident and target electrons and the nucleus.

TDCS (eq. 2) for the ionization is written in terms of direct and exchange amplitude as

$$\frac{d^3\sigma}{d\Omega_f d\Omega_e dE_i} = (2\pi)^4 \frac{k_f k_e}{k_i} \sum_{m=-1}^1 \left(|f|^2 + |g|^2 - \text{Re}(f^* g) \right)$$

where

$$f = \left\langle \chi_f^{(-)}(\mathbf{k}_f, \mathbf{r}_f) \chi_e^{(-)}(\mathbf{k}_e, \mathbf{r}_e) \middle| v_{fe} \middle| \chi_i^{(+)}(\mathbf{k}_i, \mathbf{r}_f) \chi_b(\mathbf{r}_e) \right\rangle$$

$$g = \left\langle \chi_f^{(-)}(\mathbf{k}_f, \mathbf{r}_e) \chi_e^{(-)}(\mathbf{k}_e, \mathbf{r}_f) \middle| v_{fe} \middle| \chi_i^{(+)}(\mathbf{k}_i, \mathbf{r}_f) \chi_b(\mathbf{r}_e) \right\rangle$$

The second order Born term is given as

$$f_{B2} = \left\langle \chi_1^{(-)}(\mathbf{k}_a, \mathbf{r}_a) \chi_2^{(-)}(\mathbf{k}_b, \mathbf{r}_b) \left| V \mathbf{G}_0^+ V \right| \psi_i \chi_0^{(+)}(\mathbf{k}_i, \mathbf{r}_a) \right\rangle$$

Where \mathbf{G}_0^+ is Green's function having the form;

$$\mathbf{G}_0^+ = \frac{1}{E_0 - H + i\varepsilon}$$

here H is the Hamiltonian of the target atom defined by

$$H = -\frac{\nabla^2}{2} \pm \left(\frac{z}{r_a} - \frac{1}{|r_a - r_b|} \right)$$

where the symbol \pm is for the projectile charge, E_0 represents incident energy and $\varepsilon \rightarrow 0^+$.

- * The initial-state distorted waves are generated in the equivalent local ground state potential of the atom.
- * The final-state distorted waves are obtained in the equivalent local ground state potential of the ion.
- * Hartree-Fock orbitals for the bound target state
 - * E. Clementi and C. Roetti, At. Data Nucl. Data Tab. 14, 177 (1974).
 - * A. D. McLEAN and R. S. McLEAN, At. Data Nucl. Data Tab. 26, 287 (1981).

$$|\chi^{(+)}(\mathbf{k}_0, \mathbf{r}_1)\rangle = \sqrt{\frac{2}{\pi}} \frac{1}{k_0 r_1} \sum_{L,M} i^L e^{i\sigma_L} u_L(k_0, r_1) Y_{L,M}^*(\hat{\mathbf{k}}_0) Y_{L,M}(\hat{\mathbf{r}}_1)$$

$$\langle \chi_1^{(-)}(\mathbf{k}_1, \mathbf{r}_1) | = \sqrt{\frac{2}{\pi}} \frac{1}{k_1 r_1} \sum_{L',M'} i^{-L'} e^{i\sigma_{L'}} u_{L'}(k_0, r_1) Y_{L',M'}^*(\hat{\mathbf{k}}_1) Y_{L',M'}(\hat{\mathbf{r}}_1)$$

$$\langle \chi_2^{(-)}(\mathbf{k}_2, \mathbf{r}_2) | = \sqrt{\frac{2}{\pi}} \frac{1}{k_2 r_2} \sum_{L'',M''} i^{-L''} e^{i\sigma_{L''}} u_{L''}(k_2, r_2) Y_{L'',M''}^*(\hat{\mathbf{k}}_2) Y_{L'',M''}(\hat{\mathbf{r}}_2)$$

Modified spin-averaged static-exchange potential of Riley and Truhlar (1975)

$$V_E(\mathbf{r}) = \frac{1}{2} \left[E + V_D(\mathbf{r}) - \left\{ (E + V_D(\mathbf{r}))^2 - 2\pi\rho(\mathbf{r})^2 \right\}^{\frac{1}{2}} \right]$$

The distorting potentials

$$V_D(r) = \sum_{nl} N_{nl} \int dr' \left[u_{nl}(r') \right]^2 / r_>$$

where $r_>$ is the greater of r and r' and N_{nl} is the number of electrons in each orbital nl . where $\rho(r)$ is the electron density.

Ref.:- Riley M. E. and Truhlar D. G., “Approximations for the exchange potential in electrons scattering,” J. Chem. Phys. 63, 2182 (1975).

The TDCS expression including Post Collision Interaction (PCI)

$$\frac{d^3\sigma}{d\Omega_1 d\Omega_2 dE_1} = M_{ee} (2\pi)^4 \frac{k_1 k_2}{k_0} \sum_{m=-1}^1 \left(|f_{nlm}|^2 + |g_{nlm}|^2 - \text{Re}(f_{nlm}^* g_{nlm}) \right)$$

Correlation-polarization potential

N. T. Padial and D. W. Norcross, *Phys. Rev. A* 29, 1742 (1984).

J. P. Perdew and A. Zunger, *Phys. Rev. B* 23, 5048 (1981).

PCI

S. J. Ward and J. H. Macek, *Phys. Rev. A* 49, 1049 (1994).

Positron impact ionization

- For the positron impact ionization there is no exchange amplitude
- The distorted waves for the incident and scattered positrons are generated in the static potential of the atom (target).
- The distorted waves for the ejected electron is generated in the static exchange potential of the ion.

Total Ionization Cross Section (TICS)

Using partial wave expansion and performing angular integrations the total ionization cross section is given by

$$\sigma(E_i) = \frac{16}{\pi E_i} \int_0^E dE_e \sum_{l_i, l_e, l_f} (2L + 1) |F|^2$$

where l_i, l_f are electron orbital angular momentum quantum numbers in incident and final channels respectively, l_e is the ejected electron quantum number and L is the total orbital angular momentum. Energies obey the conservation defined F is the ionization amplitude, can be written as

$$F = \sum_{\lambda} f_{\lambda}(l_b l_i l_e l_f L) \langle \chi_b \chi_i | \mathbf{V} | \chi_e \chi_f \rangle_{\lambda}$$

Total Ionization Cross Section (TICS)

The total ionization cross sections have been calculated in two variants of distorted wave approximation (DWA) namely Cowan structure calculation and HULLAC code.

The Hartree-Fock target wave function and Hartree potential with semi-classical exchange and correlation correction has been used for the semi relativistic DWA calculations with Cowan formalism.

Ionization cross sections using Cowan formalism have been calculated in fine-structure and configuration mode.

We have also used Modified Khare and modified Kim BEB Methods to calculate the TICS

Ref.:

R. D. Cowan, The Theory of Atomic Structure and Spectra (Univ. of Cali. Press, Berkeley, 1981).

A. Bar-Shalom, M. Klapisch, and J. Oreg, J. Quant. Spec. Radiat. Transf. 71, 169 (2001).

M. E. Riley and D. G. Truhlar, J. Chem. Phys. 63, 2182 (1975).

Why W

*W - the tungsten (W) and tungsten based materials have been recommended as one of the materials to be used as plasma facing components for the International Thermonuclear Experimental Reactor (ITER) [1] and the Demonstration Power Station (DEMO) as these materials have thermo-physical properties suitable for fusion application [2-4].

[1] G. Federici, Phys. Scr. T124, 1 (2006).

[2] S. Wurster et al., J. Nucl. Mater. 442, S181 (2013).

[3] J. de Prado et al., Mater. Des. 112, 117 (2016).

[4] J. W. Coenen et al., Phys. Scr. T167, 014002 (2016).

Why W

- * Tungsten is already in use as plasma facing components in tokamaks such as JET [5] and ASDEX-Upgrade [6].
- * In the fusion devices the tungsten and related materials may exhibit high melting temperature, strong resistance against sputtering and shorter penetration depth etc.

[5] M. Groth et al., Nucl. Fusion **53**, 093016 (2013).

[6] M. Mayer et al., Phys. Scr. **128**, 106 (2007).

Why Be

- * Be - recommended as surface materials in ITER project
- * Erosion of the Be walls will occur when it is in contact with the hot plasma containing hydrogen and its isotopes [7, 8].
- * This leads to the formation of gas-phase Be in various charge states and of Be hydrides, i.e. BeH₂. The presence of these species in the fusion edge and divertor plasmas influences them due to electron collision processes
- * There is not much cross section information available concerning Be and its hydrides up to now.

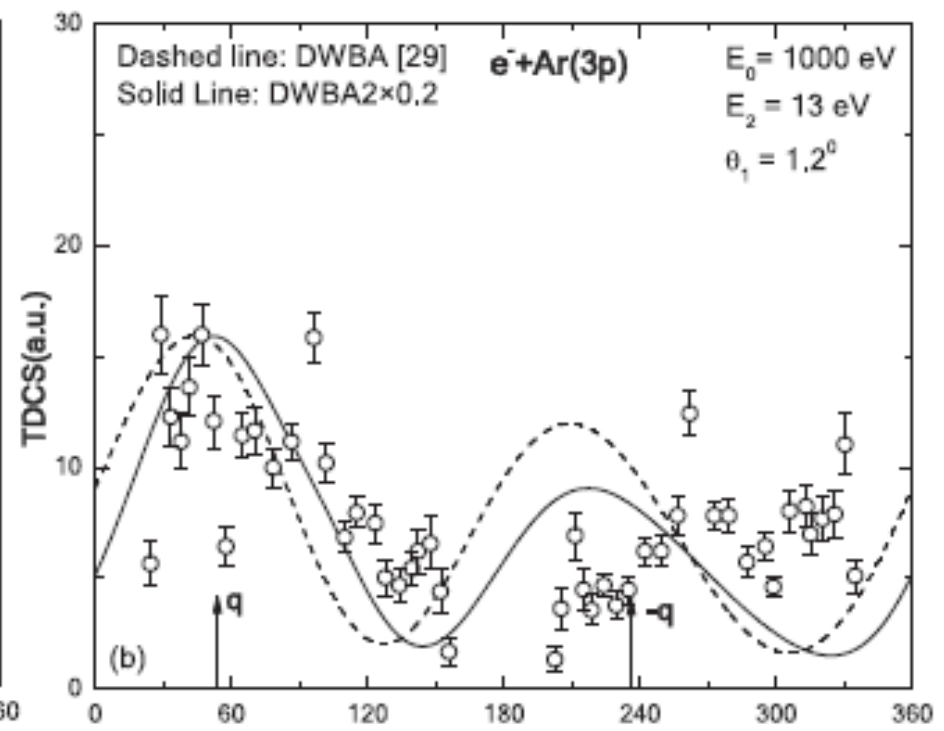
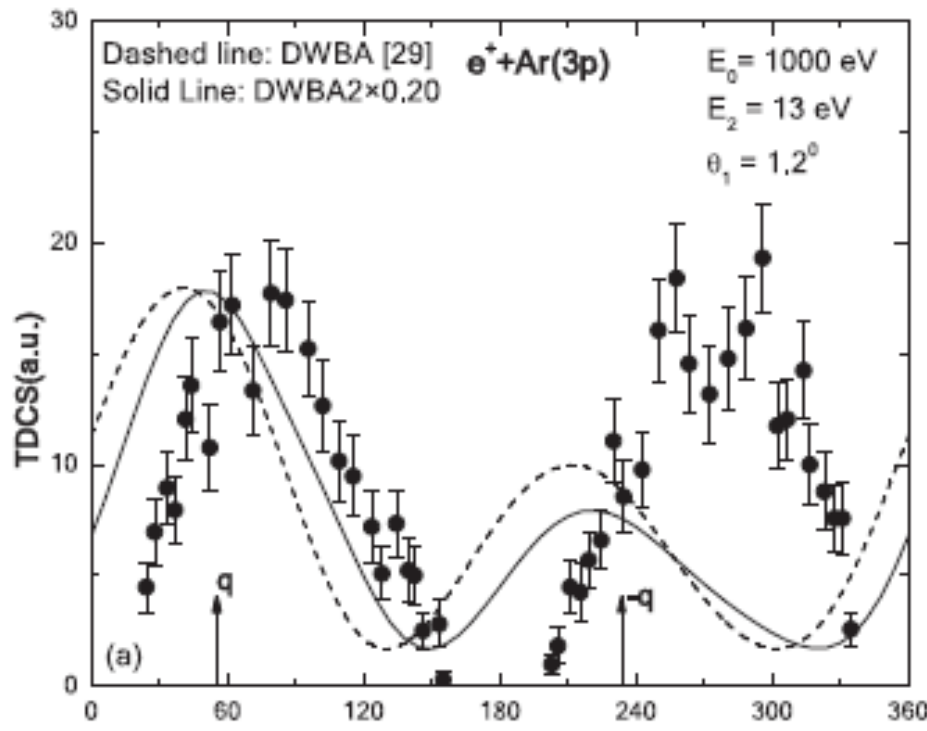
[7] R. Doerner, M.J. Baldwin, D. Buchenauer, G. De Temmerman, D. Nishijima, J. Nucl. Mater. **390**, 681 (2009)

[8] C. Bjorkas, K. Vortler, K. Nordlund, D. Nishijima, R. Doerner, New J. Phys. **11**, 123017 (2009)

W and Be

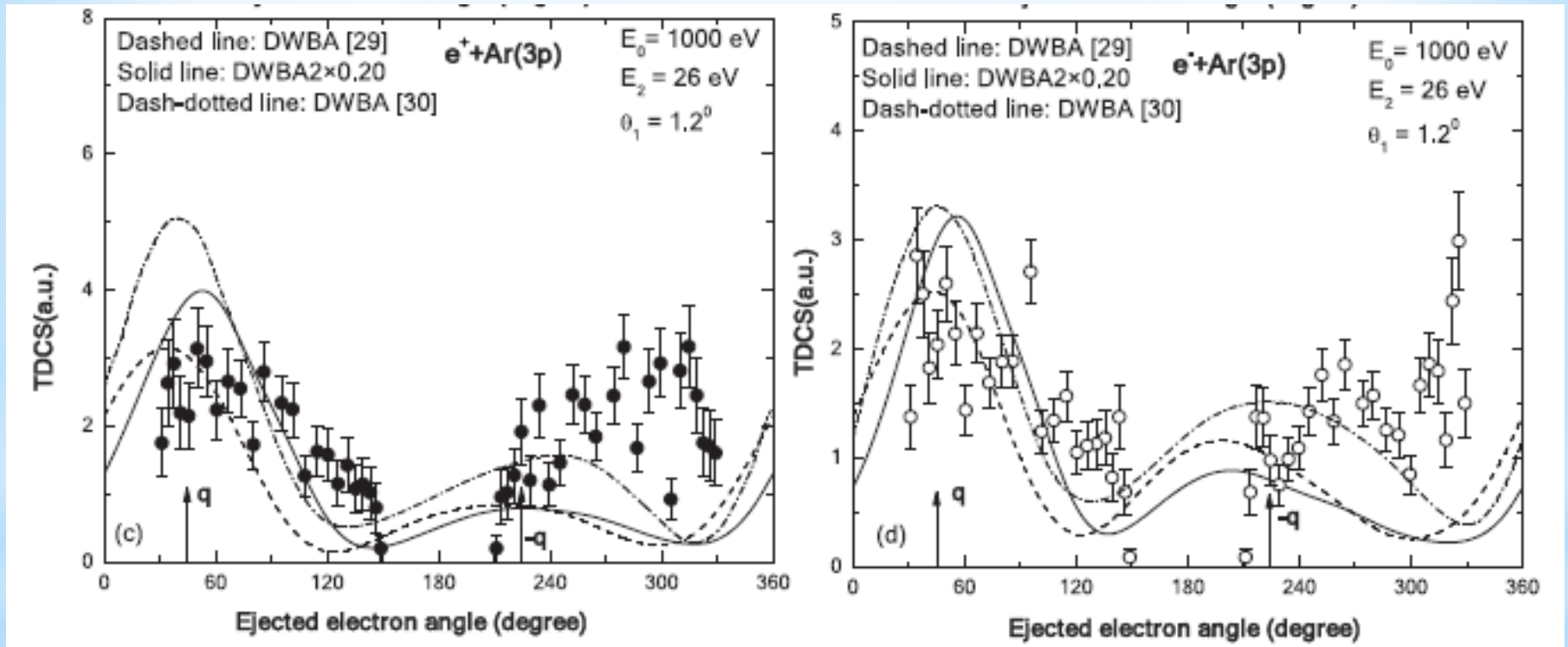
- * Electron induced processes such as excitation and ionization are prevalent in such magnetic fusion devices in a wide range of energies with significant variation of temperature and density.
- * A reliable data base is required for the electron impact ionization and excitation cross sections for W and Be atoms and their charged states to model the electron induced interactions and understand the spectroscopy involved.

Results – Coplanar ionization of Ar (3p) atoms

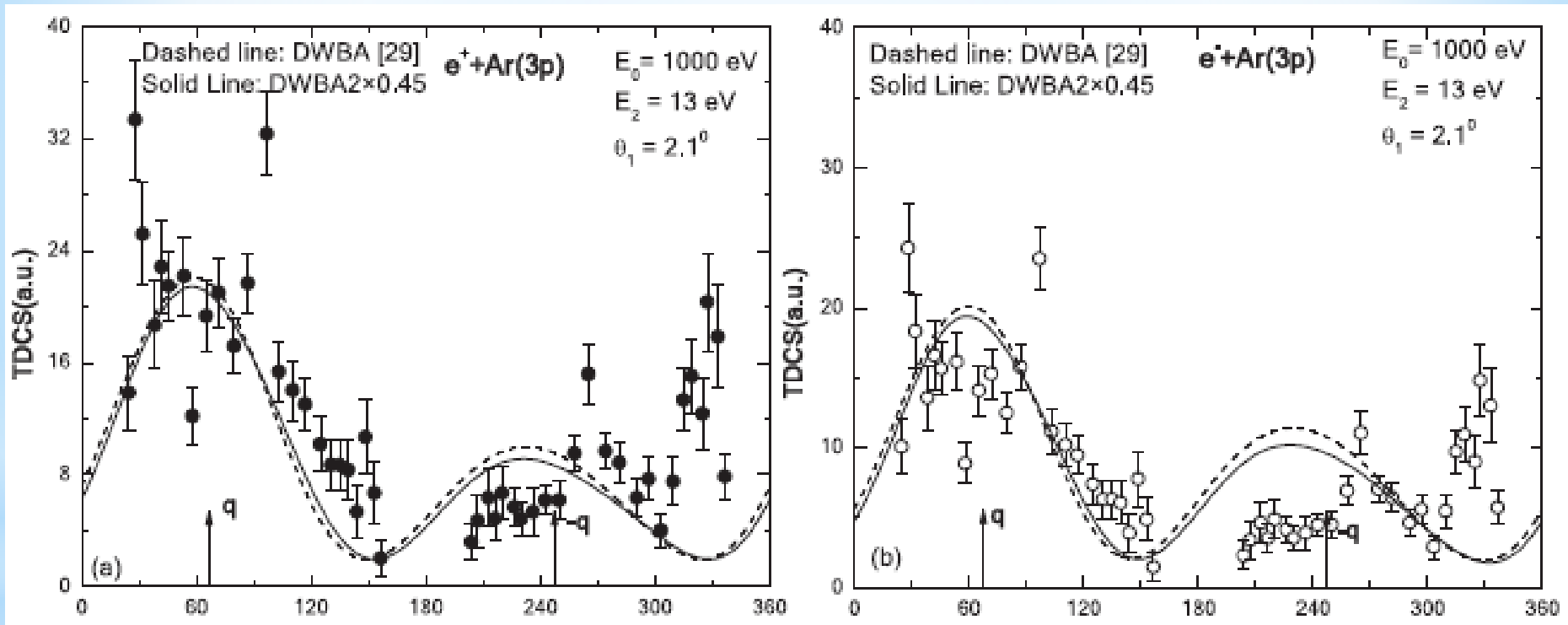


G. Purohit Nuclear Inst. and Methods in Physics Research, B 487 (2021) 52-60

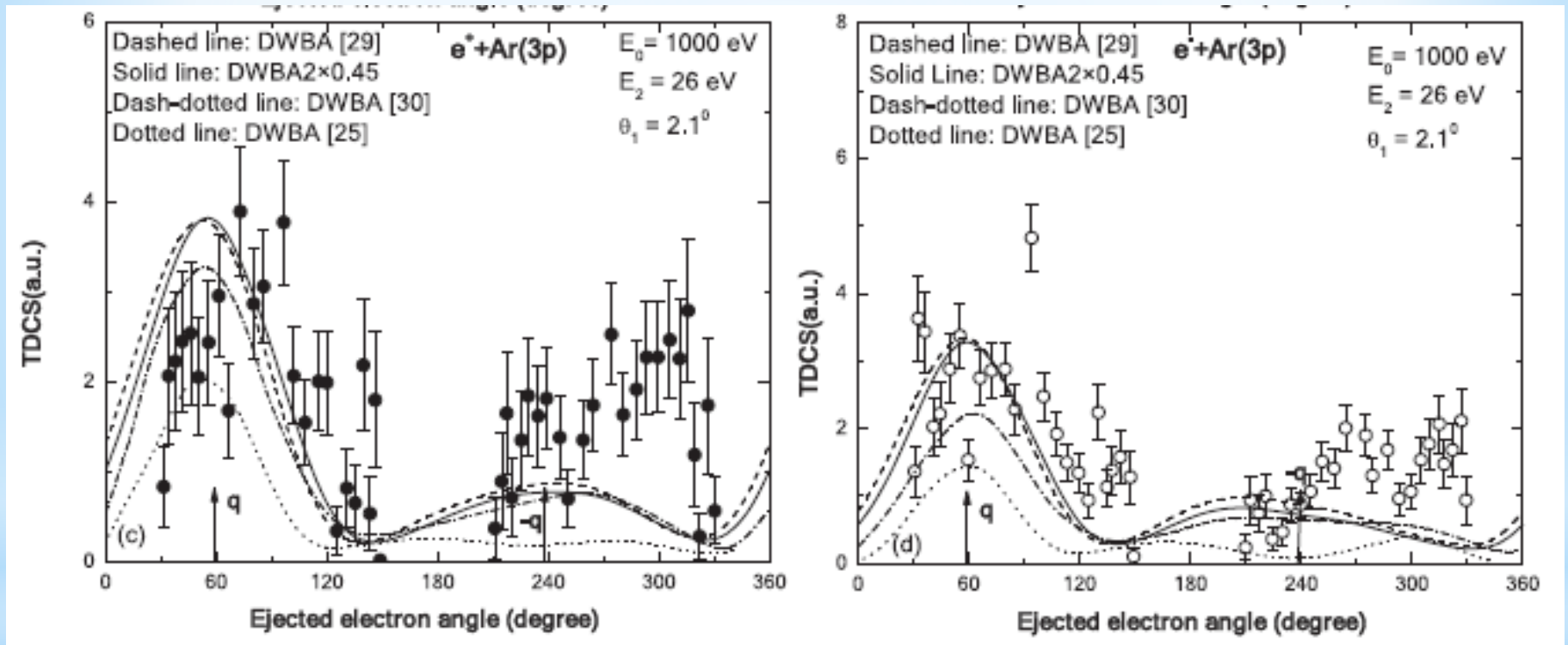
Results – Coplanar ionization of Ar (3p) atoms



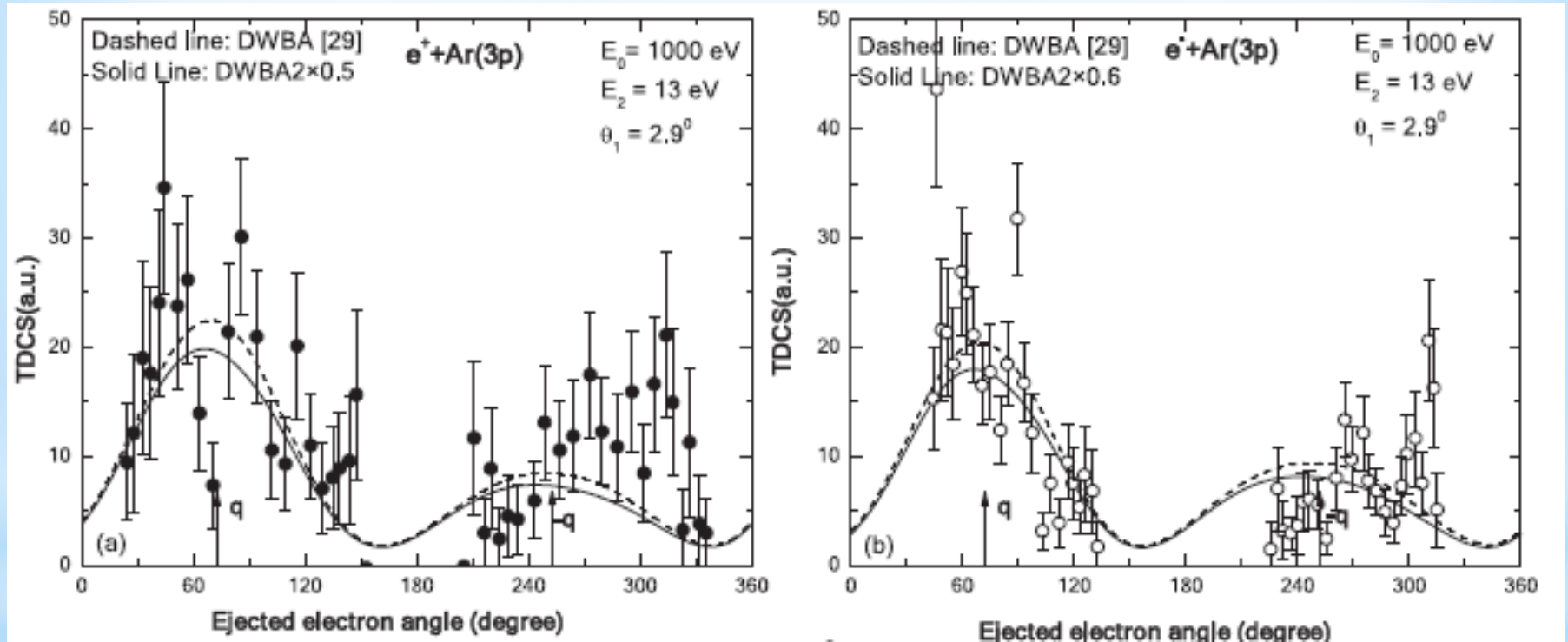
Results – Coplanar ionization of Ar (3p) atoms



Results – Coplanar ionization of Ar (3p) atoms



Results – Coplanar ionization of Ar (3p) atoms



Results – Coplanar ionization of Ar (3p) atoms

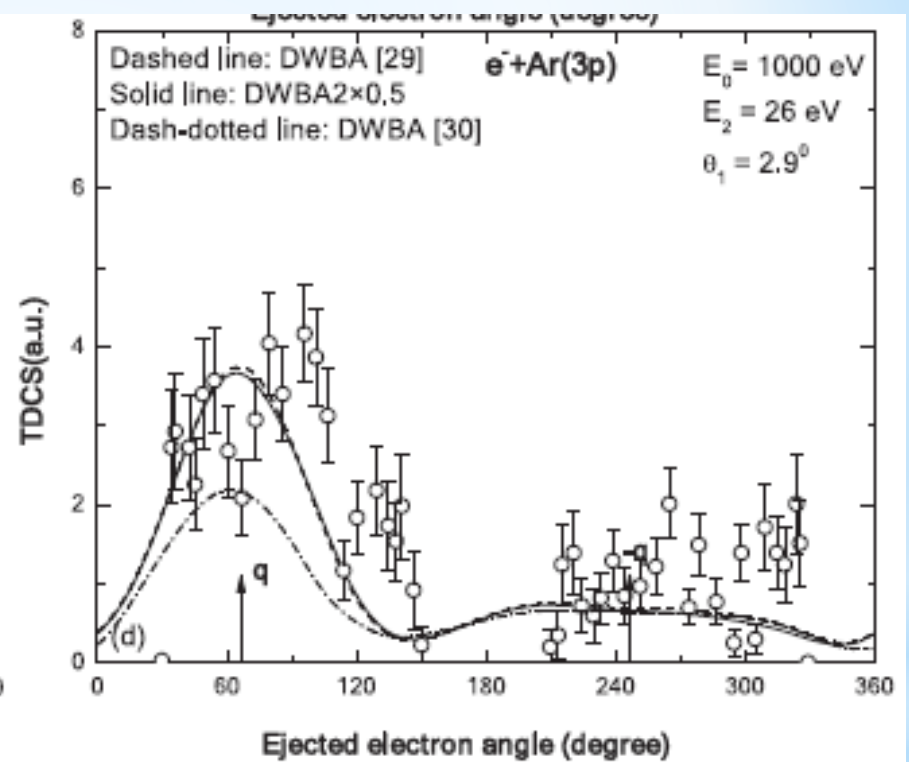
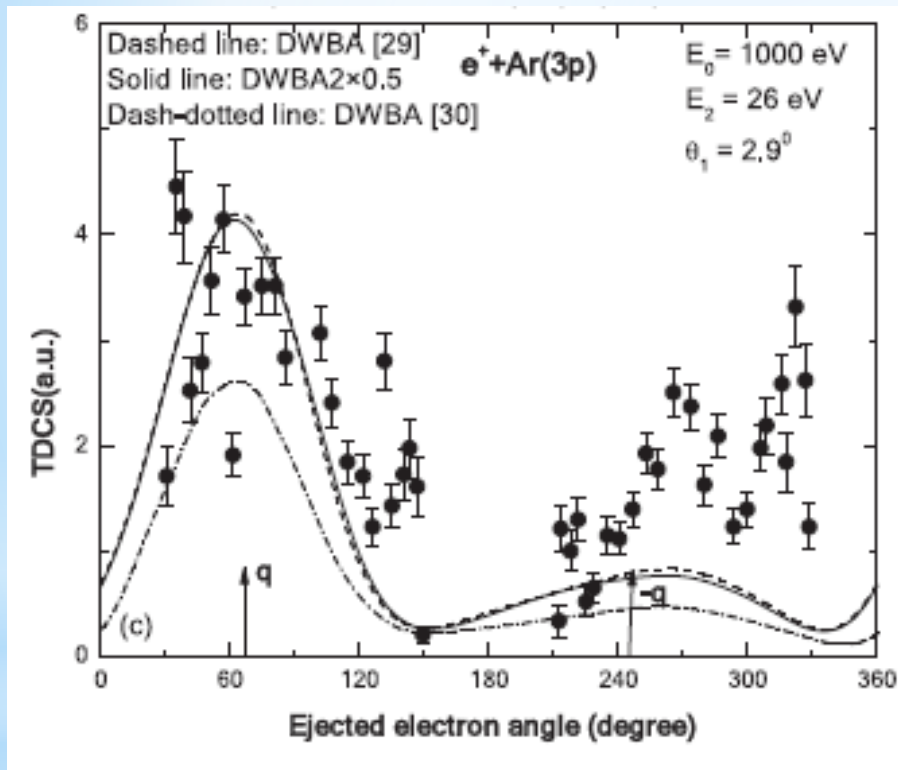
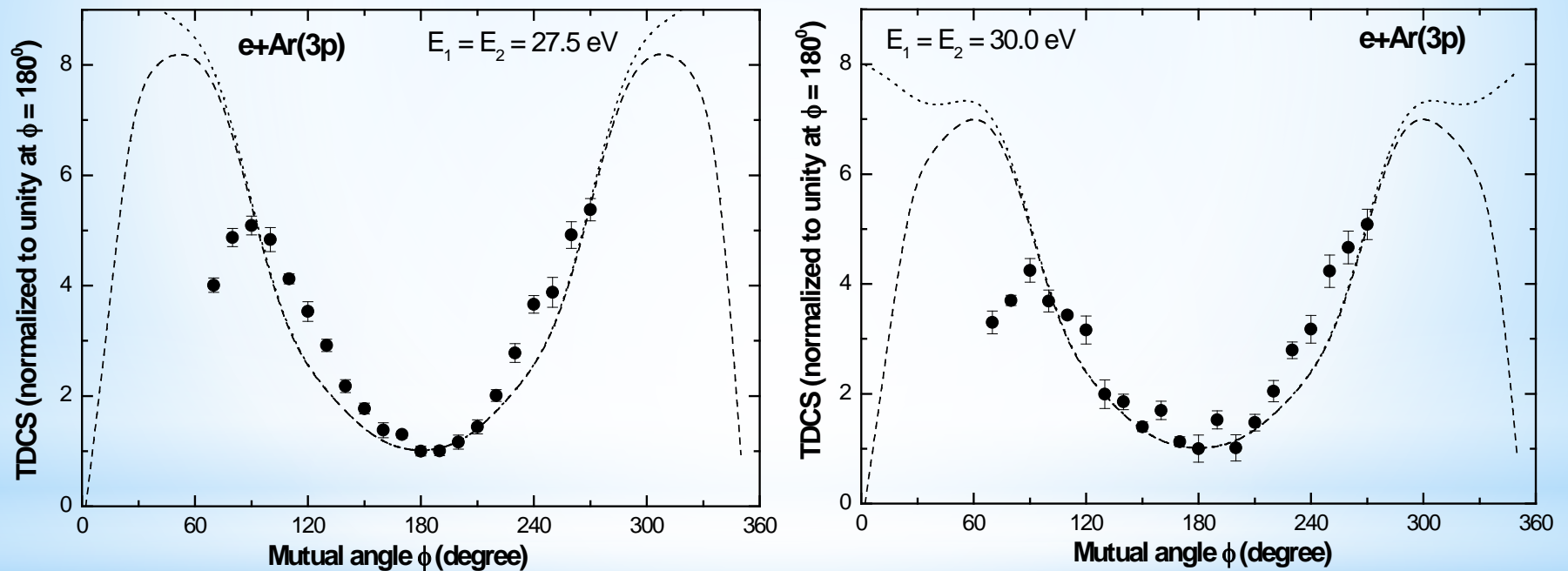


Table 1

Momentum transfer values and directions for the single ionization of Ar (3p) at 1 keV projectile energy.

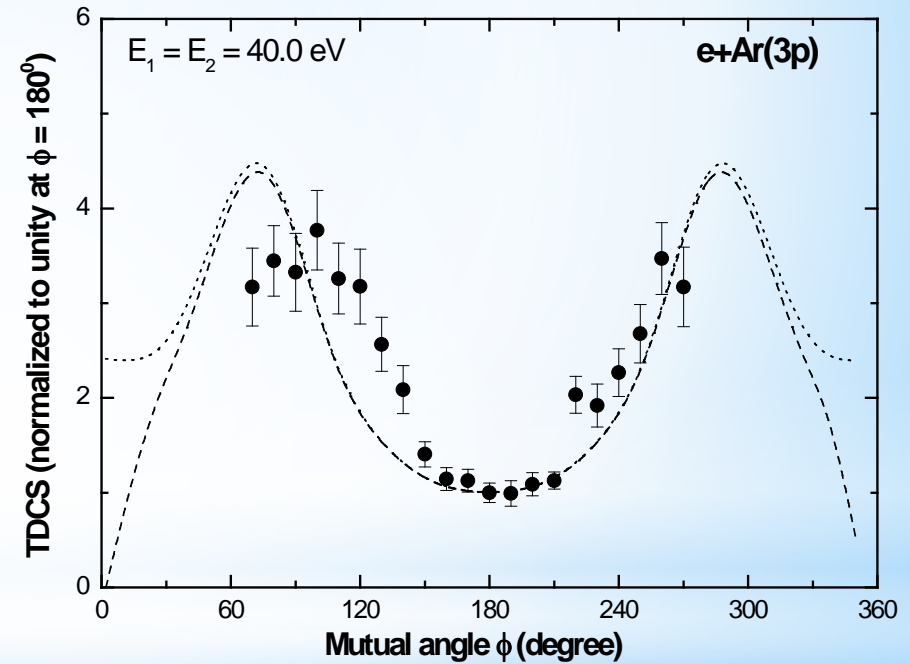
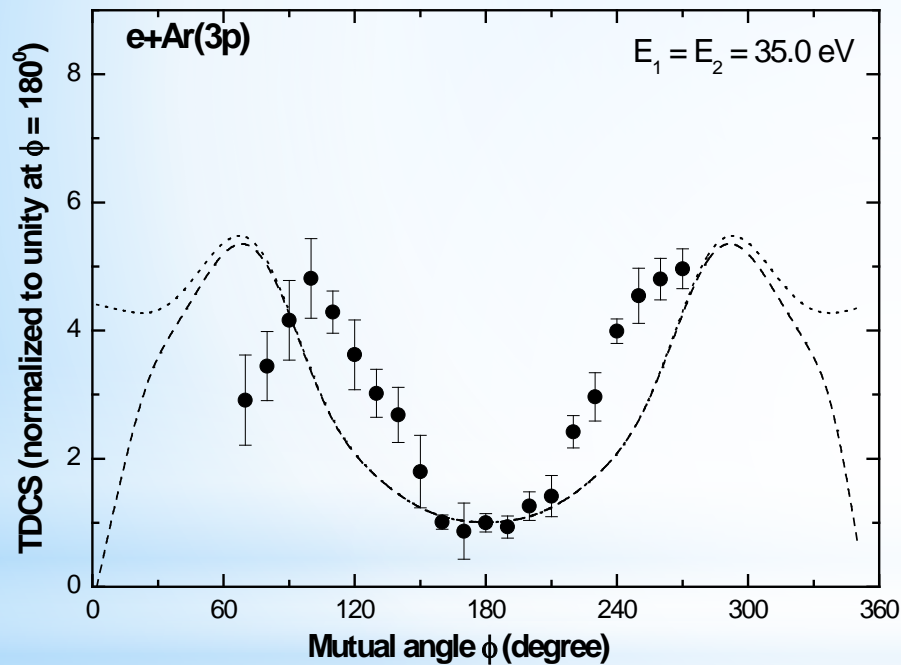
| Projectile | Ejected electron energy E_2 | Scattering angle θ_1 | Value of momentum transfer (q) (a.u.) | Expected Direction of momentum transfer (q), i.e. binary peak | Binary peak direction in DWBA | Binary peak direction in DWBA2 | Binary peak direction in measurements |
|------------|-------------------------------|-----------------------------|---------------------------------------|---|-------------------------------|--------------------------------|---------------------------------------|
| Electron | 13 eV | 1.2° | 0.22 | 54.5° | 44° | 53° | 52° |
| | | 2.1° | 0.34 | 67.2° | 61° | 59° | 54° |
| | | 2.9° | 0.45 | 72.5° | 69° | 67° | 64° |
| | 26 eV | 1.2° | 0.25 | 43.8° | 44° | 56° | 56° |
| | | 2.1° | 0.36 | 58.7° | 58° | 59° | 56° |
| | | 2.9° | 0.46 | 65.7° | 66° | 65° | 55° |
| Positron | 13 eV | 1.2° | 0.22 | 54.5° | 41° | 51° | 62° |
| | | 2.1° | 0.34 | 67.2° | 59° | 58° | 53° |
| | | 2.9° | 0.45 | 72.5° | 69° | 66° | 57° |
| | 26 eV | 1.2° | 0.25 | 43.8° | 34° | 53° | 54° |
| | | 2.1° | 0.36 | 58.7° | 52° | 56° | 61° |
| | | 2.9° | 0.46 | 65.7° | 64° | 62° | 56° |

Results – Perpendicular Plane ionization of Ar (3p) atoms

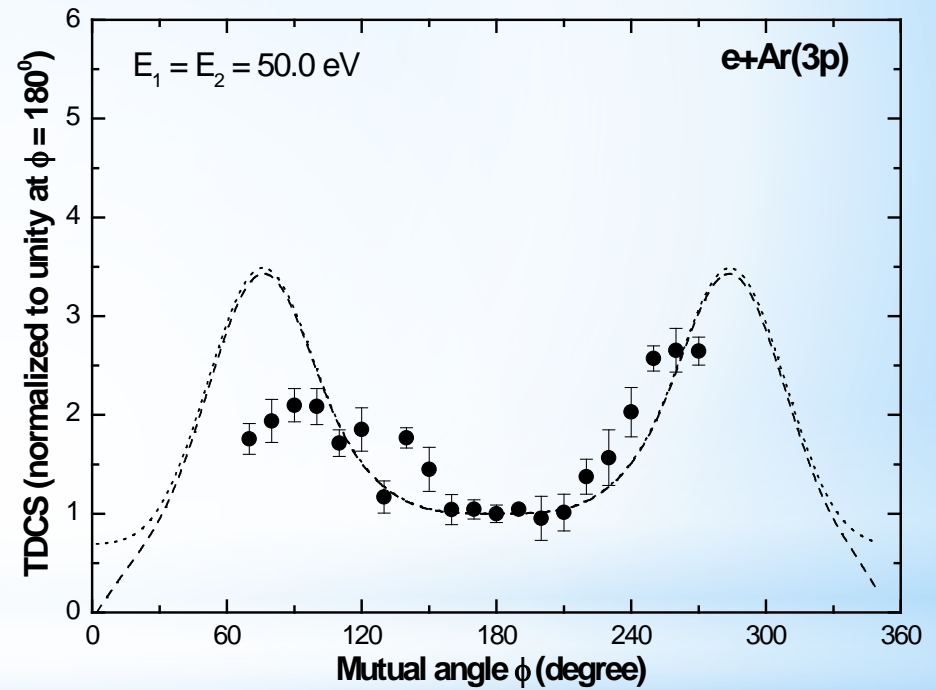
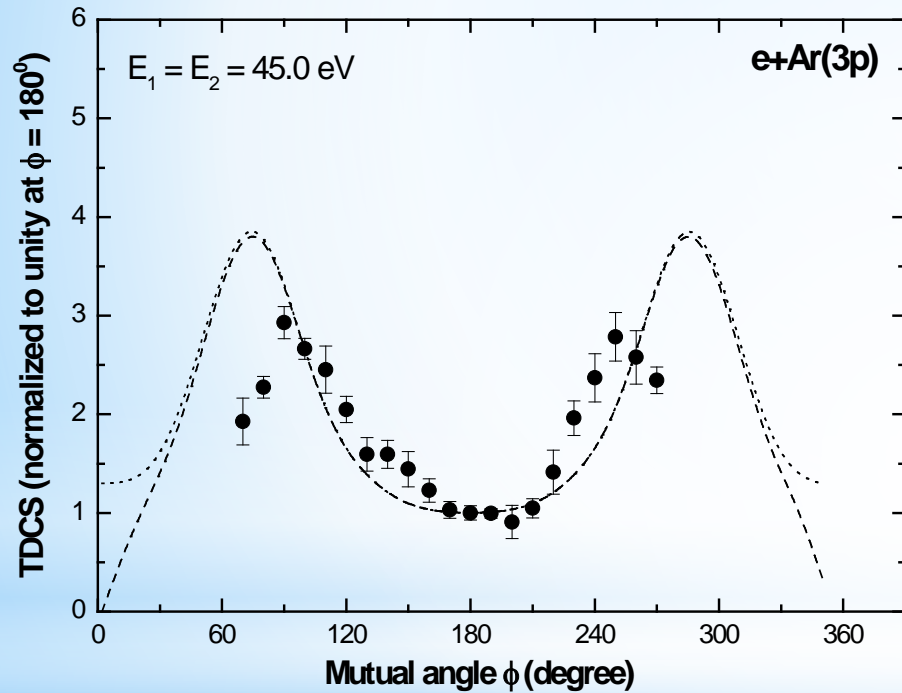


Experimental Data: Patel and Murray *Phys. Rev. A* 105, 042815 (2022)

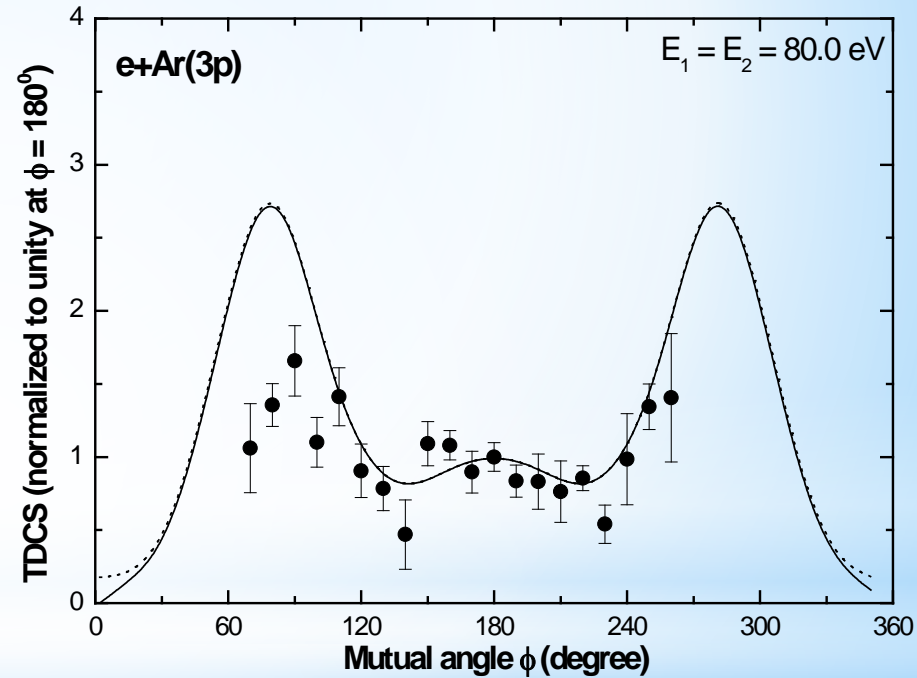
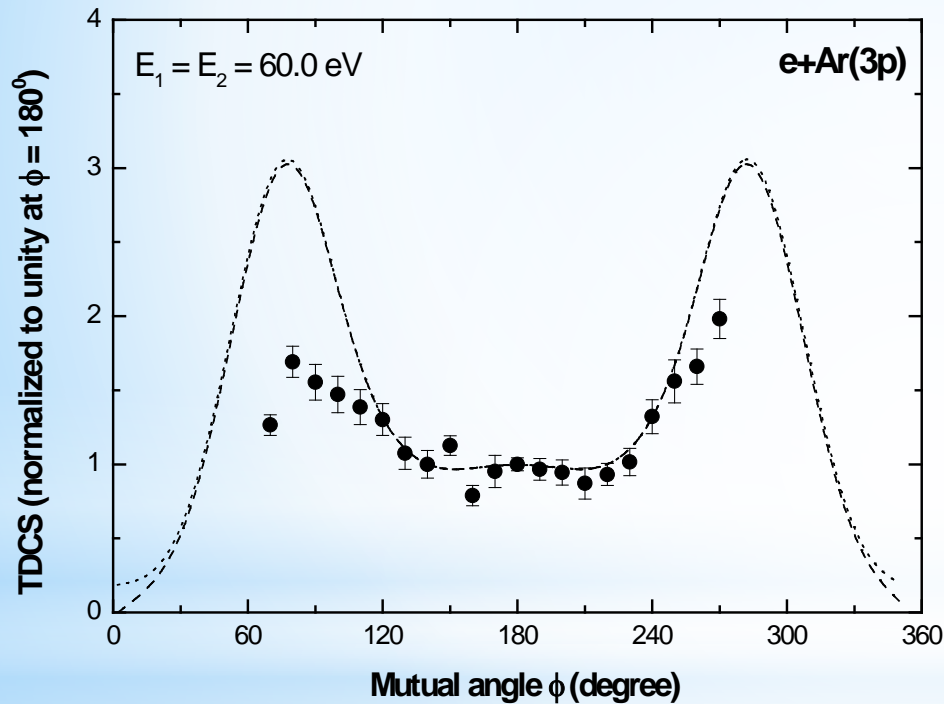
Results – Perpendicular Plane ionization of Ar (3p) atoms



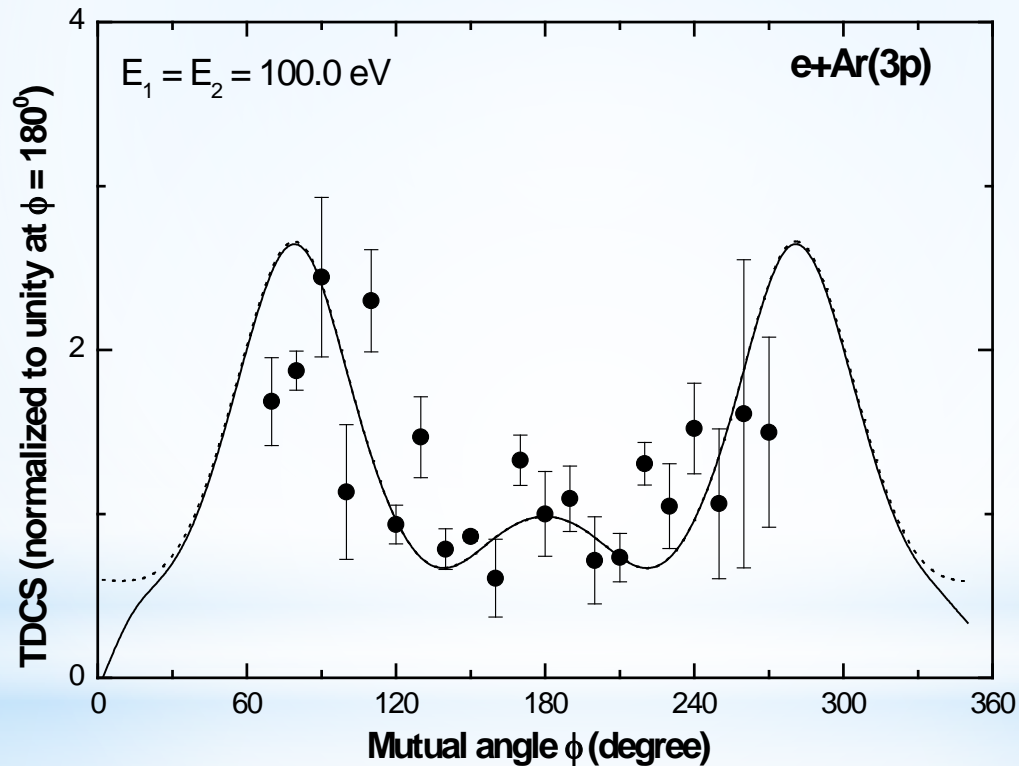
Results – Perpendicular Plane ionization of Ar (3p) atoms



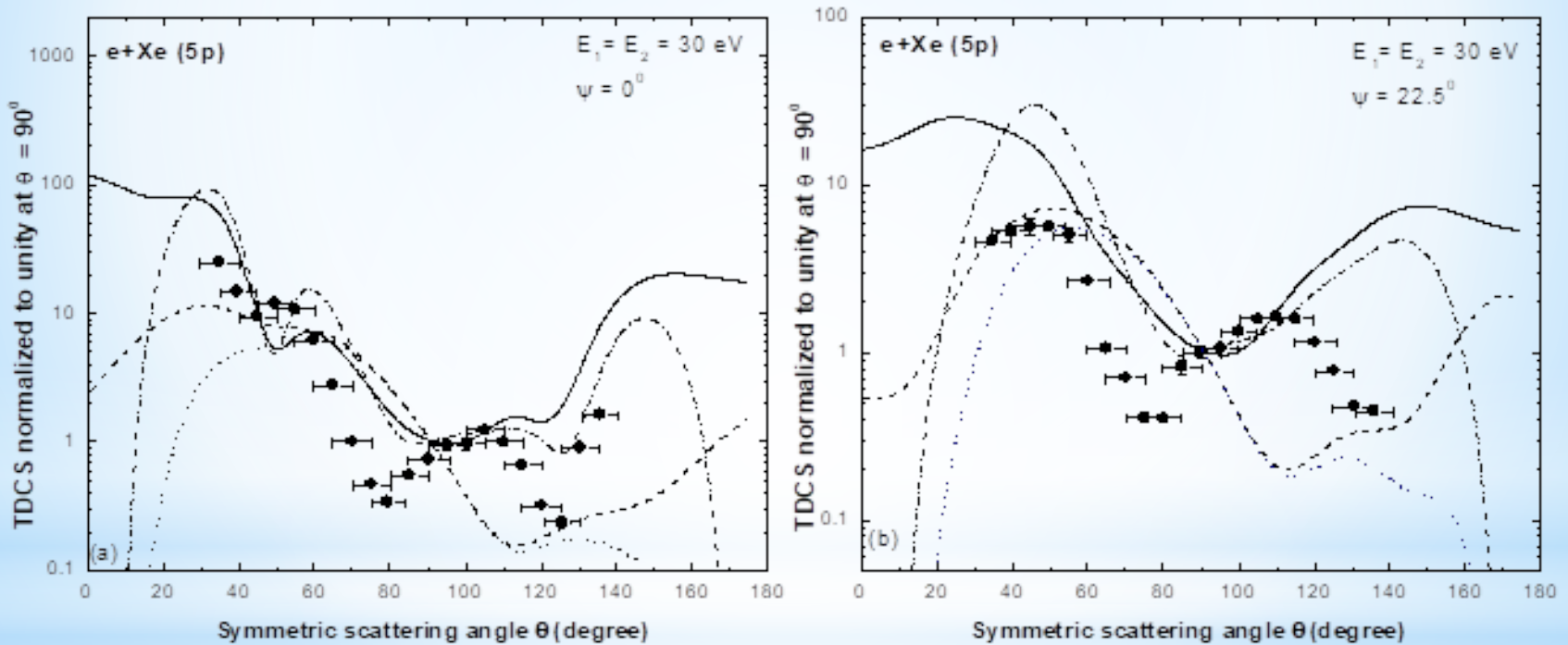
Results – Perpendicular Plane ionization of Ar (3p) atoms



Results – Perpendicular Plane ionization of Ar (3p) atoms

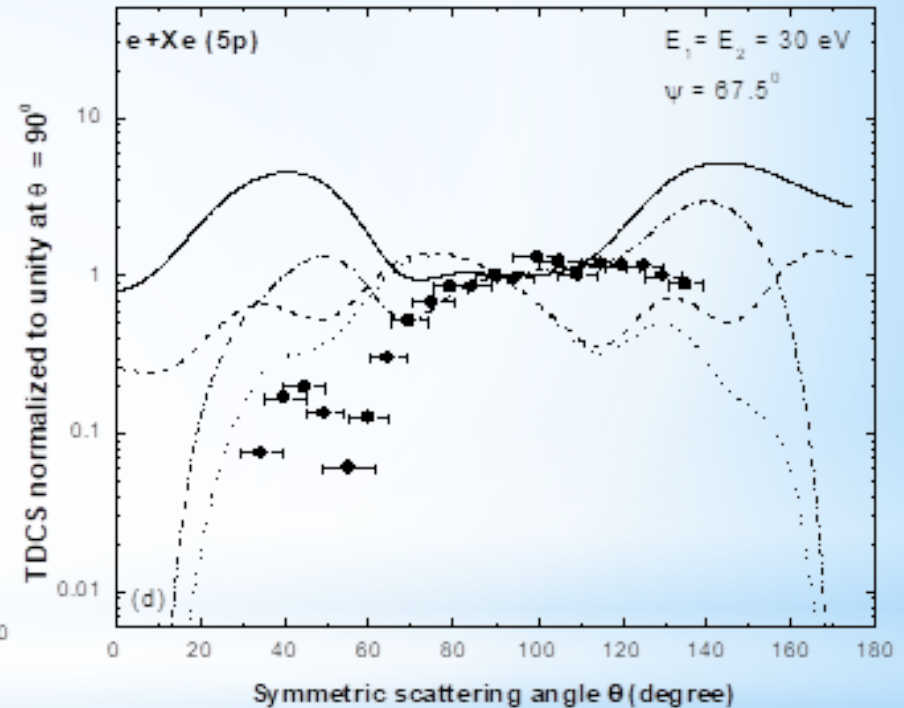
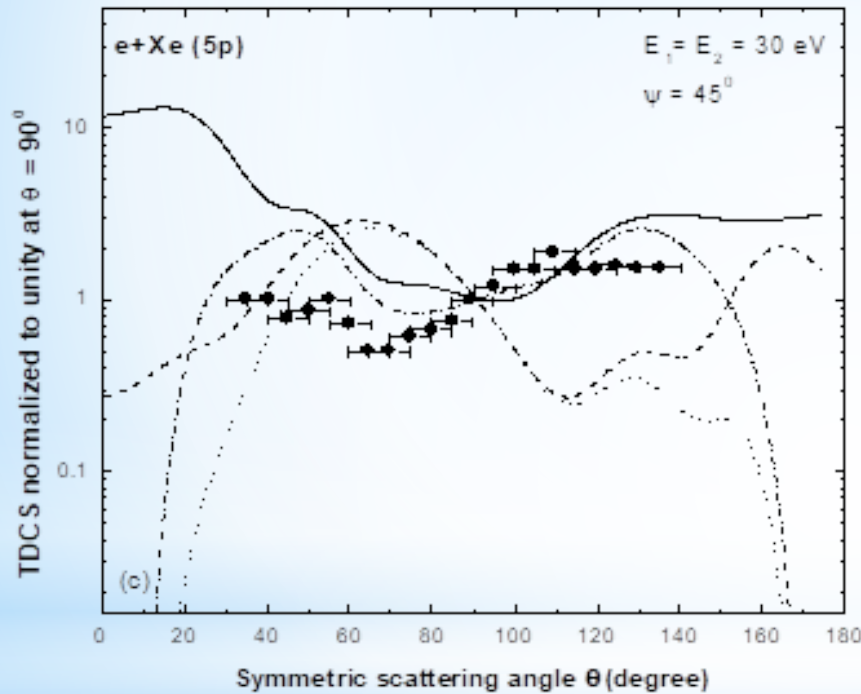


Results – Coplanar to Perpendicular Plane ionization of Xe (5p) at 60 eV above IP



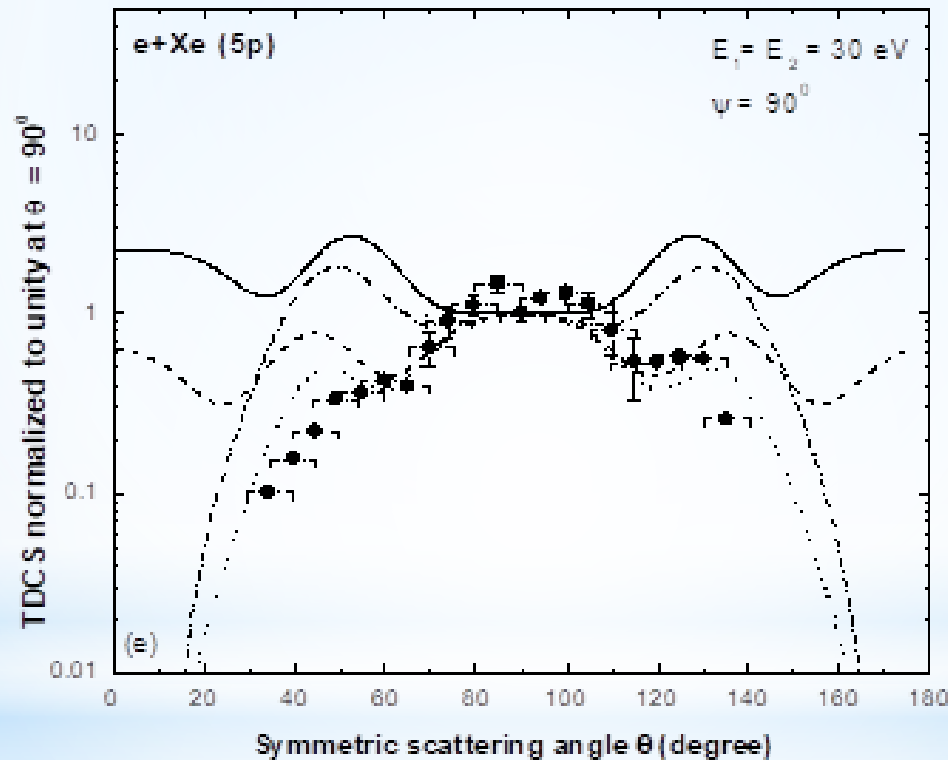
Experimental Data: Patel and Murray *Phy. Rev. A* 105, 032818 (2022)

Results – Coplanar to Perpendicular Plane ionization of Xe (5p) at 60 eV above IP



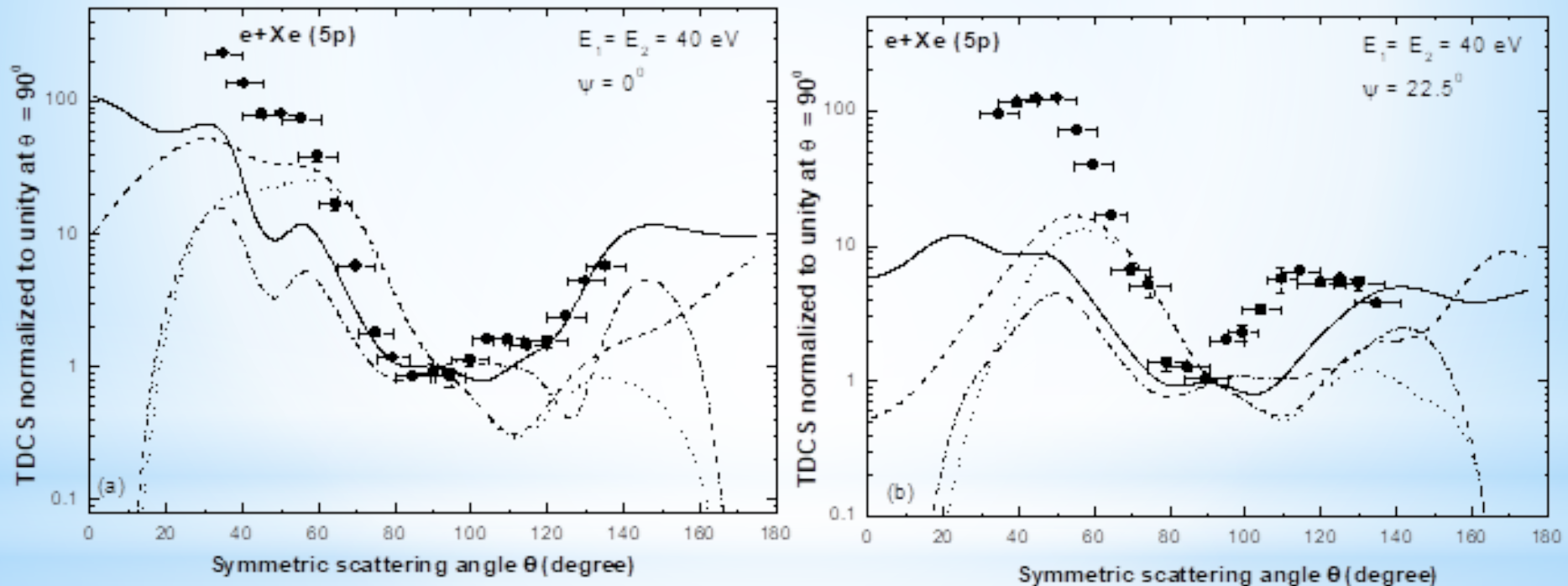
Experimental Data: Patel and Murray *Phy. Rev. A* 105, 032818 (2022)

Results – Coplanar to Perpendicular Plane ionization of Xe (5p) at 60 eV above IP

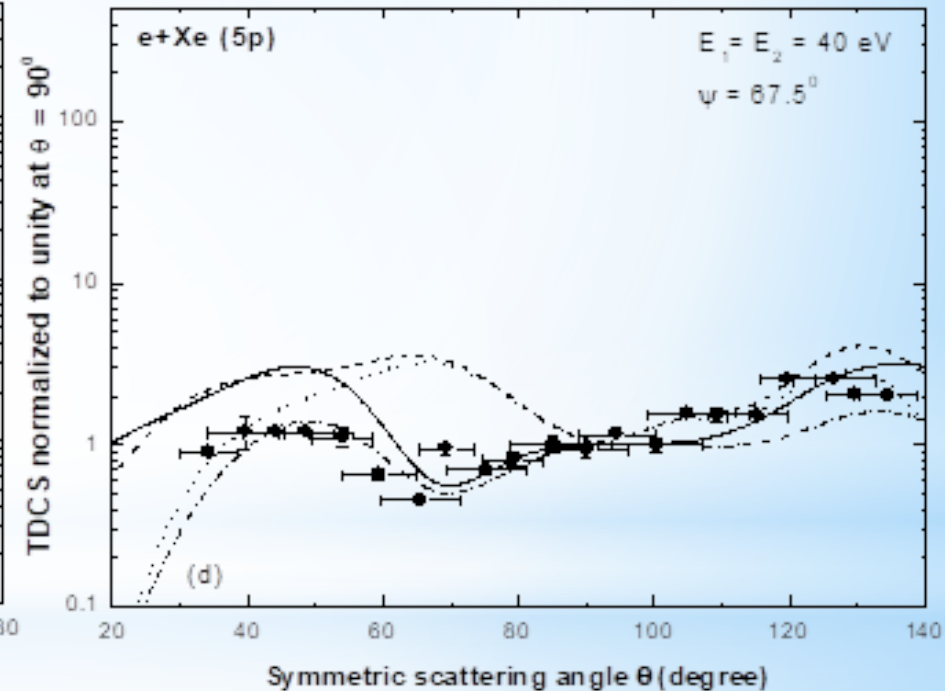
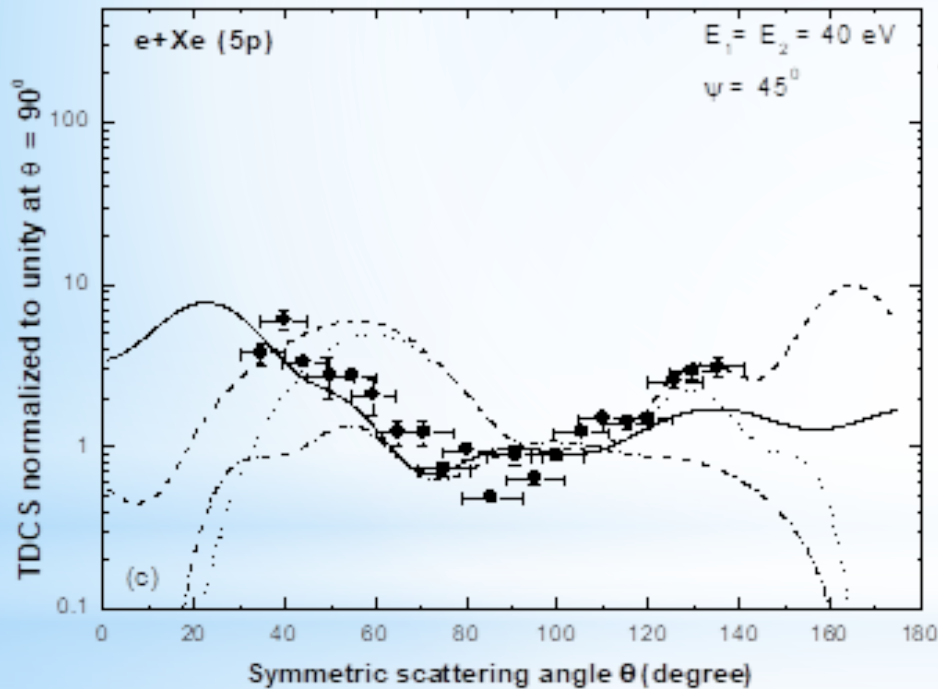


Experimental Data: Patel and Murray *Phys. Rev. A* 105, 032818 (2022)

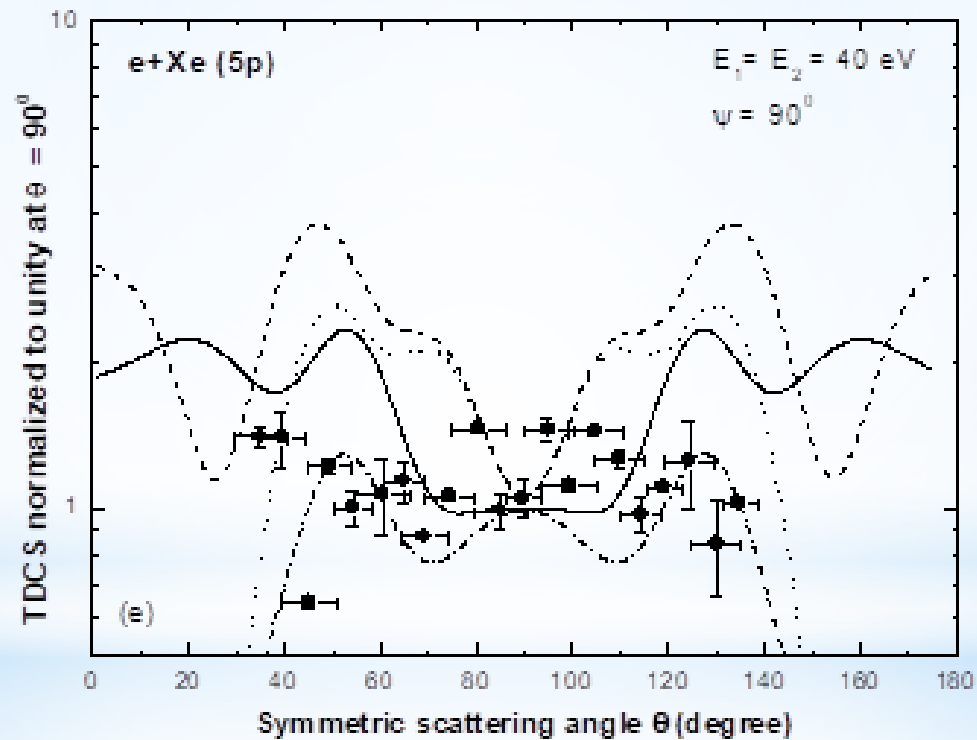
Results – Coplanar to Perpendicular Plane ionization of Xe (5p) at 80 eV above IP



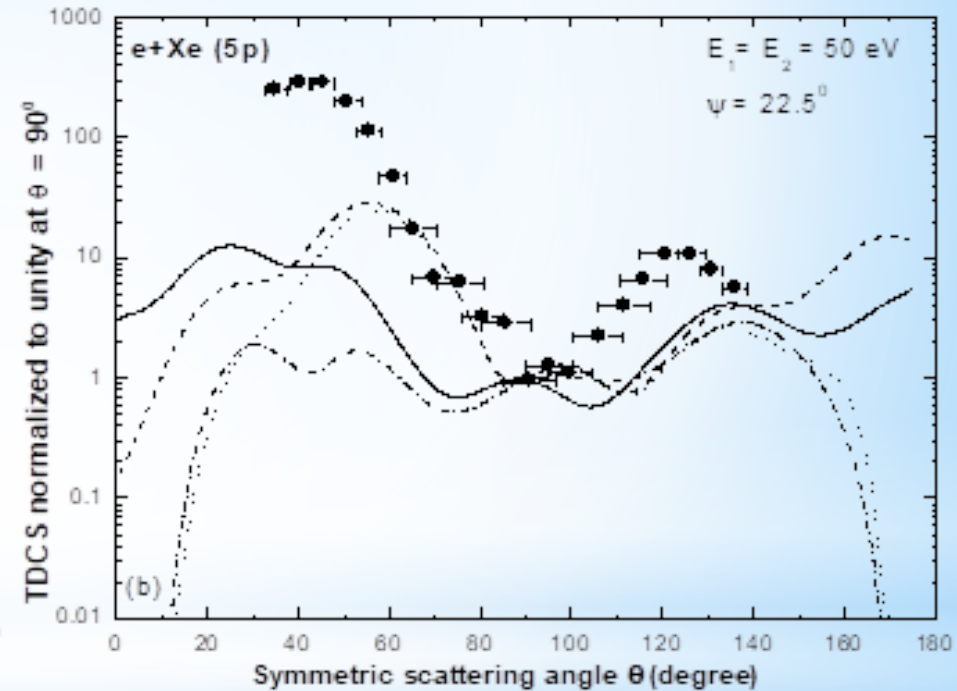
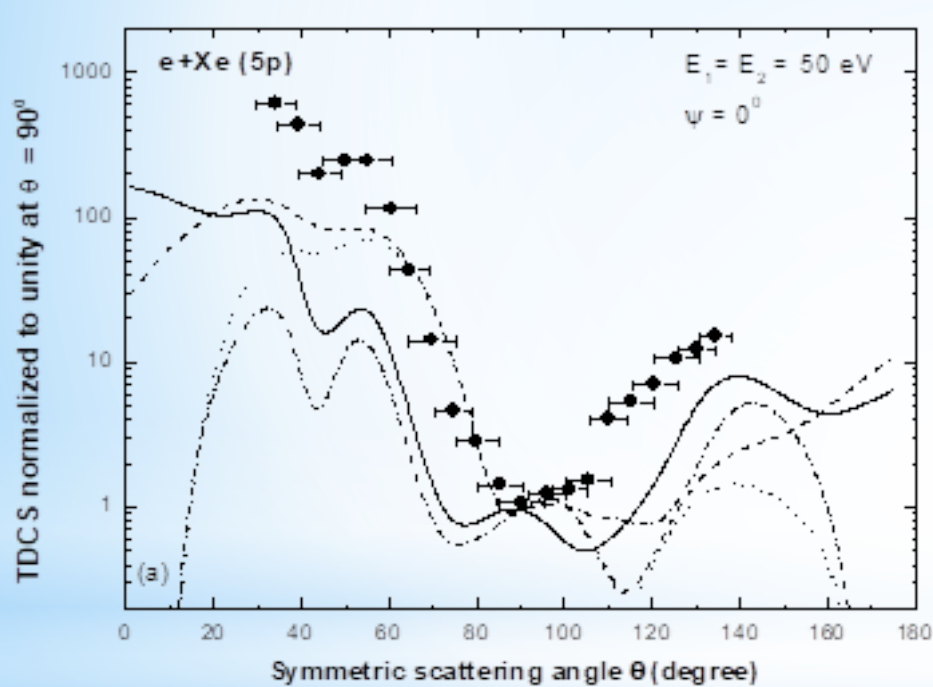
Results – Coplanar to Perpendicular Plane ionization of Xe (5p) at 80 eV above IP



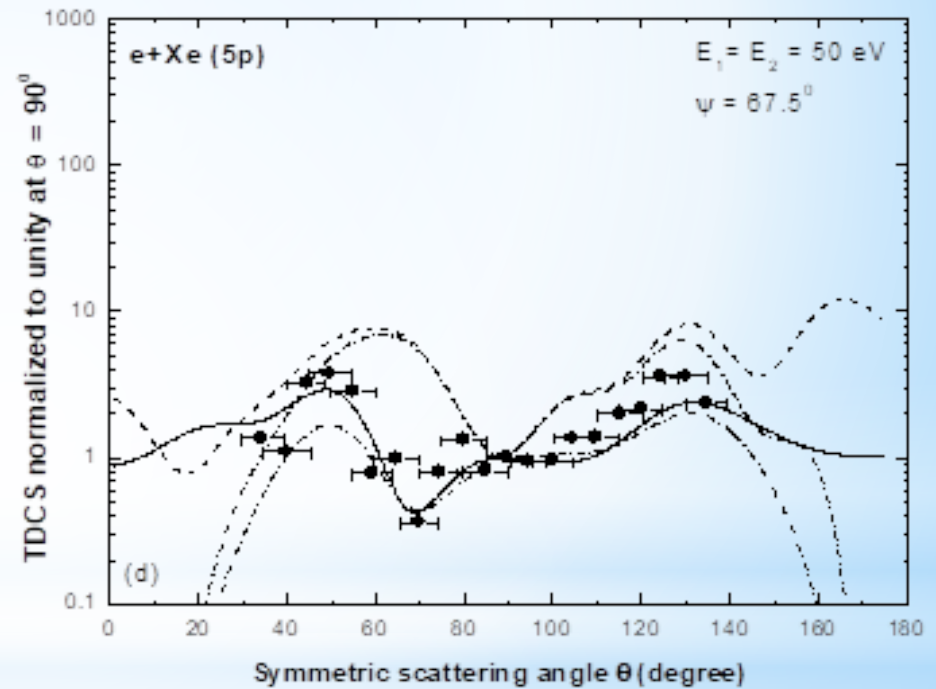
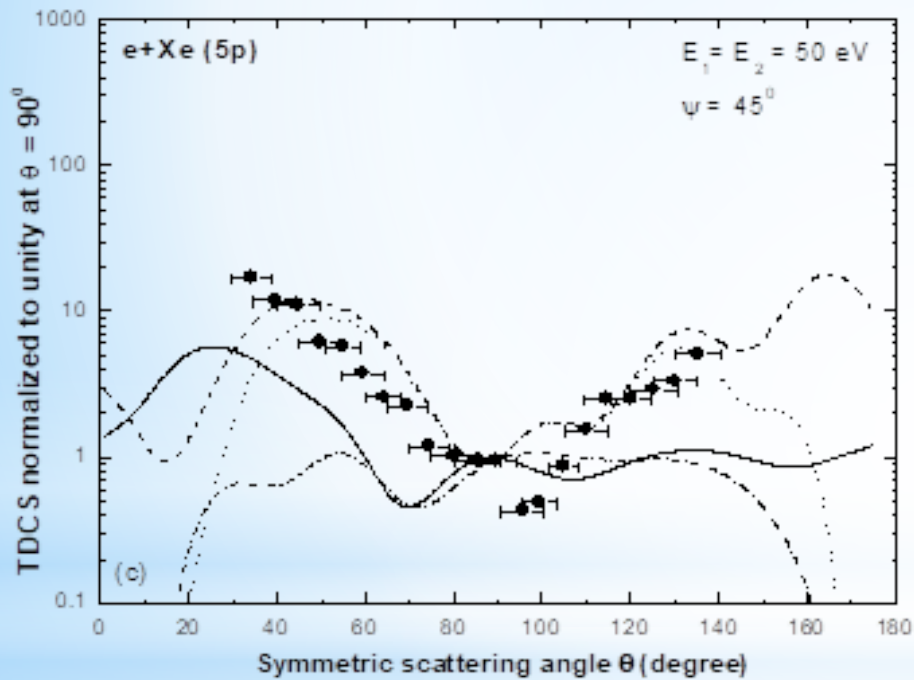
Results – Coplanar to Perpendicular Plane ionization of Xe (5p) at 80 eV above IP



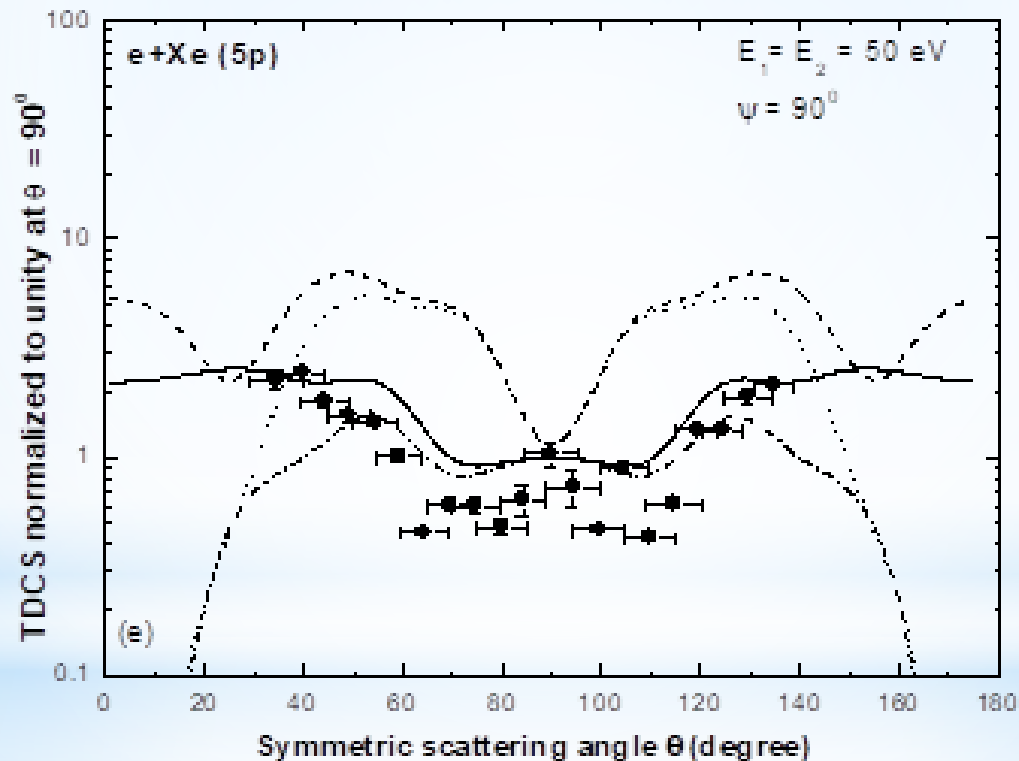
Results – Coplanar to Perpendicular Plane ionization of Xe (5p) at 100 eV above IP



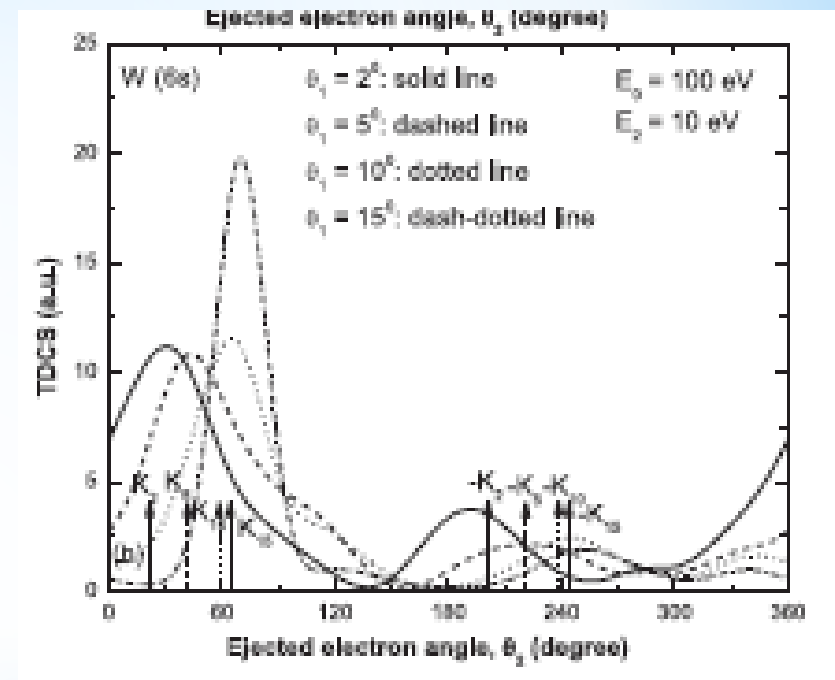
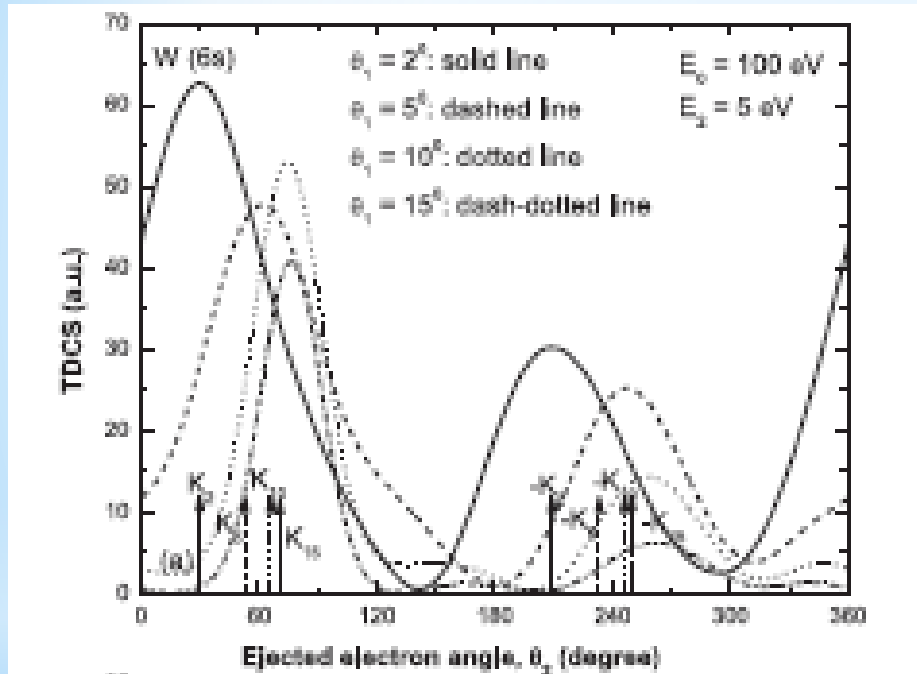
Results – Coplanar to Perpendicular Plane ionization of Xe (5p) at 100 eV above IP



Results – Coplanar to Perpendicular Plane ionization of Xe (5p) at 100 eV above IP

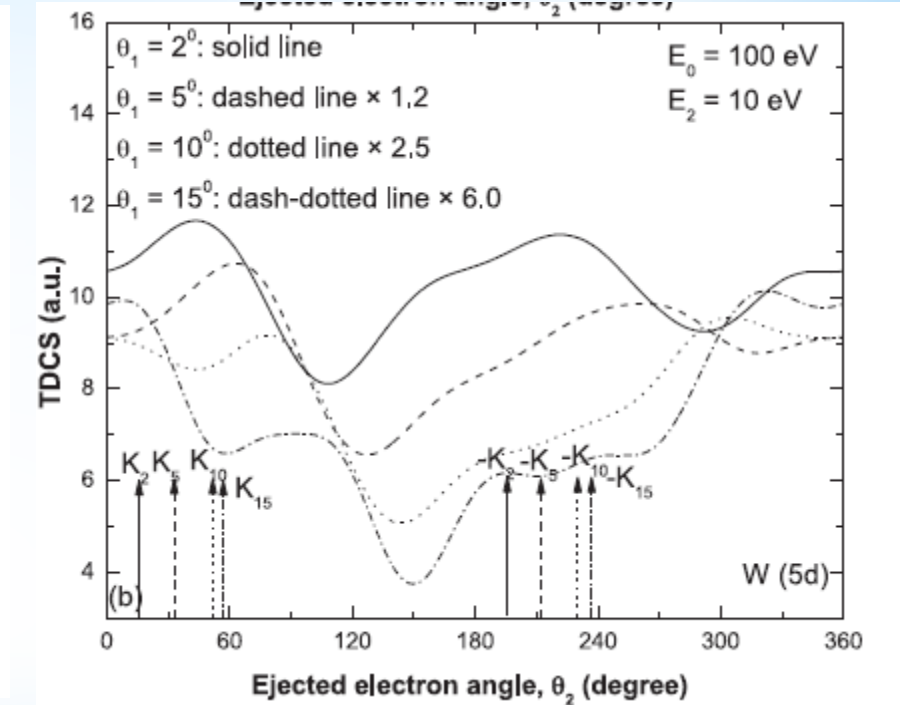
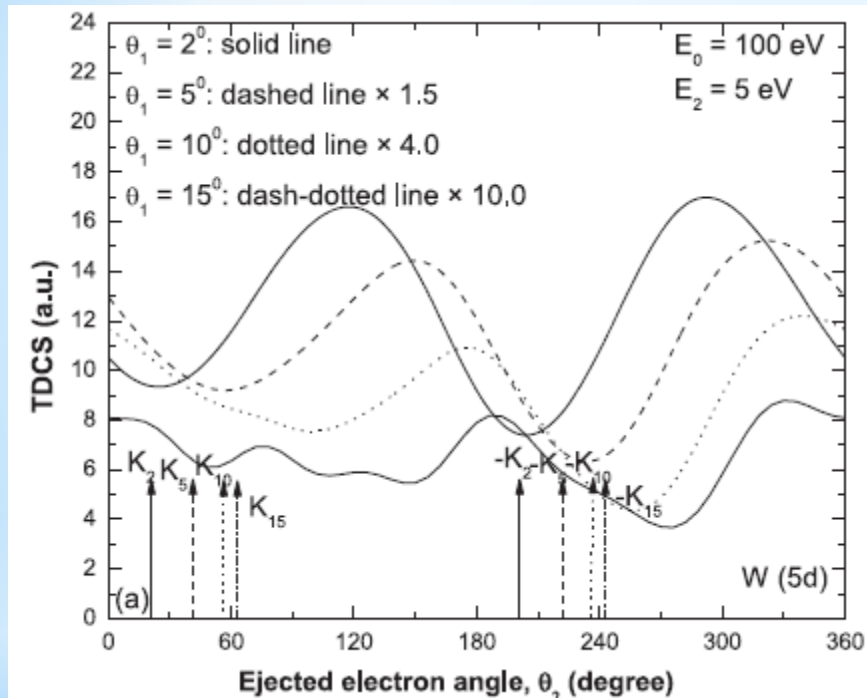


Results – Coplanar Asymmetric Ionization of W (6s) atoms



G Purohit
Journal of Physics B: Atomic, Molecular and
Optical Physics 54 (6), 065203 (2021)

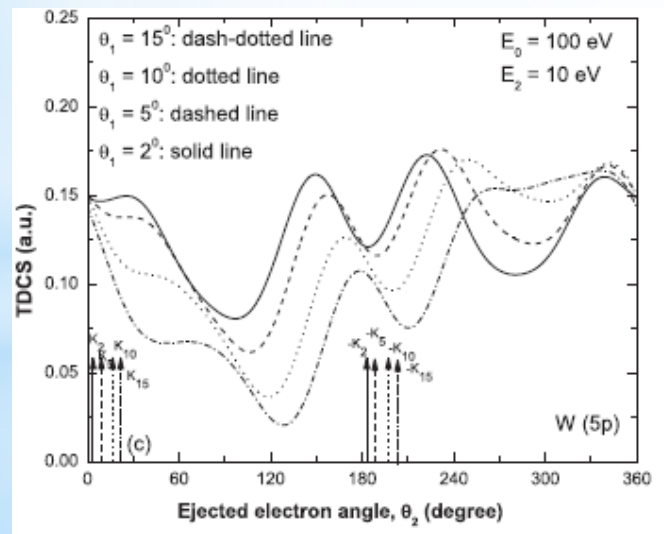
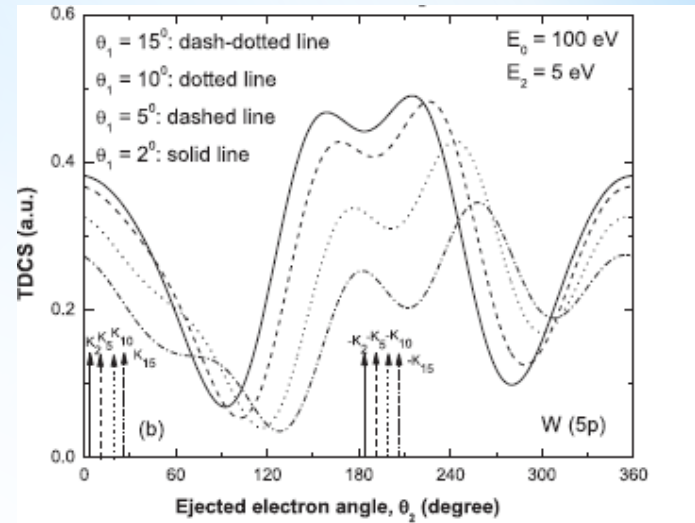
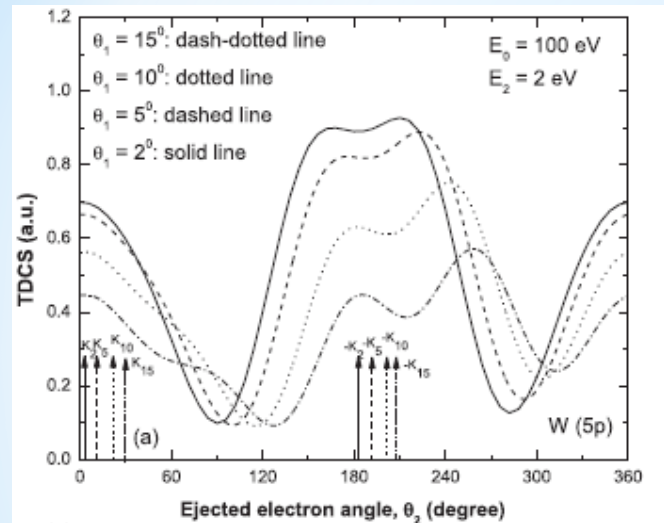
Results – Coplanar Asymmetric Ionization of W (5d) atoms



G Purohit

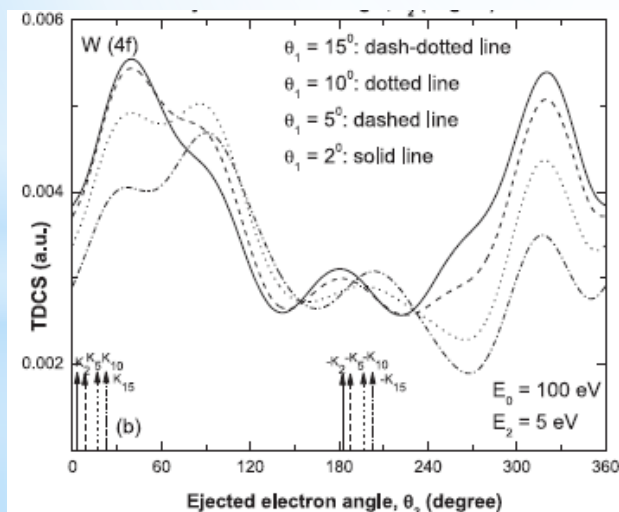
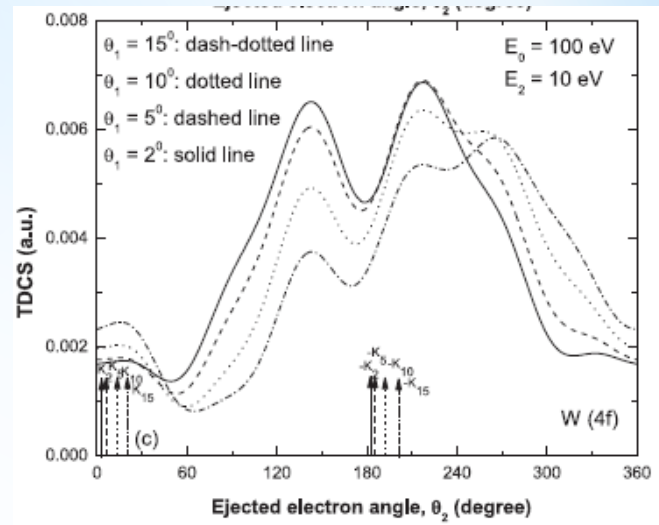
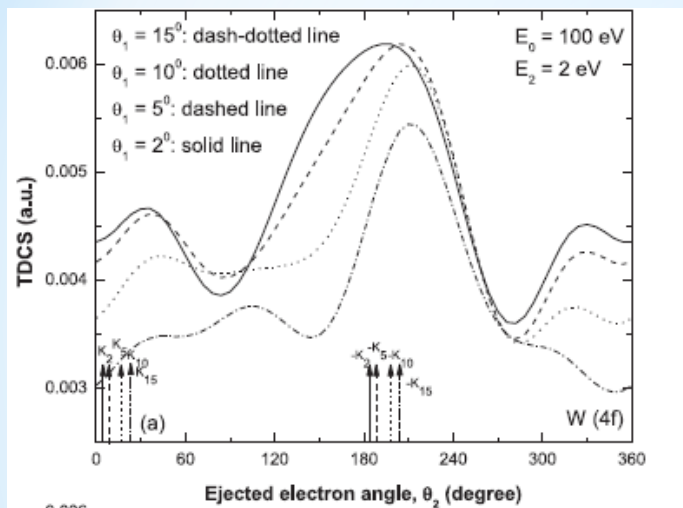
**Journal of Physics B: Atomic, Molecular and Optical
Physics 54 (6), 065203 (2021)**

Results – Coplanar Asymmetric Ionization of W (5p) atoms



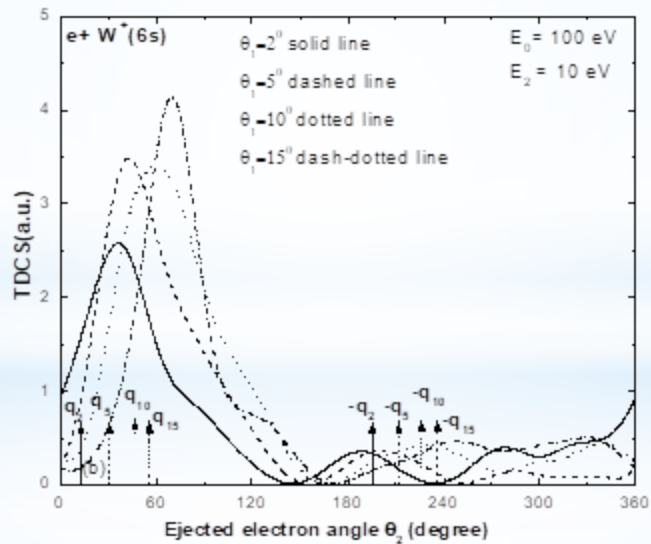
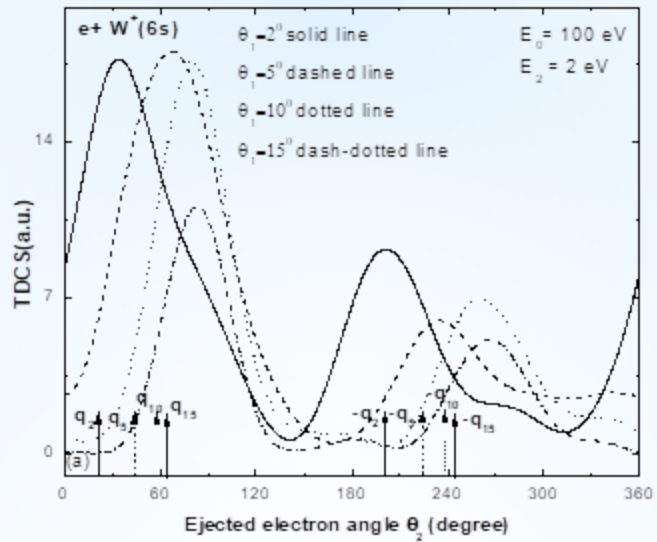
G Purohit
Journal of Physics B:
Atomic, Molecular
and Optical Physics
54 (6), 065203 (2021)

Results – Coplanar Asymmetric Ionization of W (4f) atoms

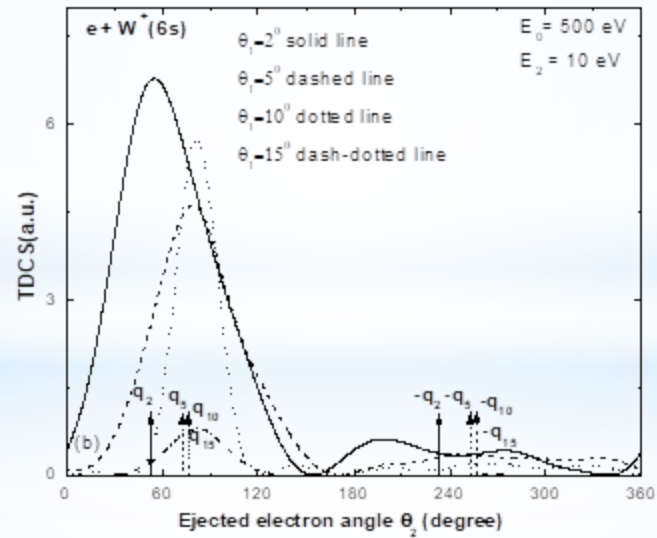
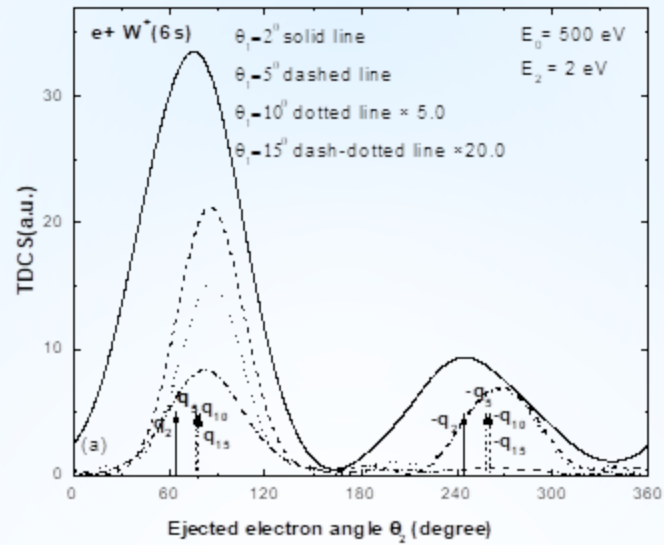


G Purohit
Journal of Physics B:
Atomic, Molecular
and Optical Physics
54 (6), 065203 (2021)

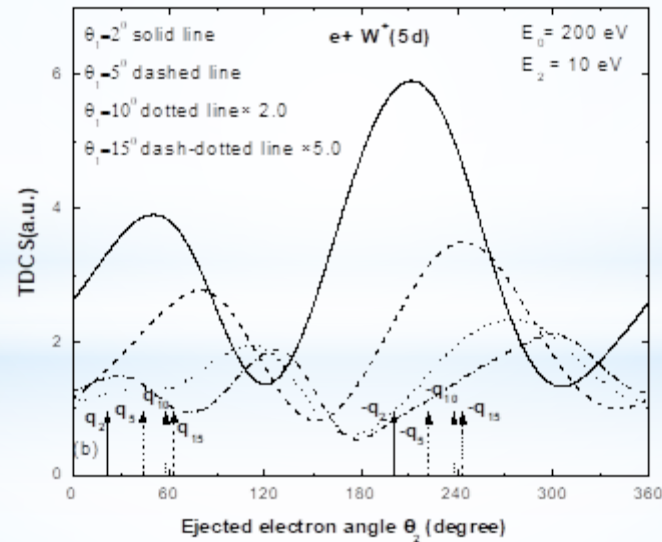
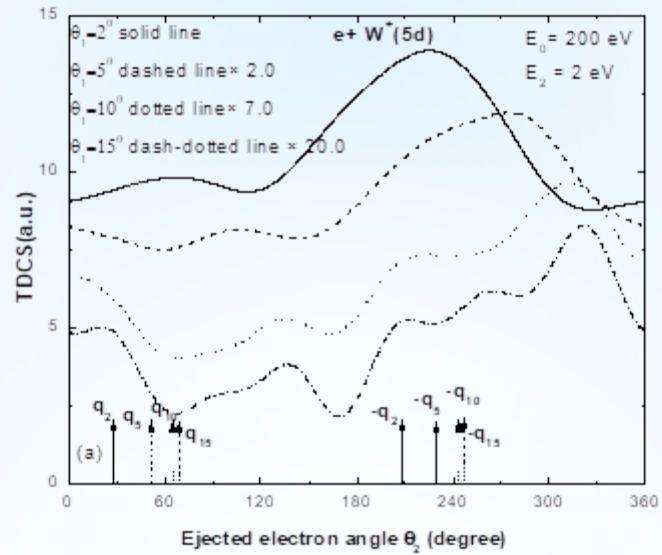
Results – Coplanar Asymmetric Ionization of W^+ ions



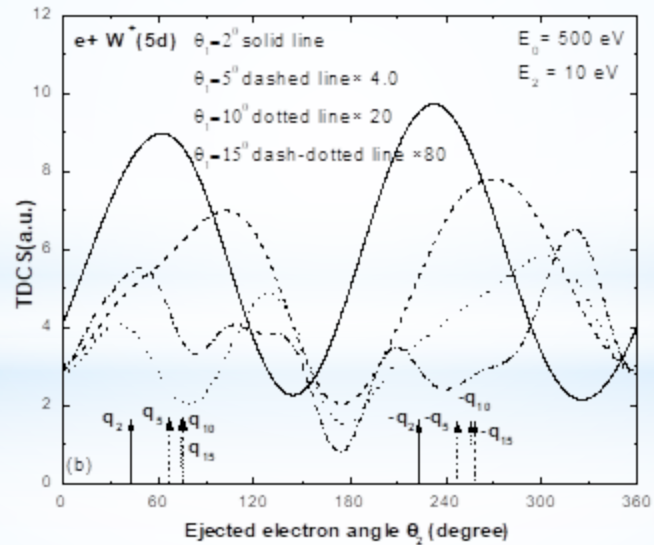
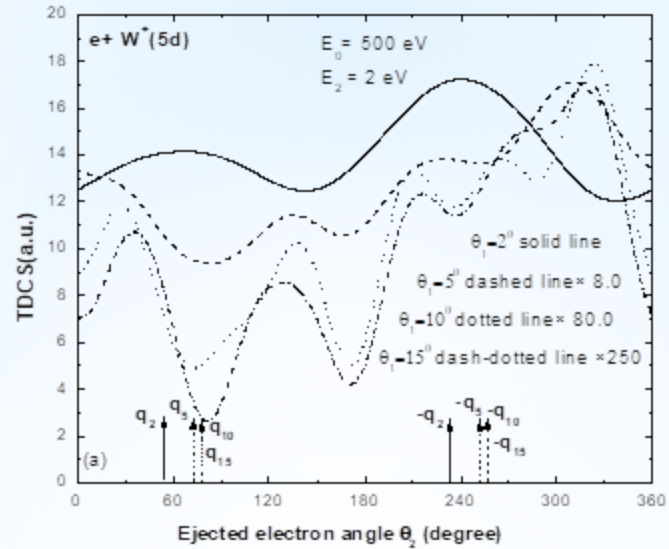
Results – Coplanar Asymmetric Ionization of W^+ ions



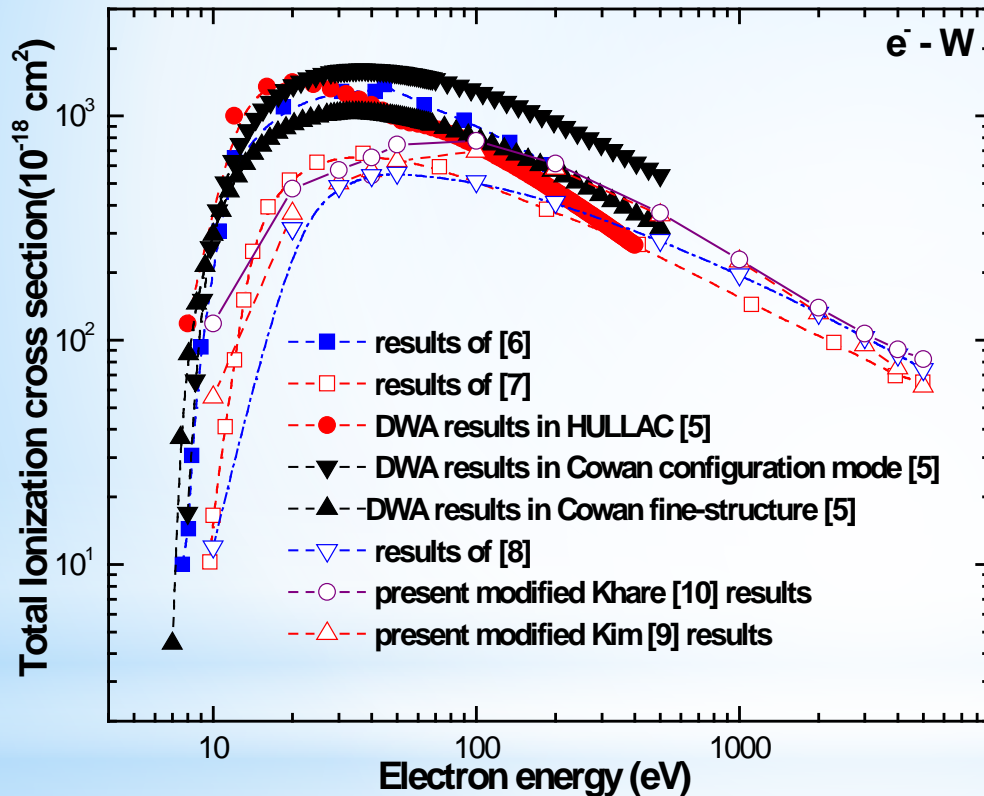
Results – Coplanar Asymmetric Ionization of W^+ ions



Results – Coplanar Asymmetric Ionization of W^+ ions



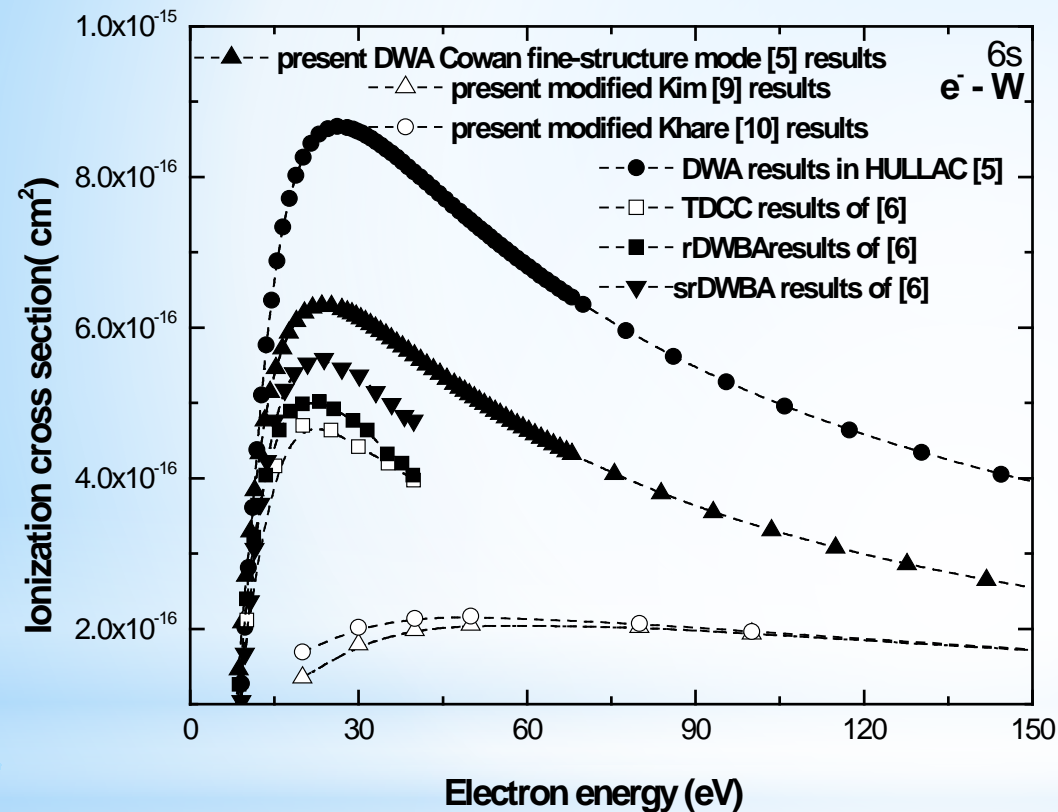
Results - Ionization cross sections for W atoms



Purohit, Kato, Murakami et al *Eur. Phys. J. D* 75, 9 (2021).

[5] G. Purohit, D. Kato and I. Murakami, *Plasma and Fusion Research* 13, 3401026 (2018). [6] M. S. Pindzola, S. D. Loch and A. R. Foster, *J. Phys. B: At. Mol. Opt. Phys.* 50, 095201 (2017). [7] F. Blanco, F. Ferreira da Silva, P. Lima-Vieira and G. Garcia, *Plasma Sources Sci. Technol.* 26, 085004 (2017). [8] B. Goswami, R. Naghma and B. Antony, *Int. J. Mass Spectrom.* 8, 372 (2014). [9] Y.K. Kim and M.E. Rudd, *Phys. Rev. A* 50, 3954-67 (1994). [10] S.P. Khare, M.K. Sharma and S. Tomar, *J. Phys. B: At. Mol. Opt. Phys.* 32, 3147 (1999).

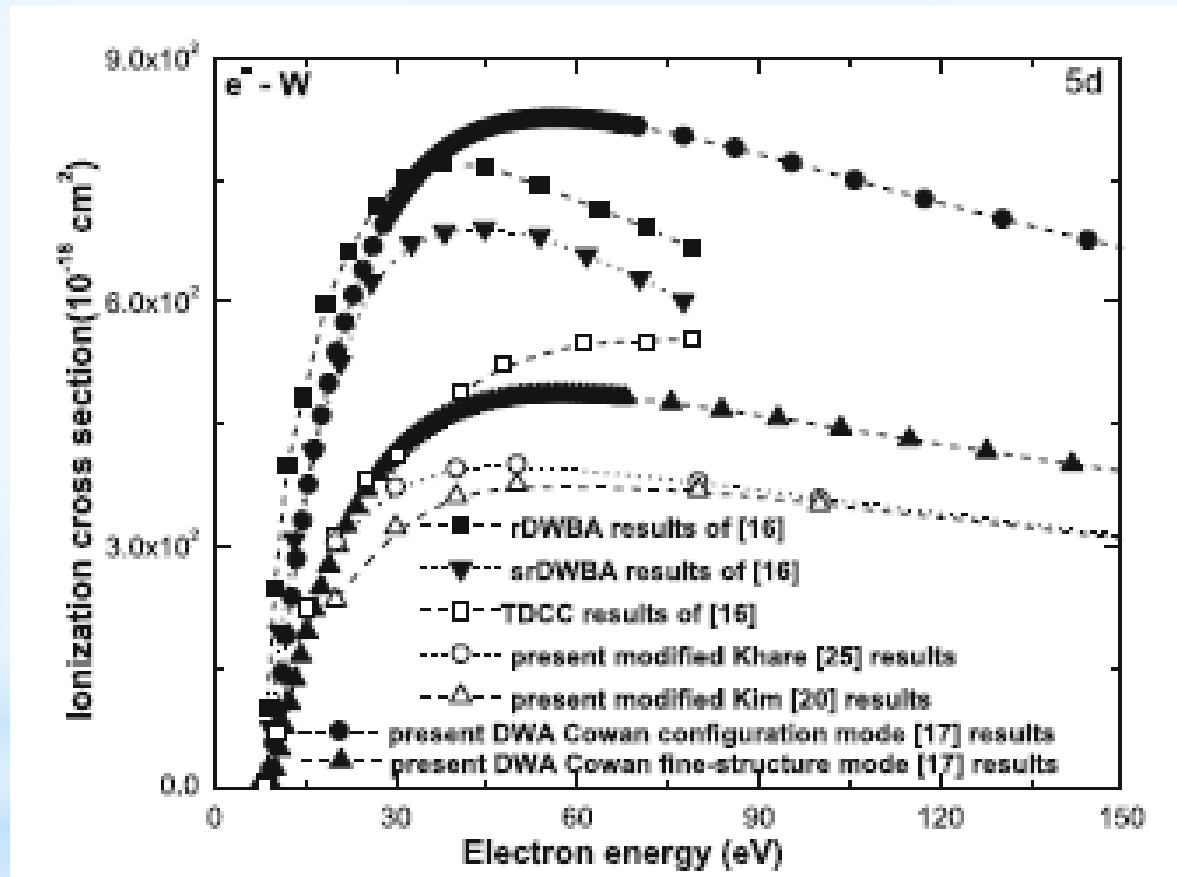
Results - Ionization cross sections for W atoms



Purohit, Kato, Murakami et al Eur. Phys. J. D 75, 9 (2021).

[5] G. Purohit, D. Kato and I. Murakami, Plasma and Fusion Research 13, 3401026 (2018). [6] M. S. Pindzola, S. D. Loch and A. R. Foster, J. Phys. B: At. Mol. Opt. Phys. 50, 095201 (2017). [7] F. Blanco, F. Ferreira da Silva, P. Lima-Vieira and G. Garcia, Plasma Sources Sci. Technol. 26, 085004 (2017). [8] B. Goswami, R. Naghma and B. Antony, Int. J. Mass Spectrom. 8, 372 (2014). [9] Y.K. Kim and M.E. Rudd, Phys. Rev. A 50, 3954-67 (1994). [10] S.P. Khare, M.K. Sharma and S. Tomar, J. Phys. B: At. Mol. Opt. Phys. 32, 3147 (1999).

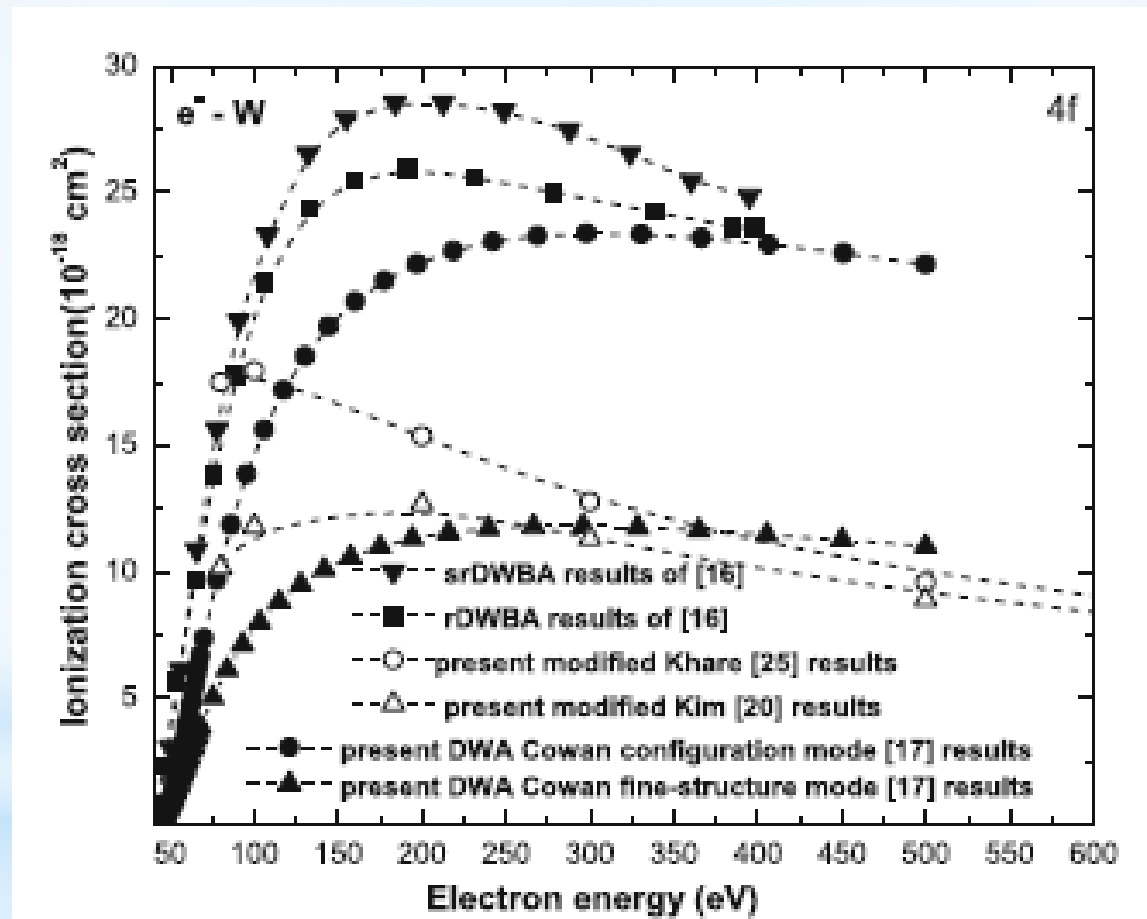
Results - Ionization cross sections for W atoms



Purohit, Kato, Murakami et al Eur. Phys. J. D
75, 9 (2021).

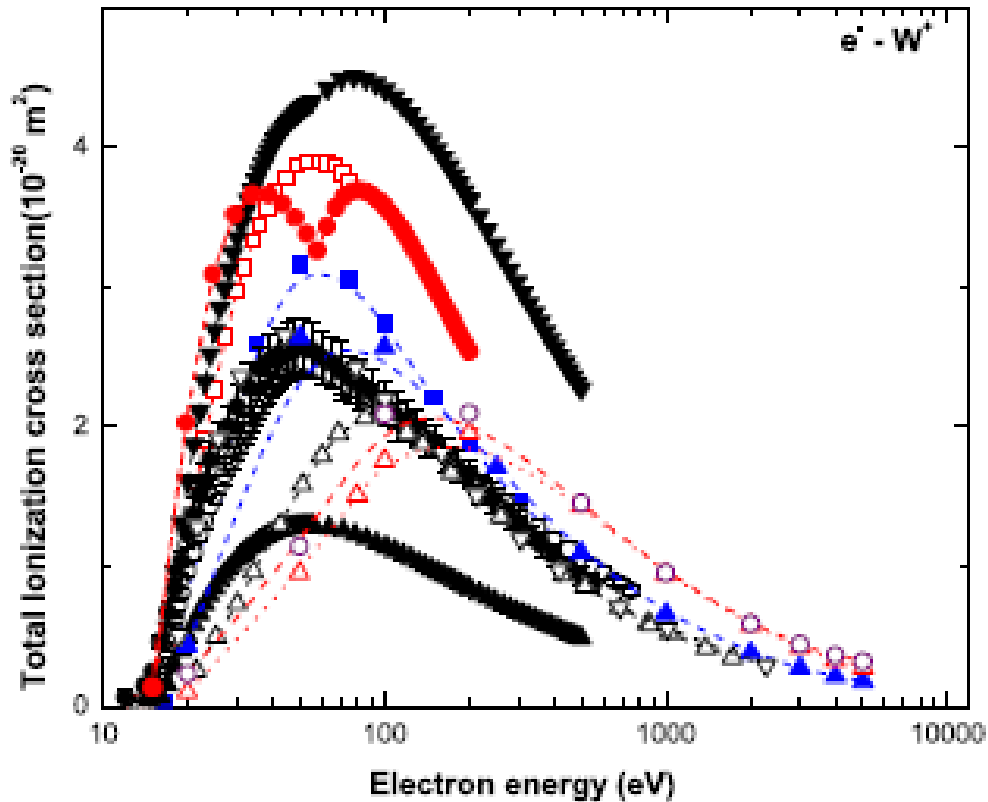
Results - Ionization cross sections for W atoms

Ionization cross sections of W
atom 4f subshell



Purohit, Kato, Murakami et al Eur. Phys. J. D
75, 9 (2021).

Results - Ionization cross sections for W^+ ions

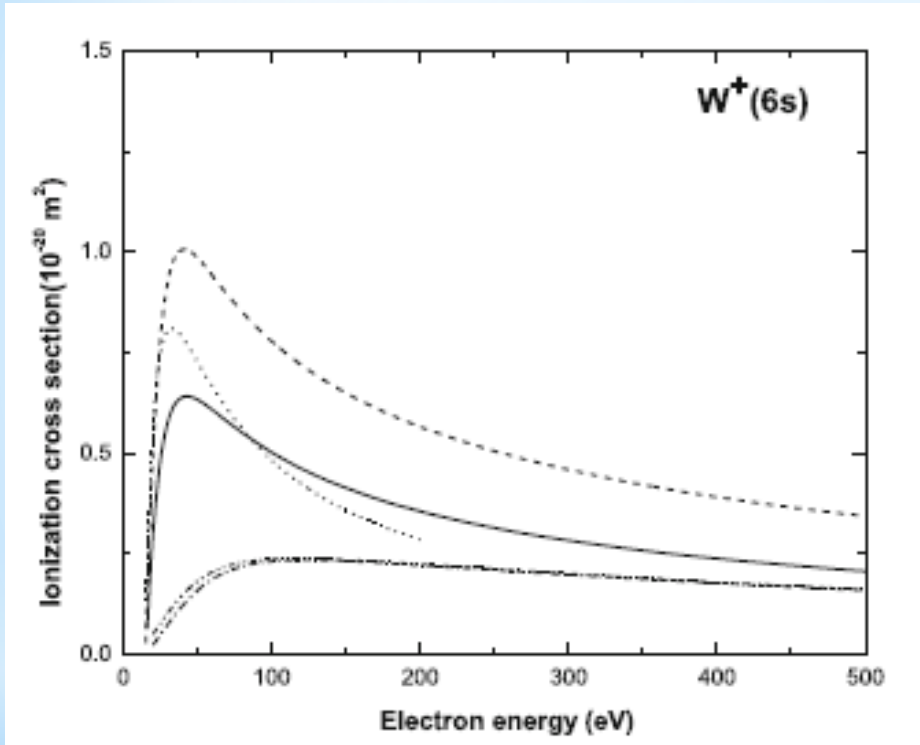


Red solid circles: DWA results in HULLAC [Plasm. Fus. Res. 13, 3401026 (2018)], black solid up- and down- triangles: DWA results in Cowan formalism with fine-structure and configuration mode [Plasm. Fus. Res. 13, 3401026 (2018)]; blue solid squares: results of [J. Phys. B At. Mol. Opt. Phys. 44, 125201 (2011)] and red hollow squares: results of [Phys. Rev. A 46, 2486 (1992)], Red hollow up triangles: present results in modified Kim [Phys. Rev. A 50, 3954-67 (1994)] and purple hollow circles: present modified Khare [J. Phys. B At. Mol. Opt. Phys. 32, 3147 (1999)] results;

solid black circles: measurements [J. Phys. B At. Mol. Opt. Phys. 28, 4853 (1995)]; black hollow circles: measurements [J. Phys. B At. Mol. Opt. Phys. 17, 2707 (1984)]; blue up triangles: results of [Int. J. Mass Spectrom. 252, 213 (2006)], black hollow up triangles: results of [Phys. Rev. A 20, 445 (1979)] and black hollow down triangles: results of [Z. Phys. 216, 241 (1968)]

Purohit, Kato and Murakami, et al. Eur. Phys. J. D 75, 219 (2021)

Results - Ionization cross sections for W^+ ions



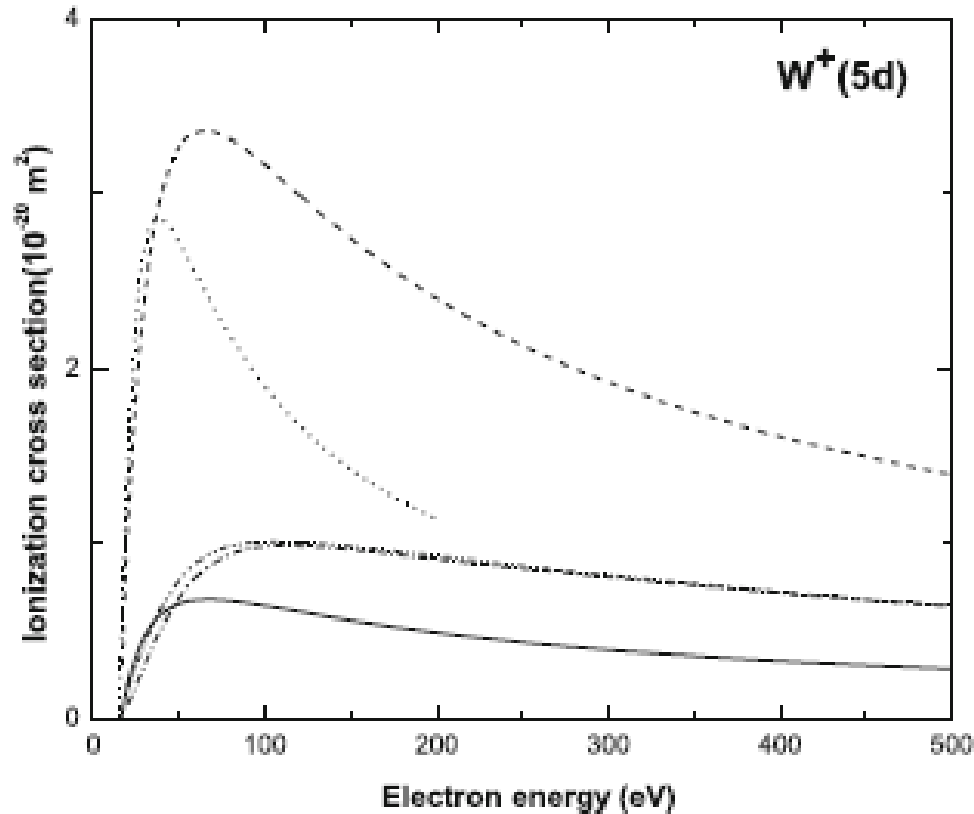
Dotted Curve: DWA results in HULLAC [Plasm. Fus. Res. **13**, 3401026 (2018)],

Solid and dashed curves: DWA results in Cowan formalism with fine-structure and configuration mode [Plasm. Fus. Res. **13**, 3401026 (2018)];

Dash dotted line: present results in modified Kim [Phys. Rev. **A50**, 3954-67 (1994)] and Dash dot dotted line: present modified Khare [J. Phys. B At. Mol. Opt. Phys. **32**, 3147 (1999)] results;

Purohit, Kato and Murakami, et al. Eur. Phys. J. D **75**, 219 (2021)

Results - Ionization cross sections for W^+ ions



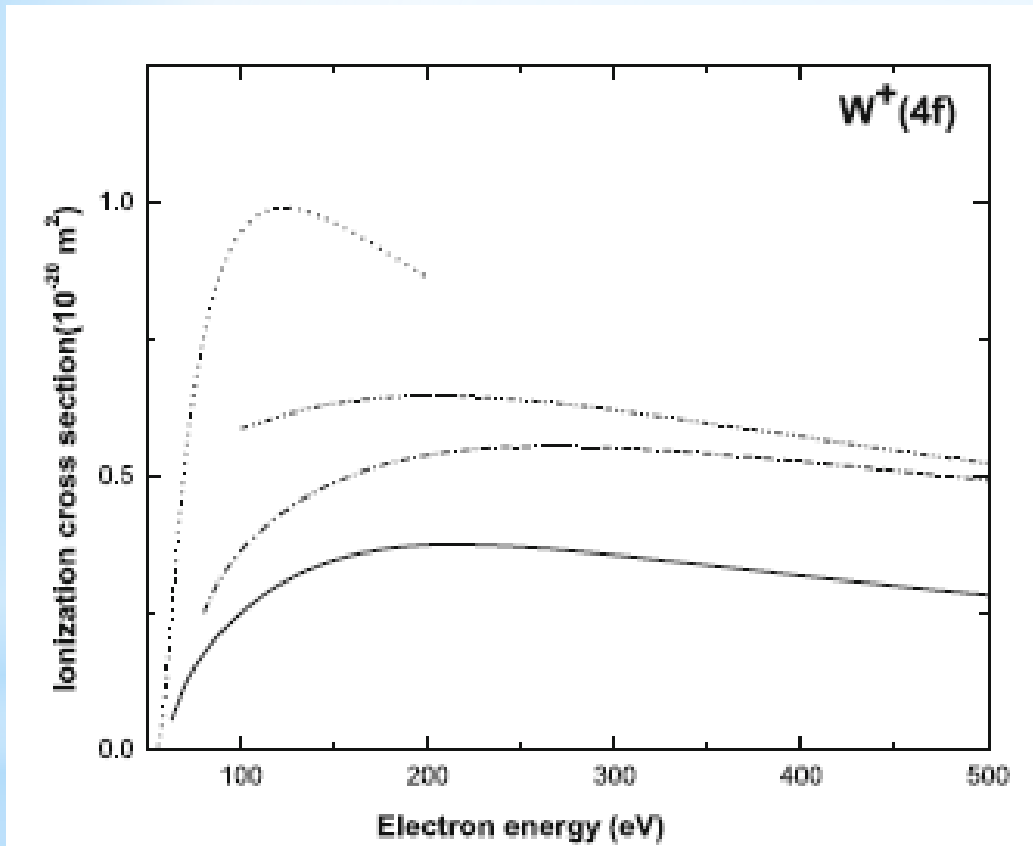
Dotted Curve: DWA results in HULLAC [Plasm. Fus. Res. **13**, 3401026 (2018)],

Solid and dashed curves: DWA results in Cowan formalism with fine-structure and configuration mode [Plasm. Fus. Res. **13**, 3401026 (2018)];

Dash dotted line: present results in modified Kim [Phys. Rev. **A50**, 3954-67 (1994)] and Dash dot dotted line: present modified Khare [J. Phys. B At. Mol. Opt. Phys. **32**, 3147 (1999)] results;

Purohit, Kato and Murakami, et al. Eur. Phys. J. D **75**, 219 (2021)

Results - Ionization cross sections for W^+ ions



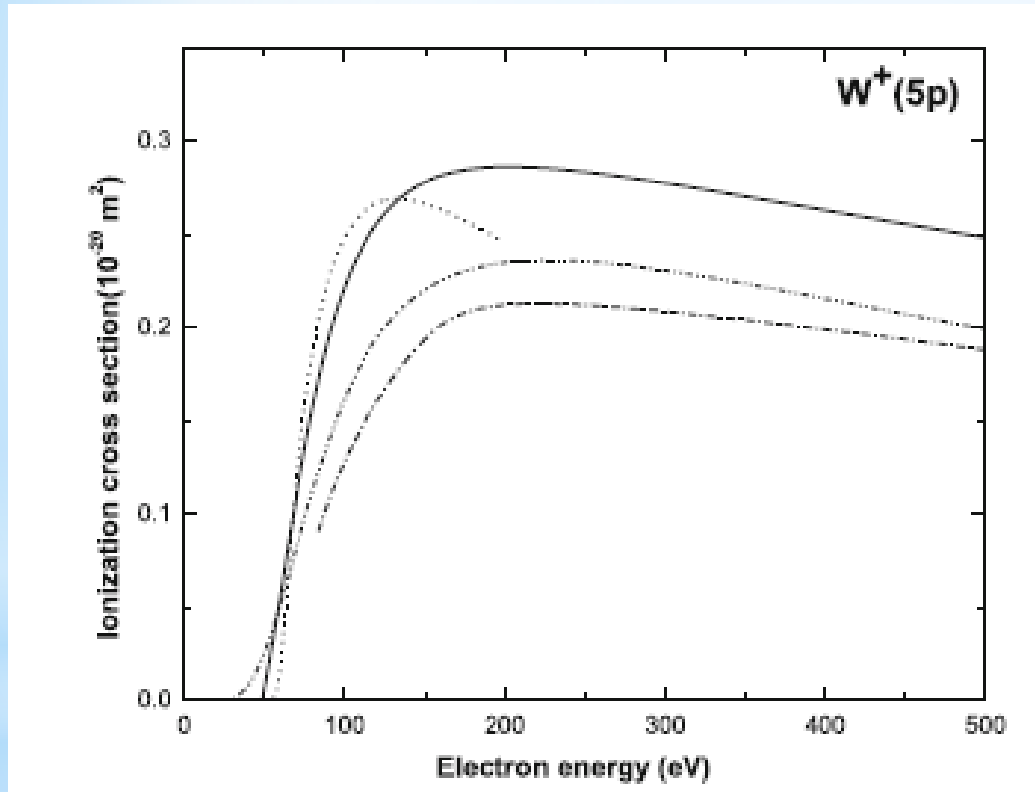
Dotted Curve: DWA results in HULLAC [Plasm. Fus. Res. **13**, 3401026 (2018)],

Solid curve: DWA results in Cowan formalism With configuration mode [Plasm. Fus. Res. **13**, 3401026 (2018)];

Dash dotted line: present results in modified Kim [Phys. Rev. **A50**, 3954-67 (1994)] and Dash dot dotted line: present modified Khare [J. Phys. B At. Mol. Opt. Phys. **32**, 3147 (1999)] results;

Purohit, Kato and Murakami, et al. Eur. Phys. J. D **75**, 219 (2021)

Results - Ionization cross sections for W^+ ions



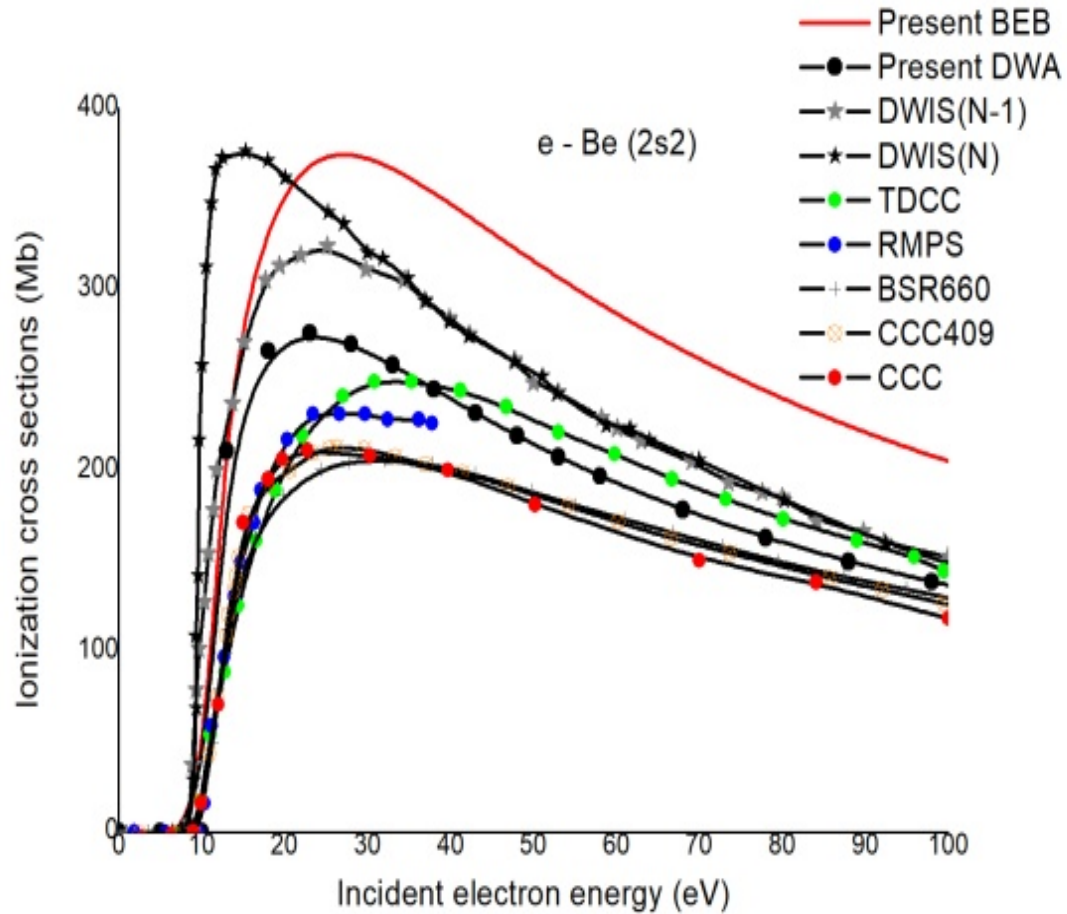
Dotted Curve: DWA results in HULLAC [Plasm. Fus. Res. **13**, 3401026 (2018)],

Solid curve: DWA results in Cowan formalism With configuration mode [Plasm. Fus. Res. **13**, 3401026 (2018)];

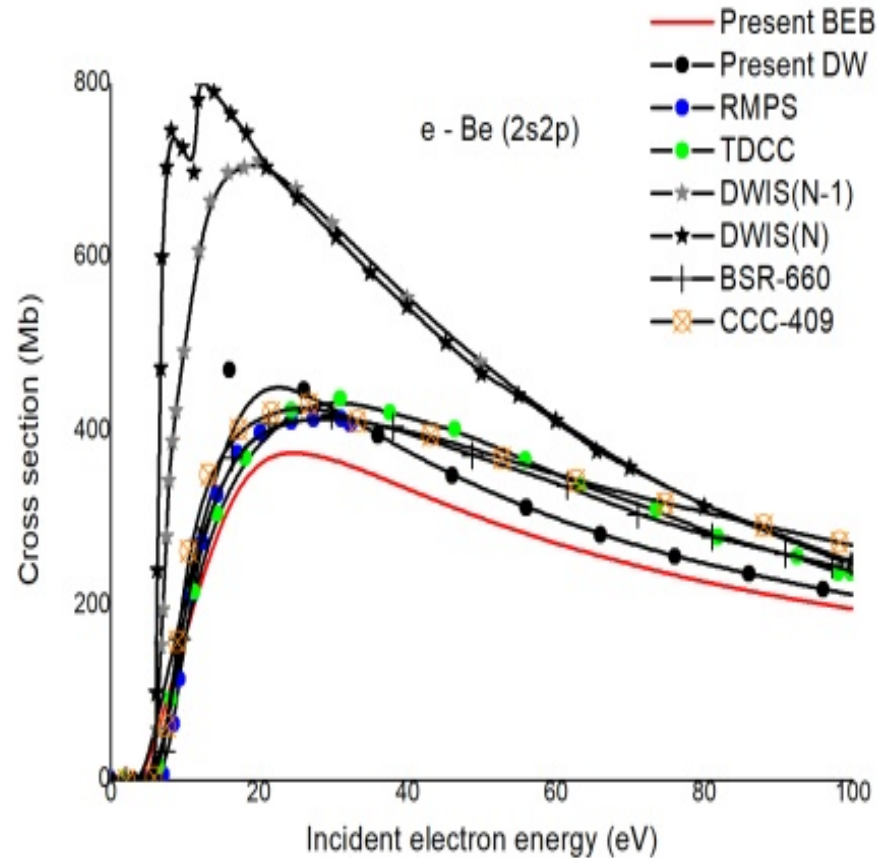
Dash dotted line: present results in modified Kim [Phys. Rev. **A50**, 3954-67 (1994)] and Dash dot dotted line: present modified Khare [J. Phys. B At. Mol. Opt. Phys. **32**, 3147 (1999)] results;

Purohit, Kato and Murakami, et al. Eur. Phys. J. D **75**, 219 (2021)

Results - Ionization cross sections for Be ($1s^2, 2s^2$)



Results - Ionization cross sections for Be ($1s^2 2s 2p$)



Molecular targets – Difficulties?

A significant challenge - distributed nuclei.

Contrasts to atoms which have a single nuclear scattering centre - can be described using a spherical basis.

Molecular wave-functions - generally not spherical, the nuclei within the molecule providing multiple scattering centres.

Molecular targets – Difficulties?

So, there is a key challenge in developing an accurate multi-centered wave-function.

A further challenge arises - difficult to align the molecules (experimentally) prior to the collision, so the models must consider the random orientation of the targets for accurate comparison.

This becomes a computationally intensive problem, and so approximations are usually made to allow these calculations to become tractable.

TDCS for Molecules - DWBA with OAMO

$$\frac{d^3\sigma}{d\Omega_1 d\Omega_2 dE_1} = (2\pi)^4 \frac{k_1 k_2}{k_0} \sum_{av} |\mathbf{T}(\mathbf{k}_1, \mathbf{k}_2, \mathbf{k}_0)|^2$$

$$|\mathbf{T}|^2 = |\mathbf{f}_{\text{dir}}|^2 + |\mathbf{f}_{\text{ex}}|^2 - \text{Re}(\mathbf{f}_{\text{dir}}^* \mathbf{f}_{\text{ex}})$$

$$\mathbf{f}_{\text{dir}} = \left\langle \mathbf{X}_1^{(-)}(\mathbf{k}_1, \mathbf{r}_1) \mathbf{X}_2^{(-)}(\mathbf{k}_2, \mathbf{r}_2) \left| -\frac{Z}{r_{12}} \right| \psi^{\text{OA}}(\mathbf{r}_2) \mathbf{X}_0^{(+)}(\mathbf{k}_0, \mathbf{r}_1) \right\rangle$$

$$\mathbf{f}_{\text{ex}} = \left\langle \mathbf{X}_1^{(-)}(\mathbf{k}_1, \mathbf{r}_2) \mathbf{X}_2^{(-)}(\mathbf{k}_2, \mathbf{r}_1) \left| -\frac{Z}{r_{12}} \right| \psi^{\text{OA}}(\mathbf{r}_2) \mathbf{X}_0^{(+)}(\mathbf{k}_0, \mathbf{r}_1) \right\rangle$$

$\psi^{OA}(\mathbf{r}_2)$ is the initial bound state wave function for the molecular target which is approximated as the orientation averaged molecular orbital

The molecular wave functions for N_2 molecule have been calculated using the density functional theory with B3LYP/TZ2P basis set [C. Lee, W. Yang and R. G. Parr, Phys. Rev. B 37, 785 (1988)]

The initial state distorting potential representing the interaction between projectile and target molecular electrons constitutes the contribution from molecular nuclei and a spherical symmetric potential obtained by averaging over all orientations using B3LYP basis sets.

The post collision interaction (PCI) has been calculated using the Ward-Macek factor (M_{ee})

$$M_{ee} = N_{ee} \left| {}_1F_1(-i\lambda_3, 1, -2k_3 r_{3ave}) \right|^2,$$

where

$$N_{ee} = \frac{\gamma}{e^\gamma - 1} \quad \gamma = -\frac{2\pi}{|k_1 - k_2|} \quad \lambda_3 = -\frac{1}{|k_1 - k_2|} \quad r_{3ave} = \frac{\pi^2}{16\varepsilon} \left(1 + \frac{0.627}{\pi} \sqrt{\varepsilon \ln \varepsilon}\right)^2$$

$$\varepsilon = (k_1^2 + k_2^2)/2$$

The TDCS expression including PCI

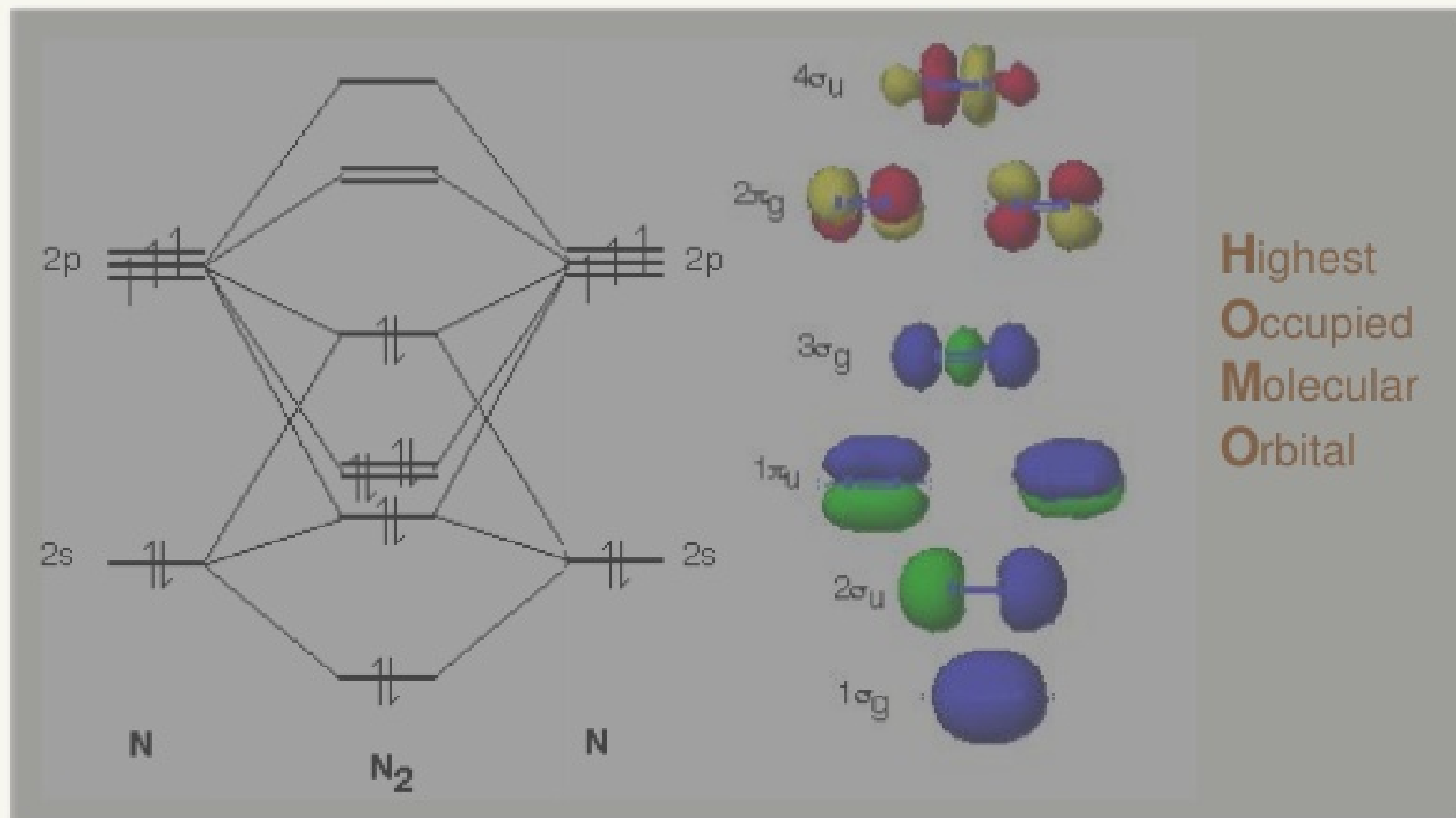
$$\frac{d^3\sigma}{d\Omega_1 d\Omega_2 dE_1} = M_{ee} (2\pi)^4 \frac{k_1 k_2}{k_0} \sum_{m=-1}^1 \left(|f_{nlm}|^2 + |g_{nlm}|^2 - \text{Re}(f_{nlm}^* g_{nlm}) \right)$$

S. J. Ward and J. H. Macek, *Phys. Rev. A* 49, 1049 (1994).

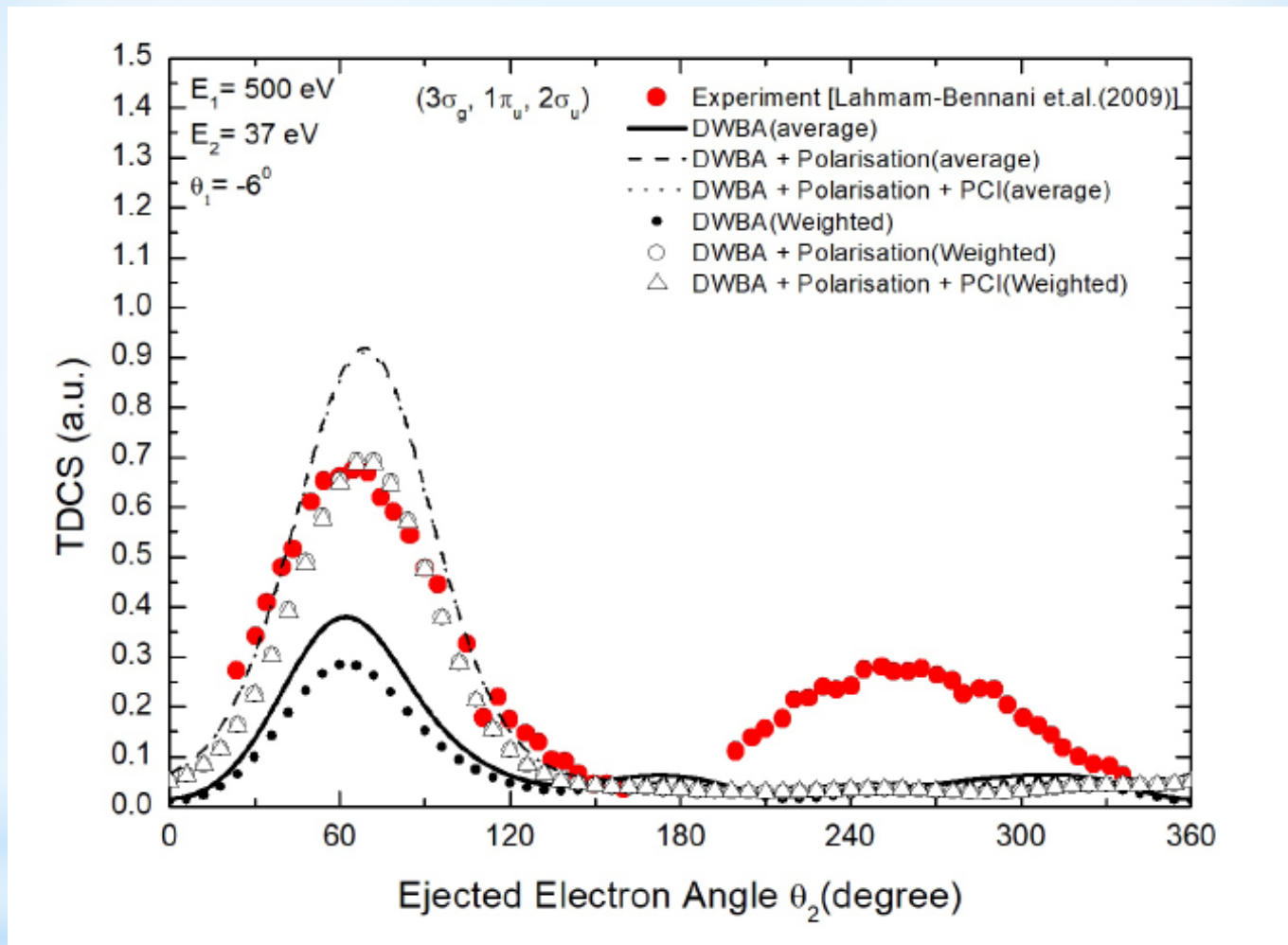
MOLECULAR ORBITALS OF NITROGEN



N_2 HOMO

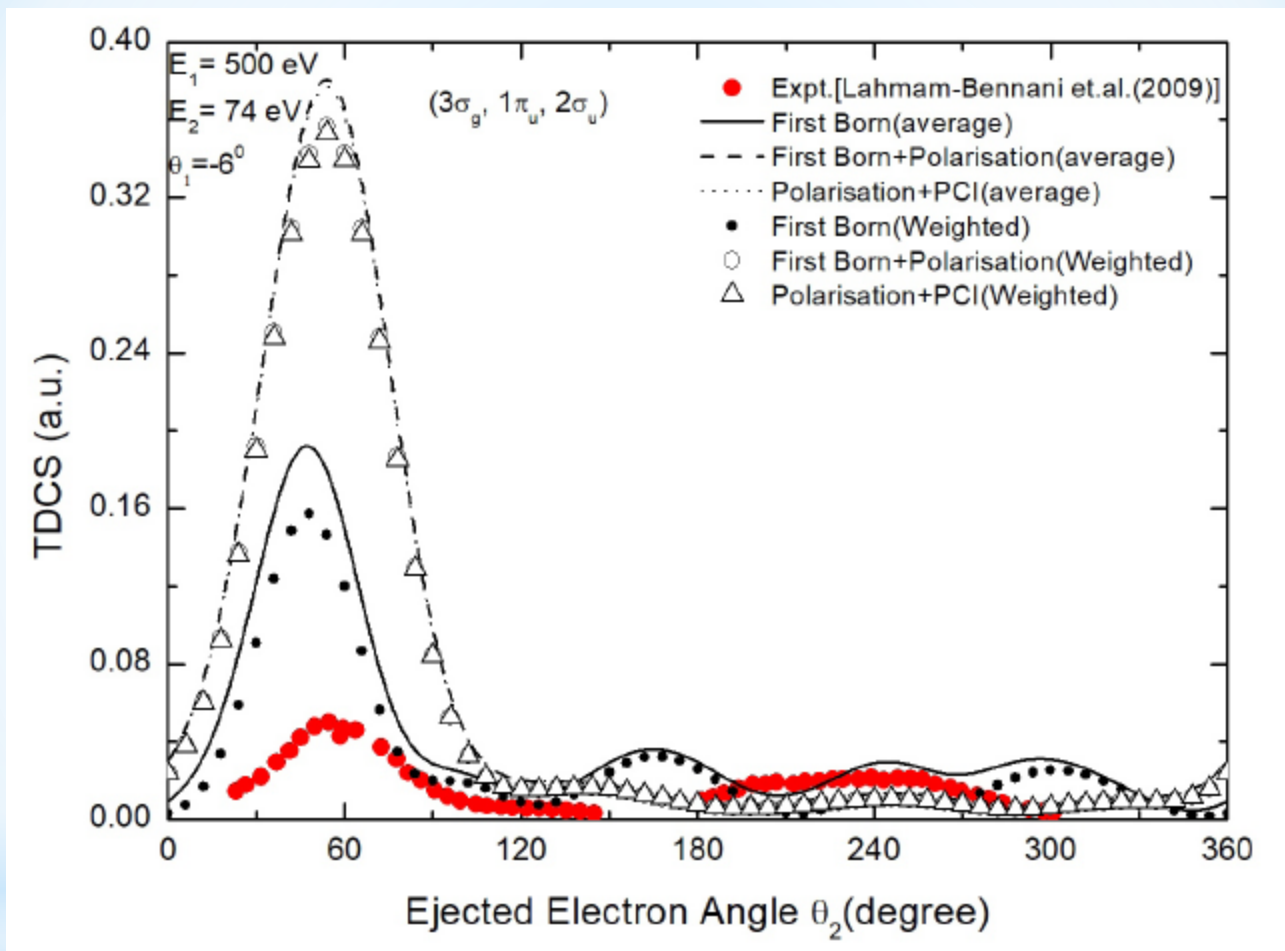


Results - Differential cross sections; N₂ molecules



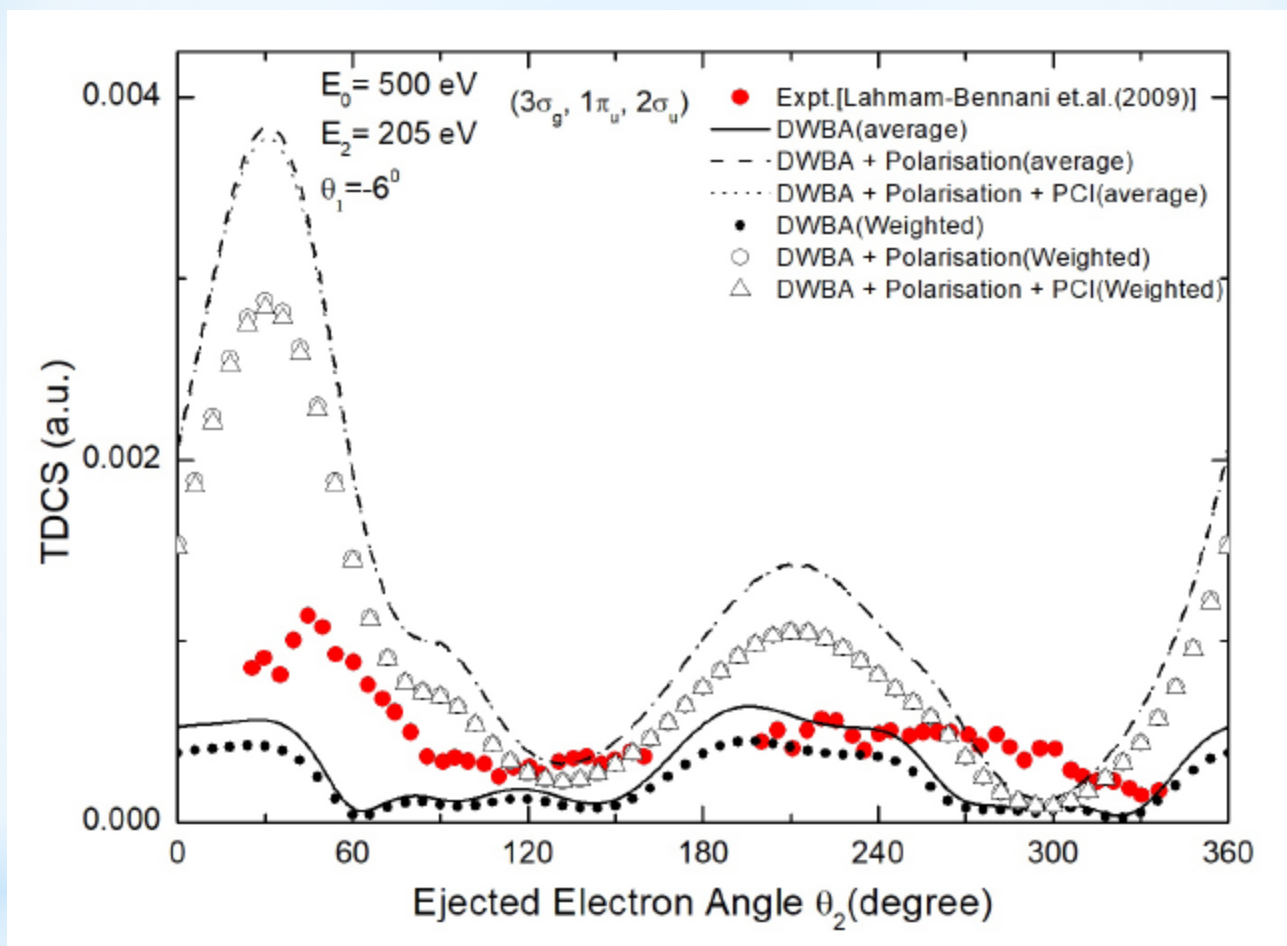
Electron-impact TDCS for N₂ molecule calculated for the weighted and average sum of the outer orbital $(3\sigma_g, 1\pi_u, 2\sigma_u)$. *The ejected electron energy is 37 eV. Kinematics and legends used are displayed in the figure frame.*

Results - Differential cross sections; N₂ molecules



Electron-impact TDCS for N₂ molecule calculated for the weighted and average sum of the outer orbital ($3\sigma_g, 1\pi_u, 2\sigma_u$). *The ejected electron energy is 74 eV. Kinematics and legends used are displayed in the figure frame.*

Results - Differential cross sections; N₂ molecules



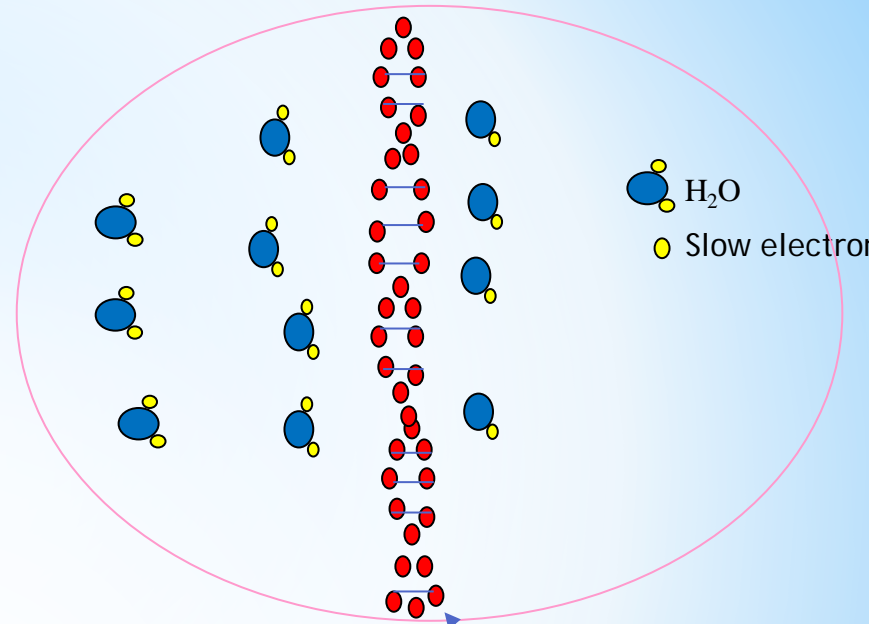
Electron-impact TDCS for N₂ molecule calculated for the weighted and average sum of the outer orbital ($3\sigma_g, 1\pi_u, 2\sigma_u$). *The ejected electron energy is 205 eV. Kinematics and legends used are displayed in the figure frame.*

Water Molecule

The third most abundant molecule on the earth - Of great importance in numerous multi-disciplinary research fields;

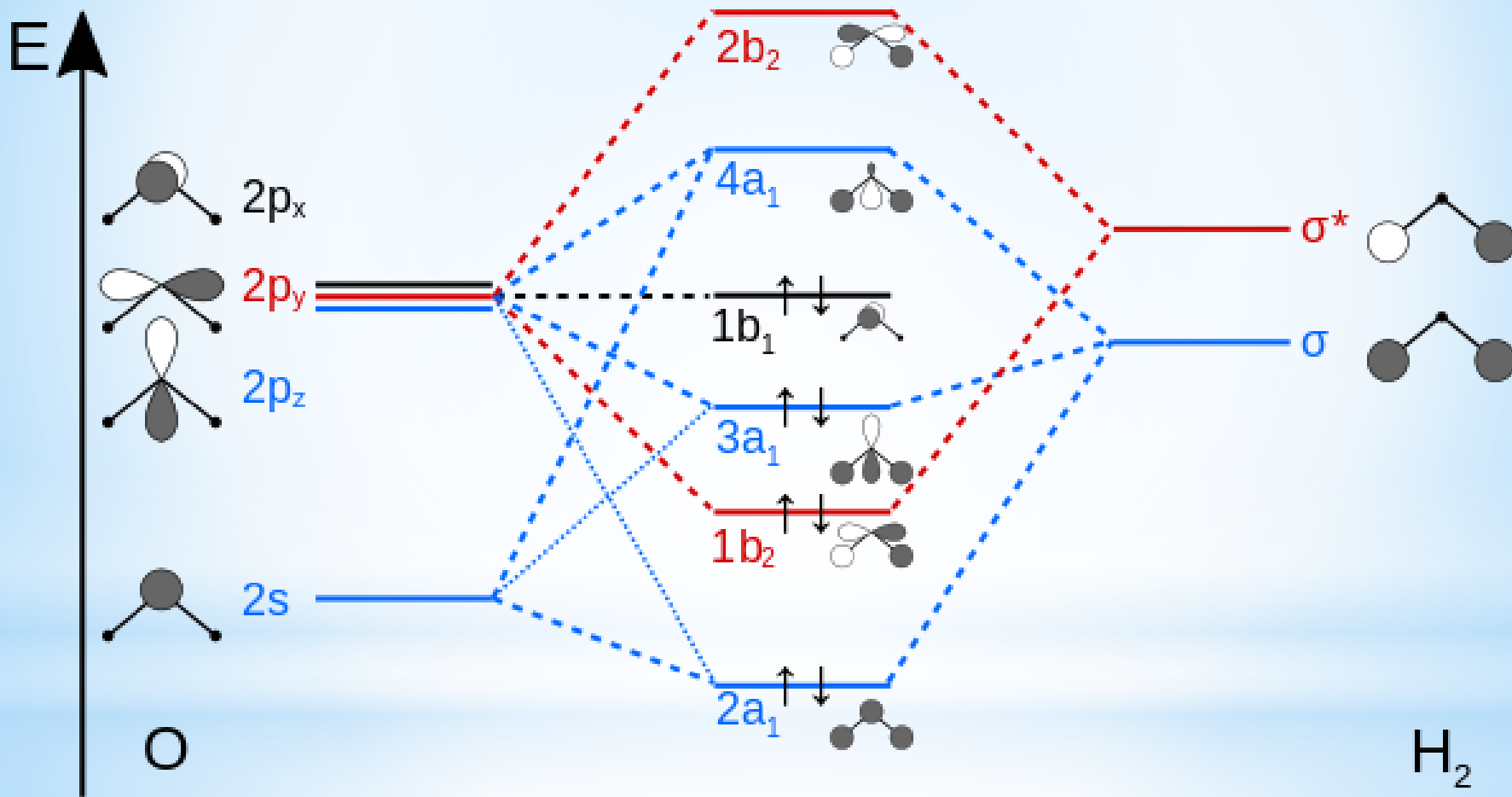
- * Radiobiology where it is commonly used as surrogate of the living matter, the latter being composed of water for about 60% in mass.
- * Energetic and angular distributions resulting from electron-induced collisions with water molecules are commonly used in charged particle track structure codes for modeling the radio-induced damages in biological samples.
- * Particularly, the knowledge of the collision dynamics of low-energy electrons with biological systems remain crucial so as to develop robust numerical models of charged particle tracking in biological matter.

Projectile



DNA

Energy deposition and angular distributions resulting from **electron collisions with water** are used in charged particle track structure analyses to model radiation damage in biological samples. These models are an active area of research since the observation that **high energy radiation that is used to treat cancers also liberates many low energy electrons, causing additional damage to cell DNA.**



The TDCS in terms of second Born approximation is given as

$$\frac{d^3\sigma}{dk_f dk_e dE_e} = (2\pi)^4 \frac{k_f k_e}{k_i} \sum_{av} |f_{B1} + f_{B2}|^2,$$

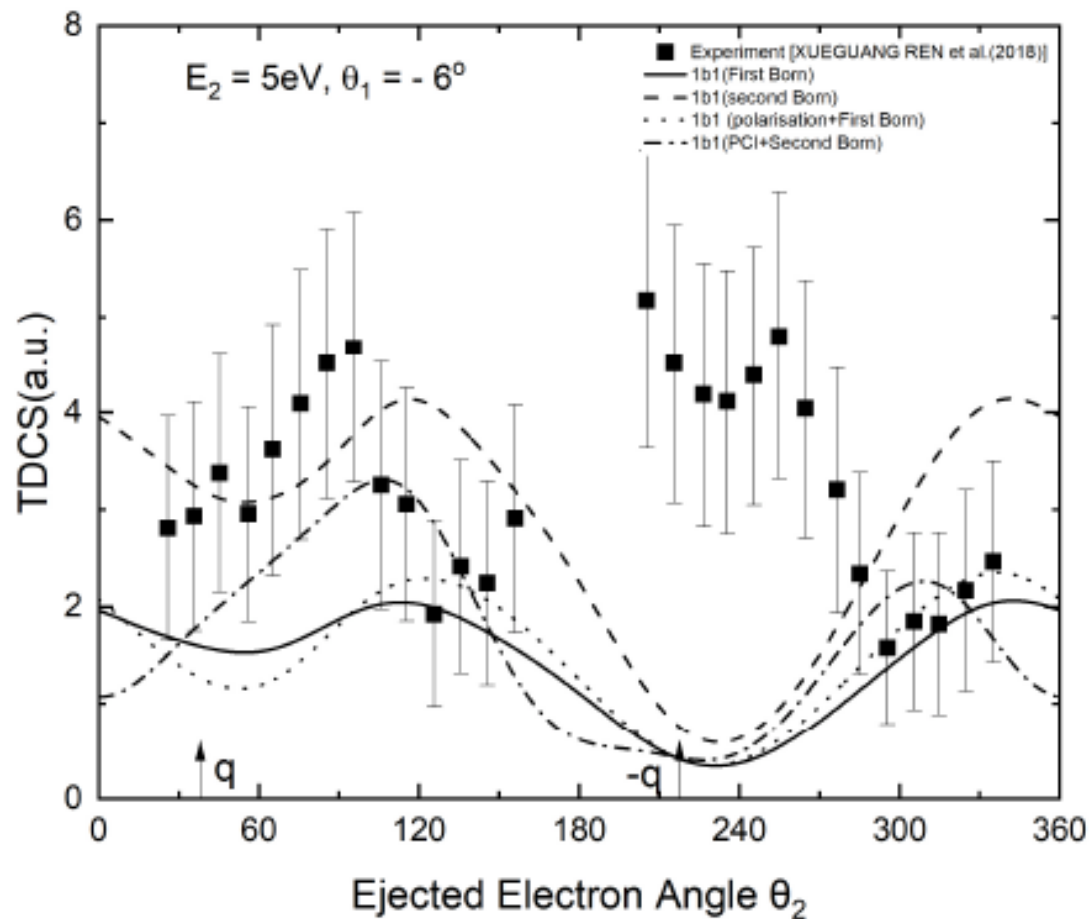
In DWBA, the first order term is calculated as follows:

$$f_{B1} = \langle \Psi_1(k_f, r_f) \Psi_2(k_e, r_i) | \pm \left(\frac{-Z}{r_f} - \frac{1}{|r_f - r_i|} \right) | \Phi_0(r_i) \Psi_i(k_i, r_f) \rangle$$

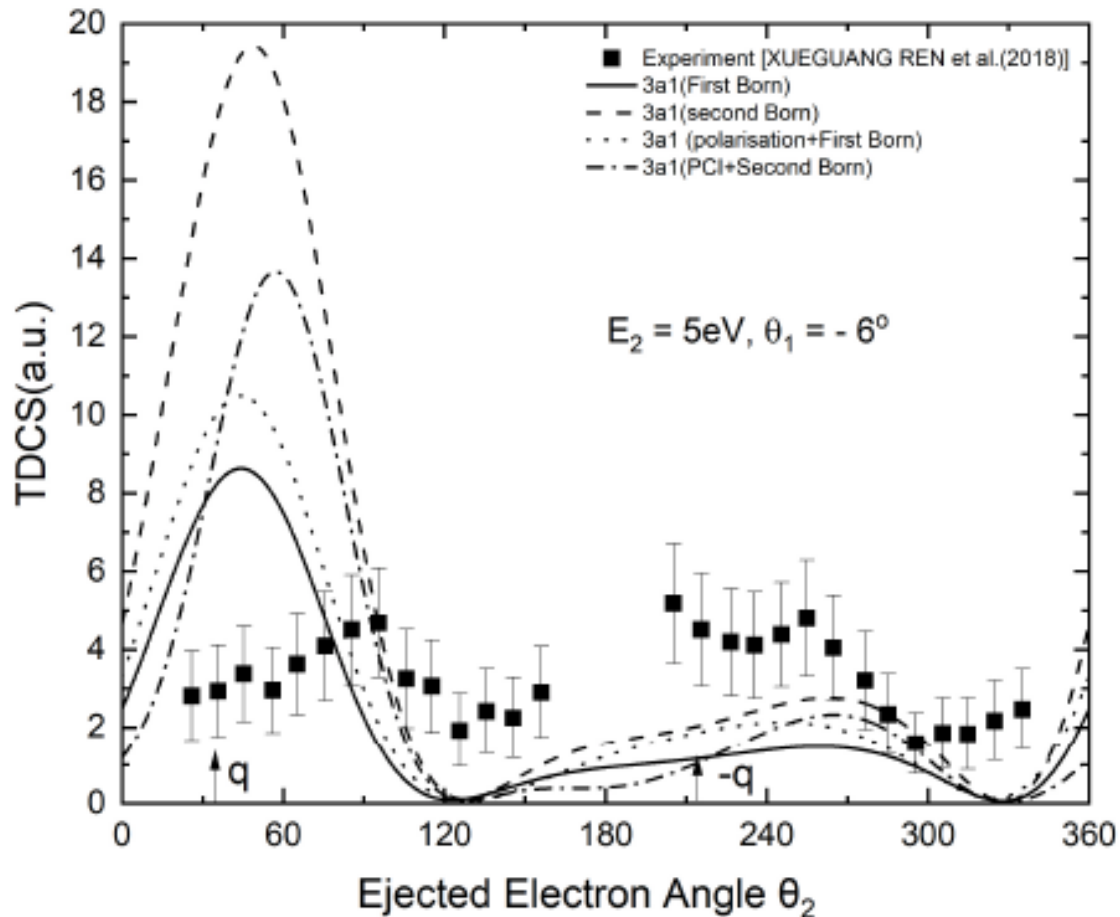
The second Born term in the DWBA is expressed by

$$f_{B2} = \langle \Psi^{(-)}(k_f, r_f) \Psi^{(-)}(k_e, r_i) | V G_0^+ V | \Phi_0(r_i) \Psi_i^{(-)}(k_i, r_f) \rangle$$

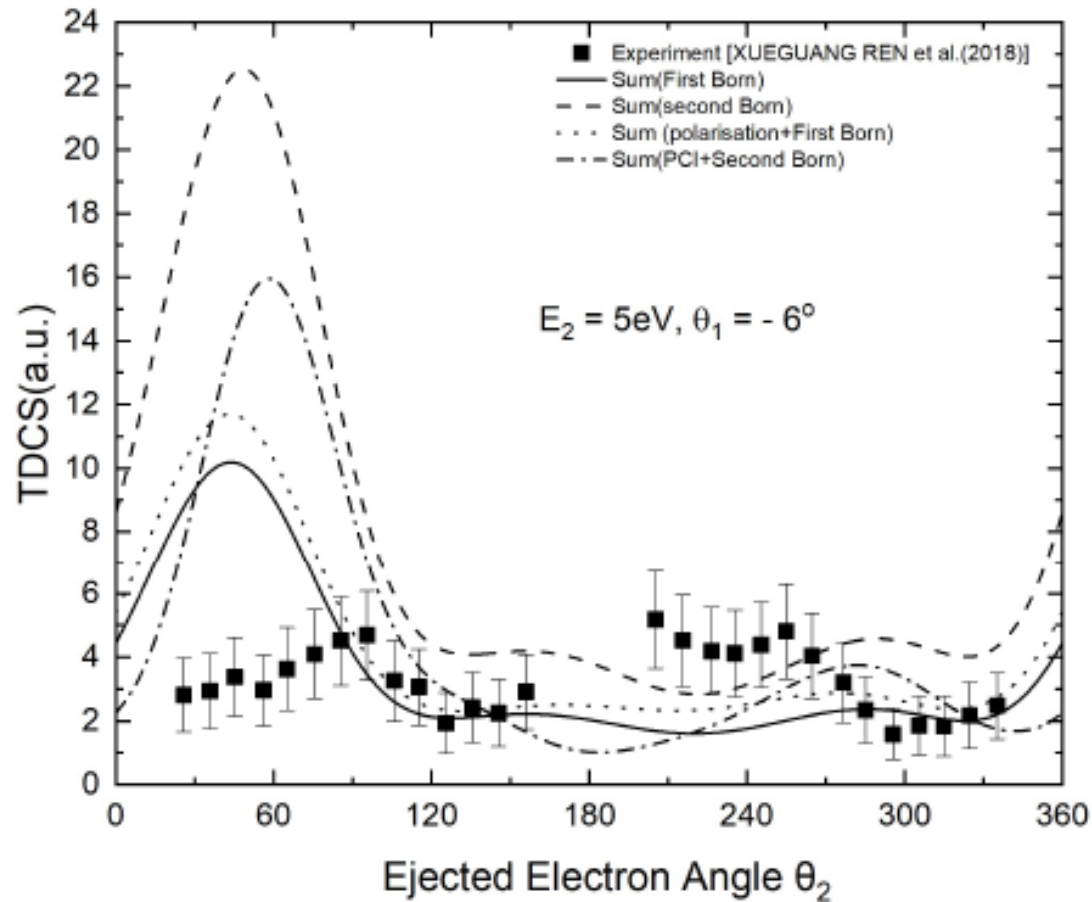
Results – Electron impact TDCS for H₂O molecules at 81 eV – Coplanar geometry



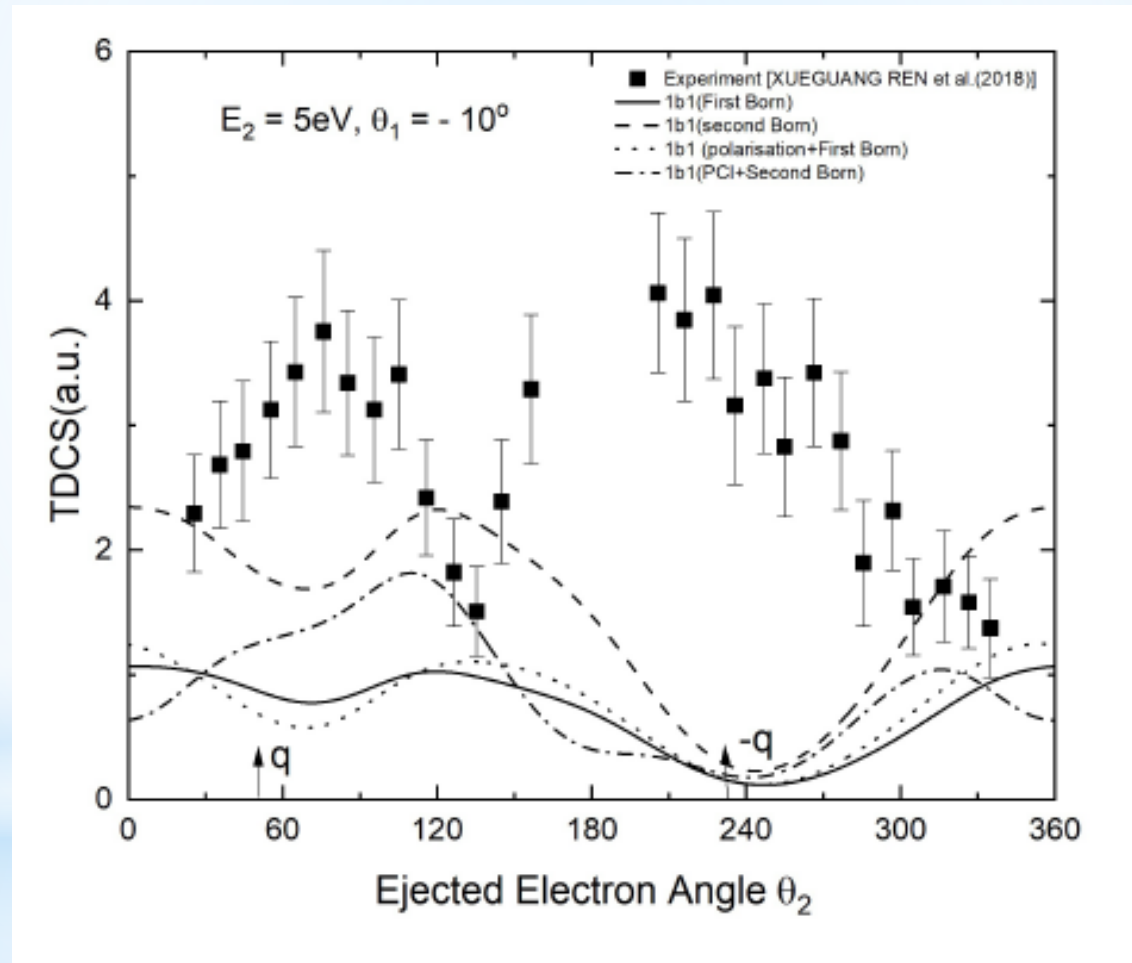
Results – Electron impact TDCS for H₂O molecules at 81 eV – Coplanar geometry



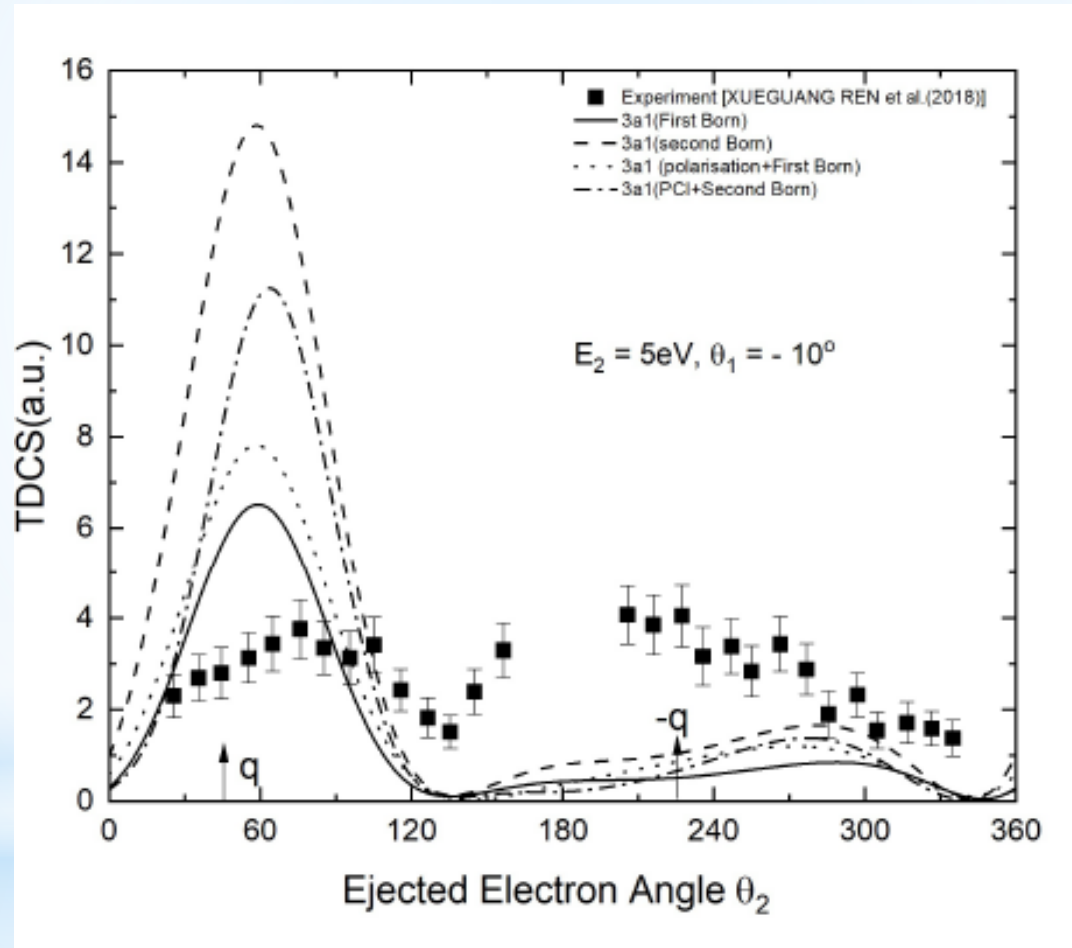
Results – Electron impact TDCS for H₂O molecules at 81 eV – Coplanar geometry



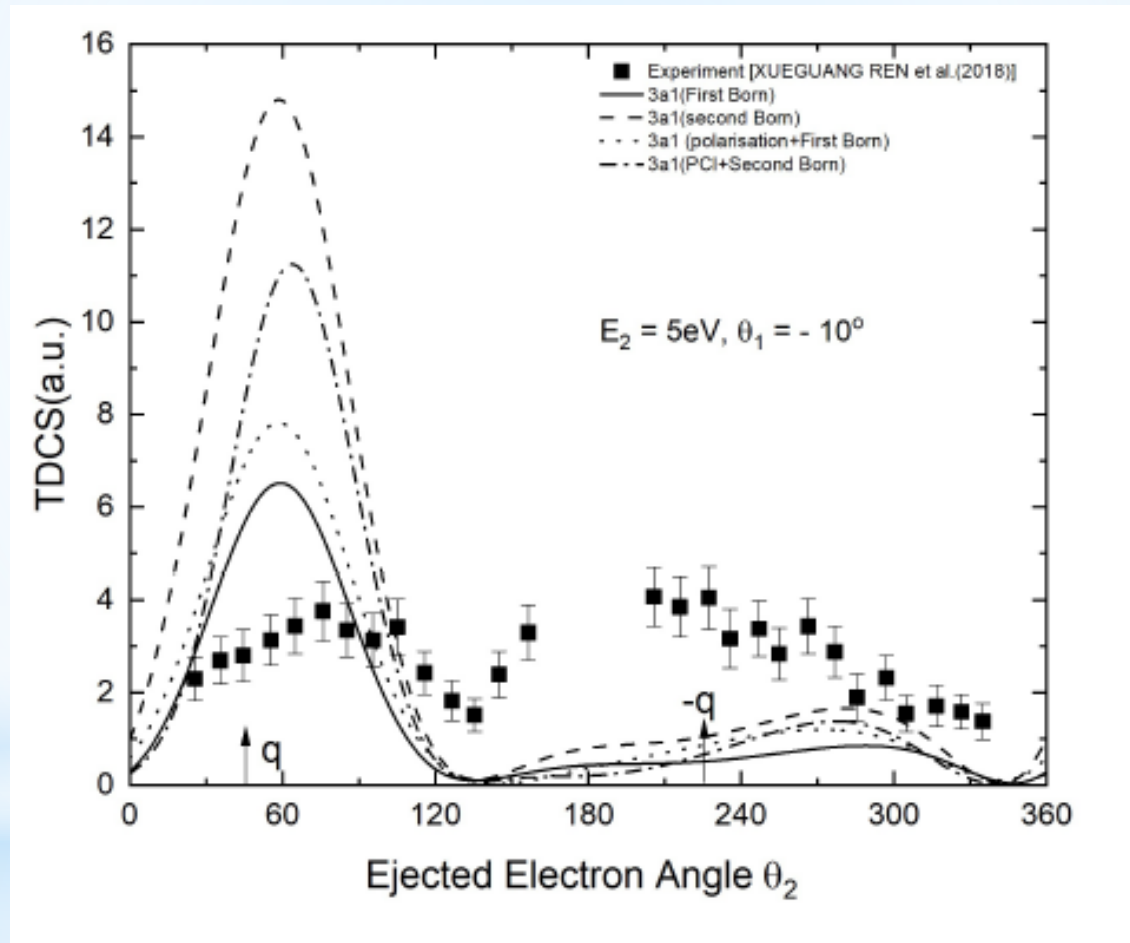
Results – Electron impact TDCS for H₂O molecules at 81 eV – Coplanar geometry



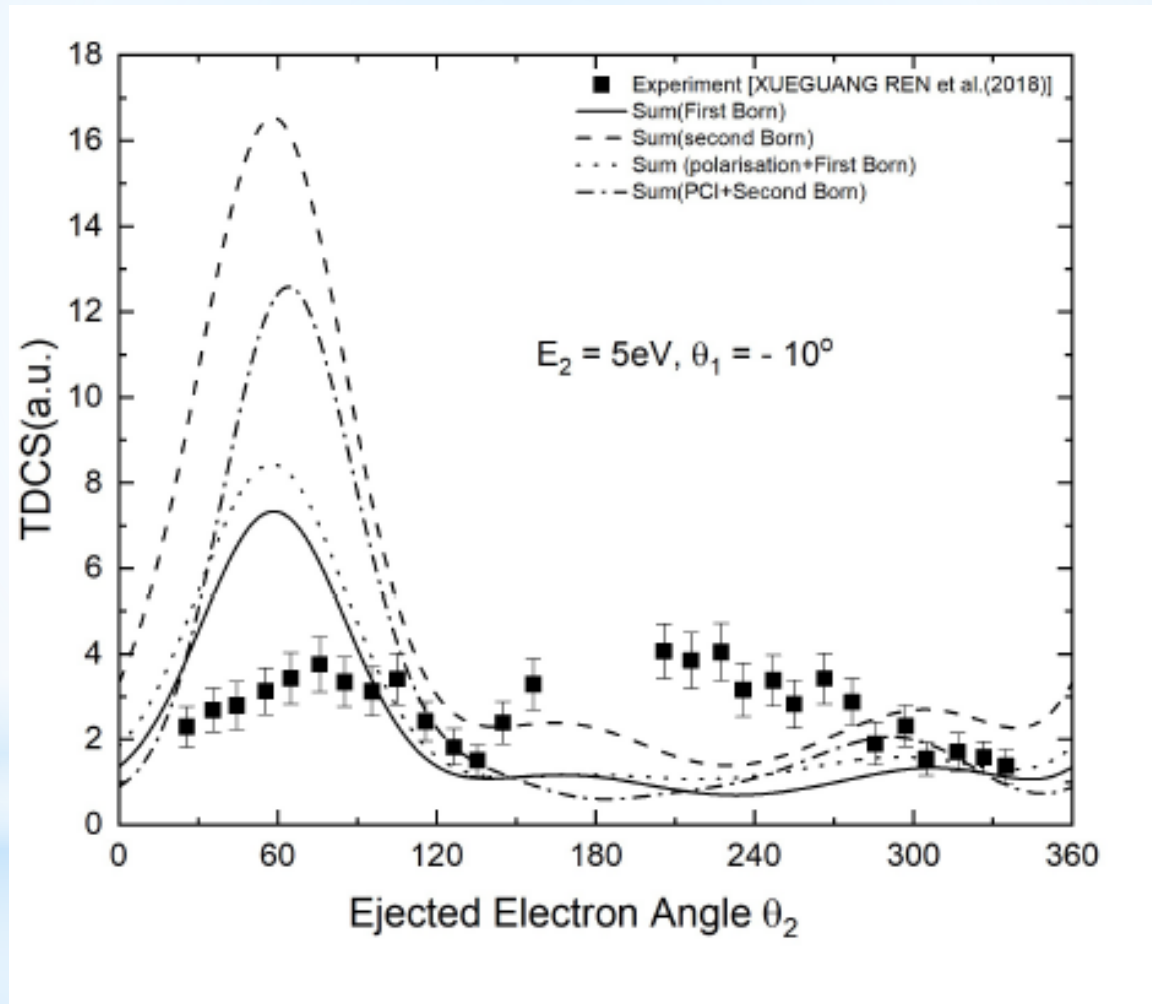
Results – Electron impact TDCS for H₂O molecules at 81 eV



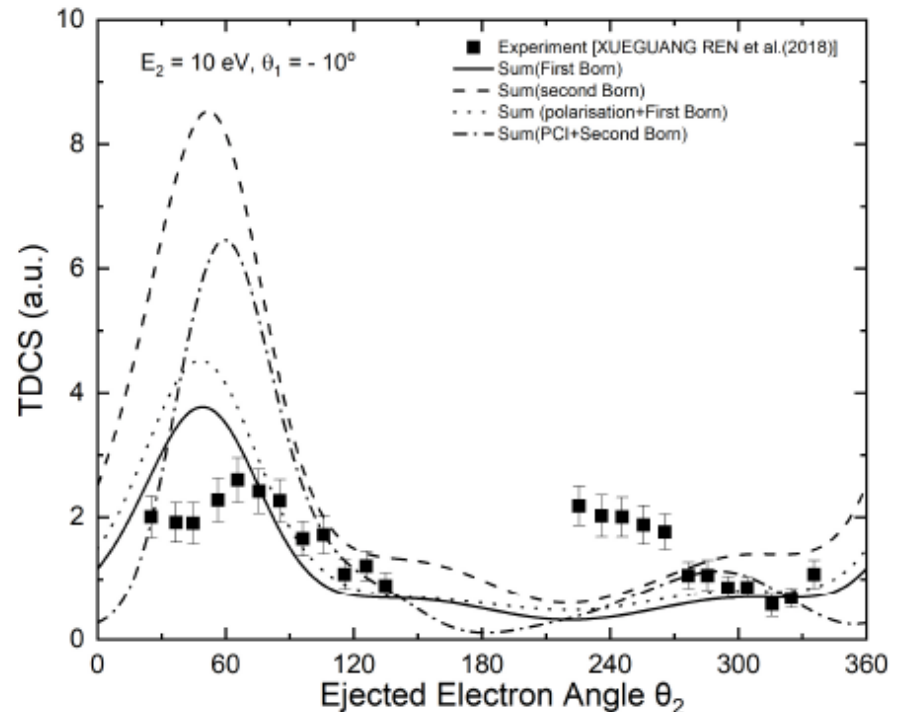
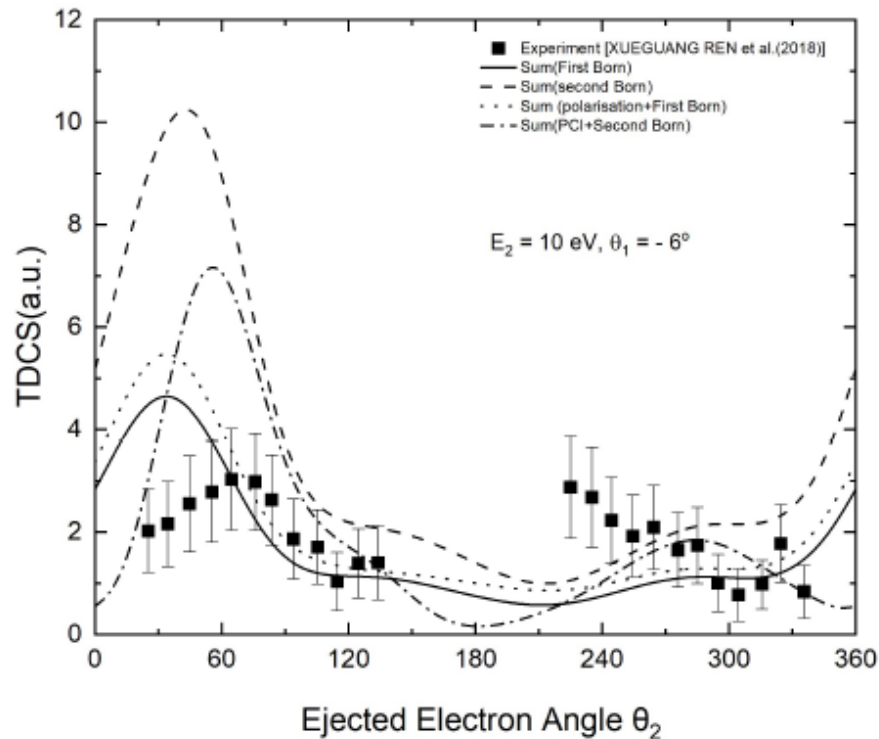
Results – Electron impact TDCS for H₂O molecules at 81 eV



Results – Electron impact TDCS for H₂O molecules at 81 eV

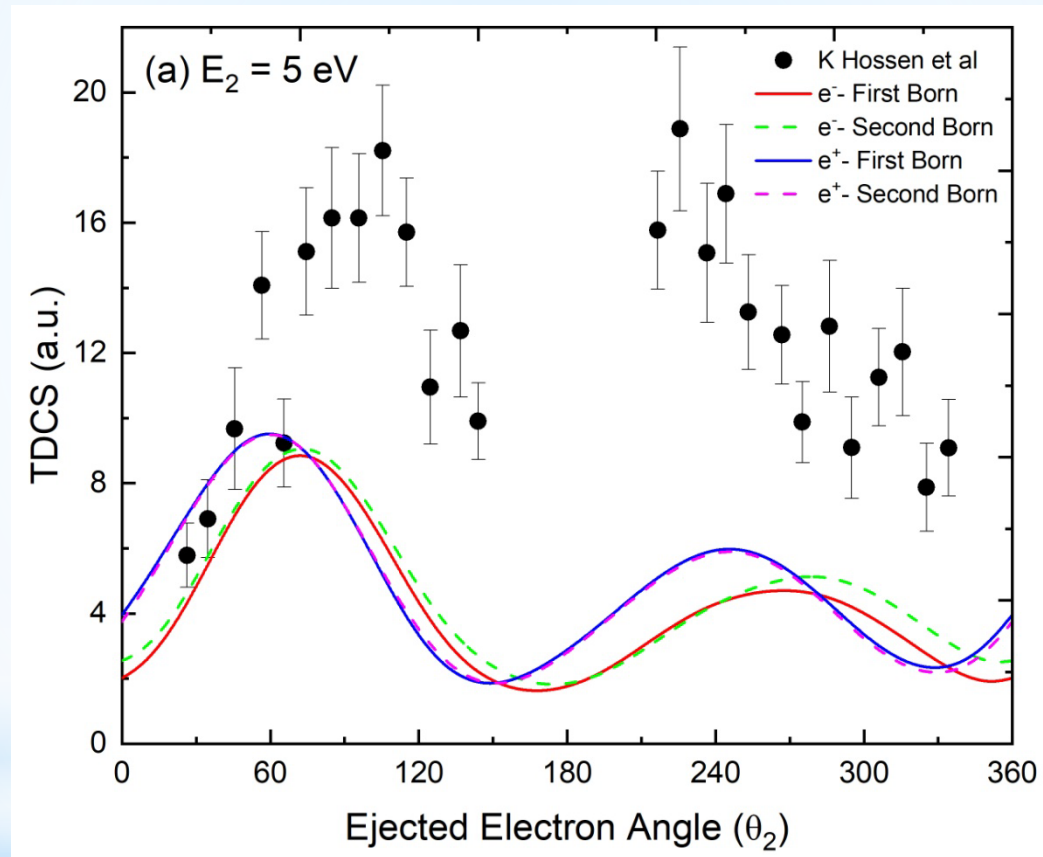


Results – Electron impact TDCS for H₂O molecules at 81 eV



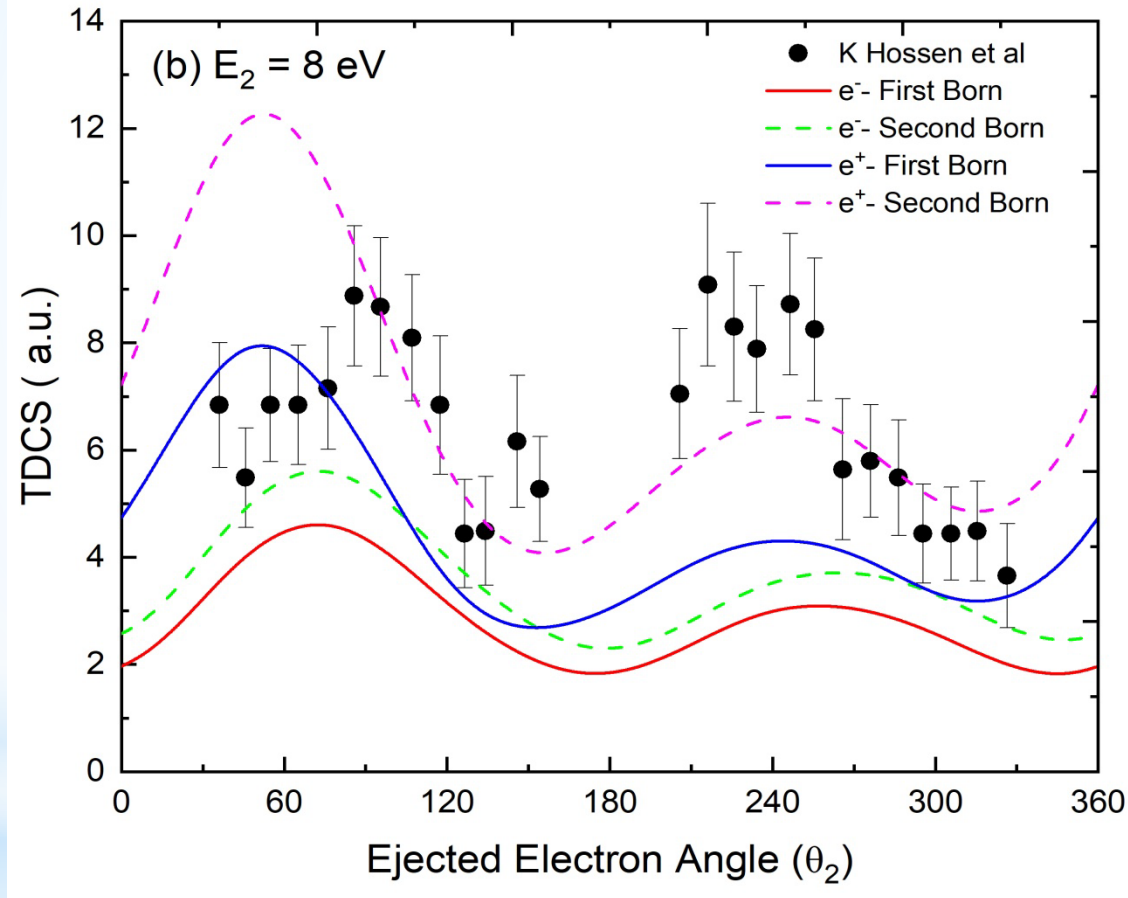
Exp. - X. Ren, S. Amami, K. Hossen, E. Ali, C. Ning, J. Colgan, D. Madison, and A. Dorn
Phys. Rev. A **95**, 022701(2017)

Results – Electron and positron impact TDCS for CO₂ molecules at 100 eV



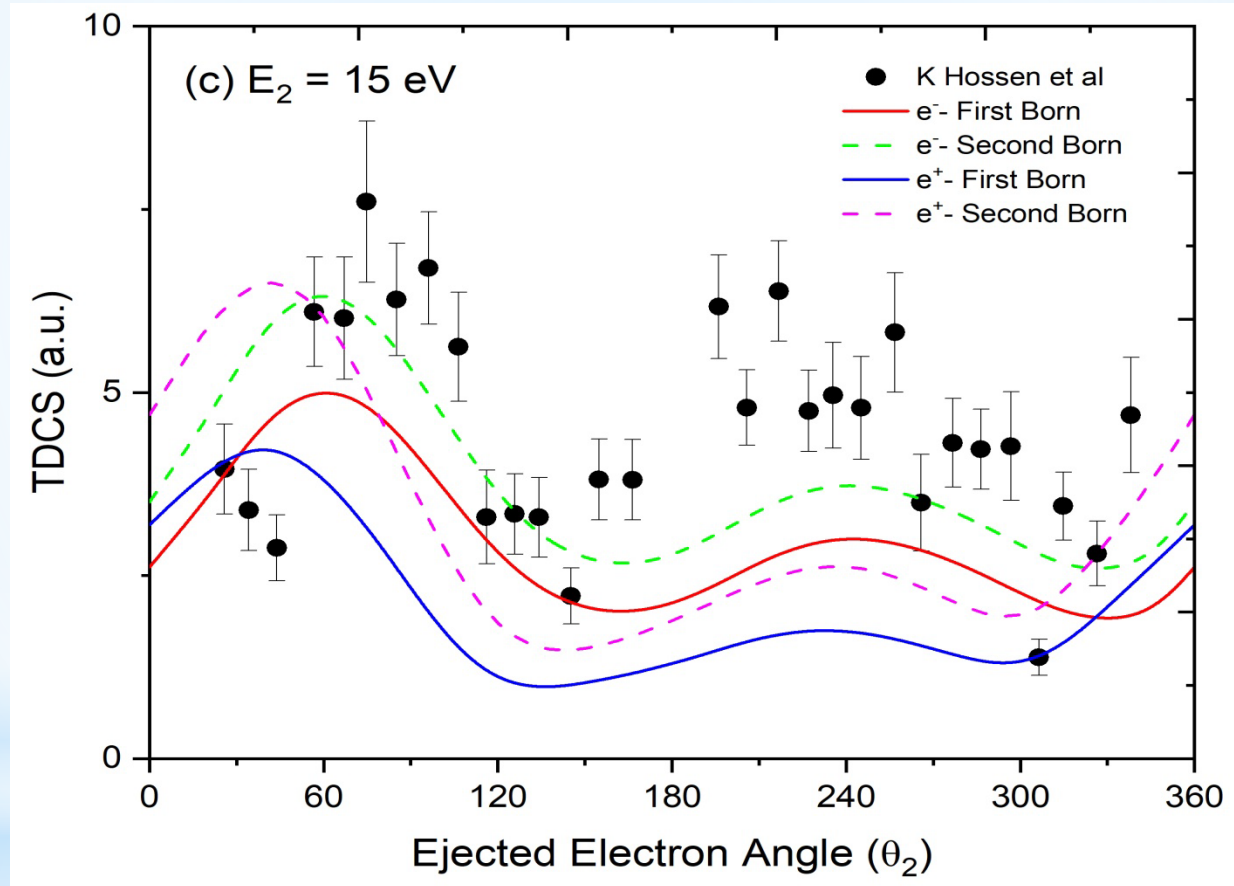
Exp. - Hossen et al. J. Phys. B: At., Mol. and Opt. Phys. 51(21), 215201 (2018)

Results – Electron and positron impact TDCS for CO₂ molecules at 100 eV



Exp. - Hossen et al. J. Phys. B: At., Mol. and Opt. Phys. 51(21), 215201 (2018)

Results – Electron and positron impact TDCS for CO₂ molecules at 100 eV



Exp. - Hossen et al. J. Phys. B: At., Mol. and Opt. Phys. 51(21), 215201 (2018)

Conclusions

Ar (3p) - electron and positron impact

- * Present attempt helps to probe the antiparticle - matter and particle-matter interactions and it is observed that the DBWA is able to produce the differences in the trends of TDCS which are projectile charge dependent.
- * The binary electron emission is increased for positron impact and the recoil emission is decreased, however in case of measurements both the binary and recoil emission increases for positron impact which may be of interest for further investigation.
- * Systematic shift of peaks, shifting away from the momentum transfer direction for positron impact and shifting towards each other for electron impact, is observed with increasing momentum transfer.
- * The post collision interaction and target polarization has not been found significant, further theoretical efforts with accurate treatment for electron exchange may be important to understand the disagreement with the experiments.

Conclusions

Ar (3p) - Coplanar Asymmetric Ionization at 1 keV

- ❖ Second Born approximation is significant at smaller scattering angles - i.e. for the small momentum transfer conditions
- ❖ Significant shift observed in the binary peak positions.
- ❖ Post Collision Interaction (PCI) and Target Polarization Potential not found to be significant in this energy regime

Ar (3p) - Perpendicular Plane Ionization

- ❖ Reasonable agreement with measurements in the 55 eV to 200 eV above IP projectile energy range.
- ❖ The DCS at the higher energies evolves into a broad flat structure with the side lobes reducing in magnitude

Conclusions

Xe (5p) - Coplanar to Perpendicular Plane Ionization

- ❖ Reasonable agreement with measurements with certain disagreement in the lower scattering angle regime
- ❖ The trends of TDCS seems to depend on kinematics rather than target

Conclusions

W and W⁺

- * Present distorted wave TICS results show nearly same magnitude as obtained by semi-relativistic distorted wave results obtained earlier for the W atoms.
- * The distorted wave TICS results for the W⁺ ions overestimate the measurements and Coulomb-Born results however the distorted wave TICS calculated with fine-structure mode for W⁺ ions show smaller values.
- * The TICS results for W and W⁺ have been in agreement with the relativistic DWA and TDCC results
- * The differential cross sections for the W atoms and W⁺ ions is found to sensitive on the direction of momentum transfer i.e. scattering angle.

Conclusions

N_2 molecule - $3\sigma_g$ orbital

- ❖ The trends of TDCS are extracted as a function of momentum transfer through various energy loss values.
- ❖ The effect of reversal of the direction of Coulomb field between the projectile and molecular target is studied through the relative intensities of binary lobe for positron and electron impact and the directions of the binary lobes.
- ❖ There are points of agreement and disagreement between the theoretical and experimental results with large discrepancies.

Conclusions

N_2 molecule - $3\sigma_g$ orbital

- ❖ Both the theory and measurements show enhanced binary emission of electron for positron impact ionization.
- ❖ Nearly same recoil intensities for positron and electron impact are observed for the higher momentum transfer both in the theoretical and experimental results.
- ❖ There are significant discrepancies in the relative magnitude of binary lobes for electron impact case.
- ❖ The binary lobe positions obtained by the theoretical results are shifted towards lower values of ejected electron angles in comparison to the experimental positions

Conclusions

H₂O molecule - $1b_1 + 3a_1$ orbital

* In conclusion present DWBA2 results obtained for water molecule are in reasonable agreement with the measurements with certain discrepancies in terms of binary to recoil peak ratios and positions of peaks.

CO₂ molecule

- ❖ Two peak structure is observed in the present DWBA calculations as measurements
- ❖ Better agreement with measurements observed for higher ejected electron energies
- ❖ Second order Born effects found to be significant
- ❖ Further investigations underway

Future Plan

- * Electron impact cross sections of beryllium hydrides and Boron hydrides
- * Electron impact cross sections of W ions, $q=2,3,\dots$
- * Study of electron / positron / ion impact processes on simple to complex molecules of biological importance
- * Study of electron impact processes on high Z targets

Research Collaborators

- * Prof. Daiji Kato, NIFS, Toki, Japan
- * Prof. Fumihiko Koike, Sophia University, Tokyo, Japan
- * Prof. Yoshiro AZUMA, Sophia University, Tokyo, Japan
- * Prof. Alexander Dorn, Max Planck Institute for Nuclear Physics, Heidelberg, Germany
- * Dr. Christophe Champion, University of Bordeaux, France
- * Prof. Masahiko Takahashi, Tohoku University, Japan
- * Dr. Didier Sebielleu, University of Rennes, France
- * Dr. Chuguang Ning, Tsinghua University, Beijing, China
- * Prof. L. C. Tribedi, TIFR, Mumbai, India
- * Dr. Jiro Itatani, ISSP, Tokyo University, Japan
- * Prof. Yasuyuki Nagashima, Tokyo University of Science, Tokyo, Japan
- * Prof. Wolfgang Quint, GSI, Germany (new initiative)

Acknowledgments

I acknowledge NIFS, Toki, Japan for inviting as Visiting Associate Professor

I also acknowledge the Quantum Plasma Processes Unit, NIFS for accommodating me, with special thanks to Prof. Izumi Murakami and Prof. Daiji Kato

Thanks to Dr. Priti for help in calculations of Be and W

I acknowledge the grant received from Science and Engineering Research Board(SERB), New Delhi in the form of SERB CRG project (CRG/2019/001059).

Thanks

ありがとうございました